

CHAPTER 1: INTRODUCTION

Distillation column is one of the most important components in a separation system. Separation process between mixtures occurs inside the distillation column and it produces two types of products, which are the top and bottom products. Most of the time, the top product will be the main product of the separation and the bottom product will undergo another separation for another desired product. However, some of the fore mentioned products will be recycled back into the column as reflux. This is where the distillation process in distillation column gets complicated (Seader & Header, 2006).

It is difficult to maintain the stability in the process and the quality of the product as it is correlated. The process in distillation column proves to be complicated and difficult to handle as it is complex and highly un-predictive in nature (Seader & Header, 2006). It is a challenge to maintain the stability and desired quality that meets the customers' requirements. Distillation column is a well-known unit operation in industry. Through the 20th century, distillations are widely used for separating liquid mixtures of chemical compounds. Approximately two thirds of the energy for distillation is consumed by petroleum refinery. Distillation is favorable for separating crude oil into petroleum fractions, light hydrocarbon and aromatic chemicals (Seader & Header, 2006).

Separation of other chemical compounds, often in the presence of water, is a common practice in the chemical industry. The success of a distillation column as a method of separation is due to its operational flexibility. For a distillation column, proper control strategies are selected through appropriate implementation. This is very important because the controller has significant effect on product quality, production rate, and energy usage. In a distillation process, controlling a column is challenging since it involves nonlinearities, dual compositions control and disturbances. In refining industries, the product quality of a debutaniser column is always important and the main

focus of its operation is namely to produce the Liquefied Petroleum Gas (LPG) and light naphtha (Gupta et al., 2009), (Hori & Skogestad, 2007)

The debutaniser column is operated at one of Malaysia's crude oil refinery. The refinery produces almost 49 000 barrels of Malaysian light, sweet crude oil on a daily basis. After a recent addition of a Condensate Spiller Unit, the plant produces 74 300 barrels of naphtha condensate per day. This product is used as the main feed stream in the aromatics plant. The plant receives its feedstock mainly from Bintulu and Terengganu and it contains low amount of sulphur. The main focus of this research is to predict the product quality which involves the composition and temperature of the Debutaniser column in the Crude Distillation Unit (CDU) of the Kerteh Refinery. To achieve high purity product, an extensive study is conducted to maximize the product (n-butane and i-butane).

The debutaniser column is a type of fractional distillation column that is used to separate butane from natural gas, especially during the refining process which is usually controlled by manipulating the reflux and re-boiler flow rates of the column to ensure the desired purity of the products. Most of the complexity of the process of controlling the column comes from the unique characteristics of the column itself, including its complex dynamics, high nonlinearity and interaction between the control loops (Gupta, Ray & Samanta, 2009).

1.1 Problem statement and motivation

Petroleum industry is one of the most prolific and dynamic industries of modern civilization. Because of the highly competitive market and stringent environmental laws, strict quality control of refinery products is a must. The Crude distillation unit (CDU) is one of the systems through which the entire crude entering a refinery is to be processed. Thus close monitoring and control of CDU product properties will help in

controlling the properties of the refinery products. It is often sufficient to characterize refinery products in terms of certain properties such as Reid Vapor Pressure for volatile products, Flash Point for light distillate, Pour Point for heavy distillate and etc. Continuous control of the unit demands that these properties should be measured on-line so that it can be effectively controlled through a feedback mechanism.

The debutaniser column of the PETRONAS Penapisan Terengganu Sdn Bhd (PPTSB) produces LPG (liquefied petroleum gas) as the top stream and light naphtha as the bottom stream. The controlled outputs, which are the critical product quality to be measured, are the concentration of the top and the bottom stream. Currently, few methods are governed in determining these product qualities in PPTSB. The laboratory sample of both top and bottom products are taken. Sample is taken to the laboratory and product quality has to be determined experimentally using the appropriate ASTM Method. LPG composition is measured based on ASTM D2163 for composition test. The composition measured is Propane, i-Butane, n-Butane, i-Pentane and n-Pentane they are measured by using gas chromatography.

PPTSB uses Inferential Calculation to measure Debutaniser Overhead percentage of C₄ (n-butane). It is generated using simple linear regression method by comparing the actual %C₄ result versus Process Data (can be obtained from PI system). Calculation description for %C₄ is given below;

$$\%C_4 = a * PCT + b \quad (1)$$

Where;

PCT = Pressure compensated temperature of top temperature (Different calculation to measure composition in Debutaniser Column based on Temperature and Pressure)

a = Gain coefficient between the PCT and %C₄ lab result

b = bias (Updated based on lab result)

However, from the industrial perspective, the problem with the existing old method is that, laboratory measurement procedures are slow, tedious and time consuming. Therefore, inferential model using linear regression usually encounters colinearity problem, which adversely affects long-term prediction performance since the outputs of the debutaniser column usually depend on the feed composition which also cannot be determined online. In addition its variation significantly affects the output values. Thus, alternative method has to be used to generate a better model.

The purpose of this research is to develop NN based models in predicting the critical product qualities i.e. composition and temperature prediction and to control top and bottom temperatures of the debutaniser column of the PPTSB. Neural Network is expected to be able to generate a better model for the prediction of the product qualities and the hybrid neural network model is expected to improve the prediction of the composition and temperature of the column. Neural network forward and inverse models are able to simulate the dynamic response of the column to estimate composition and to control temperature which can be used as a neural network controller.

The challenges for the soft sensors which are;

- The integration, coupled with unceasing electronic miniaturization, will make it possible to produce extremely inexpensive sensing devices
- The automatic adaptations to changes in environment and requirements
- The coordination applications are better realized using localized algorithms

There are some work based soft sensors that have a number of advantages which are;

- They are cheaper compared to hardware sensors
- They work in parallel with hardware sensors, giving important information for fault diagnosis
- They can be easily be implemented on existing hardware that are available in the industry and can easily be used for tuning PID controller when system parameters changes
- They can estimate real time data, overcoming the delays introduced by slow hardware sensors

In this application, available process information given by engineers is used to select the important input variables and it requires a huge amount of existing working data, to be collected in the refinery over a period of five years. The set of data is used to tune the parameters of a Nonlinear Autoregressive network with exogenous inputs (NARX) structure implemented using appropriate lagged inputs to the process model. This ensures that the developed process model is dynamic in nature and not in the steady state of the process. NN based modeling is a useful strategy, It is used in a number of industrial applications, when real-time estimation of plant variables is required for monitoring and control purposes and on-line sensors may give variable measurements with small delays (Fortuna, Graziania & Xibilia, 2005) This is often applied to the petrochemical plants. The importance of equation based models is that it is robust in nature and it could relate the relationship between input and output predictions and hence it is can be easily applied as a soft sensor. Furthermore it is MIMO (Multi input multi output) based model that can predict the composition and temperature through the use of a single vector equation.

This work indicates that neural network can be applied as a controller to better understanding the oil refinery industry. In this work, we have carried out an advanced

control strategies and hybrid modelling to predict the composition and temperature for a real plant debutaniser column in the refinery industry. The non-linear controllers for the distillation column can be developed. NN offer an alternative approach to model non-linear process and result in a controller that overcomes the issues of on-line computation. The data obtained are collected from the actual plant. Some of the data that is not available are obtained using simulation.

1.2 Objectives

The main focus of this research is to achieve a control strategy that can help to maximize the product output at the Debutaniser column. The desired output is n-butane and i-butane. The objectives of the current work are as follows;

1. Data generation (using open loop, closed loop and extract from close loop) and validation for a real debutaniser columnso as to develop a neural network process model using black box for the column.
2. To develop a neural network process model using equation based for the column to predict the composition and temperature.
3. To develop an equation based hybrid model NN of 1 hidden layer to control temperature and estimate composition of a debutaniser column.
4. To implement an advanced process control for the column to control temperature and to estimate composition using equation based models.

Since there are delays for composition prediction, soft sensors are proposed to overcome this delay for the column.

1.3 Scope of work

The scopes of work for this research are as follows:

1. The steady state and dynamic simulation for the debutaniser column are developed.
2. The process variable for controller settings based on actual plant data and simulation are analyzed.
3. The performance of models generated by NN and current methods using black box model are used in predicting critical product quality for debutaniser column. The selected component composition in the top and bottom products, top and bottom temperatures using equation based neural network model are compared.
4. The composition and temperature for the column using hybrid neural network equation based are estimated using the combination of the residual prediction and the first principle model.
5. The advanced process control for the column using equation based is developed.

The scope of study is mostly on the development of the neural network model, hybrid prediction and advanced process control performance of the column. MATLAB version 2006 is used for obtaining the neural network model, hybrid model and advanced control. SIMCA-P is used for principal component analysis and partial least square analysis to analyze the variables surrounding the column. Both of the software are used throughout the development of the study.

1.4 Novelties

The novelties of the work are;

1. Neural network architecture which is used to train the network for the composition and temperature is implemented by means of an equation based method. The equation-based method is used to replace the black box model neural network architecture.
2. The equation based neural network forward model is used to predict the debutaniser composition and temperature. The residual neural network model is used to develop the hybrid model for the column by predicting the composition and temperature.
3. The forward model for the temperature is used to develop the inverse model to be applied as a controller. On the other hand the forward model for the composition is used as neural network estimator. The debutaniser column is a MIMO based controller.

1.5 Dissertation Organization

This thesis has been organized into chapters as listed below:-

- (a) Chapter 1 introduces the work objective and dissertation organization.
- (b) Chapter 2 presents the literature review and highlights the important concept of artificial neural network and its application including the theory of principal component analysis and partial least square analysis.
- (c) Chapter 3 outlines the plant description and case study for the column, data generation for open and closed loop, data pre-treatment using PCA and PLS.

- (d) Chapter 4 discusses the simulation work process model for composition and temperature applying equation based neural network for the column.
- (e) Chapter 5 focuses on the implementation of hybrid model based monitoring strategies for composition and temperature.
- (f) Chapter 6 highlights the findings and results for advanced process control using direct inverse control and internal model control using network and neural network equation based in terms of set point changes and disturbances applied for the column.
- (g) Chapter 7 is a derivation of the conclusion and recommendations for future work.
- (h) Further sections outline the references and appendices used in the dissertation.

CHAPTER 2: LITERATURE REVIEW

2.1 Introduction

In this chapter, the background of neural network and its architecture are outlined. NN model is similar to the newborn human where it needs to be developed, trained, and taught in order to perform a specific task. The methods in which data are trained are highlighted in the next section. It shows the procedure to obtain reliable neural network models. A number of researchers have worked on neural network application, principal component analysis and partial least square analysis (Liu et al., 2009), (Zamproga et al., 2005), (Chen et al., 1998), (Kano et al., 2000), (Zamproga et al., 2004), (Fortuna et al., 2005), (Singh et al., 2007), (Zilochan & Bawazir, 2001), (Prasad & Wayne Bequette, 2003). Literature is cited, highlighted and indicated the possible neural networks application for process system engineering which leads to control strategies and the development of hybrid models.

2.2 Neural network introduction

An ANN, usually called NN, is a mathematical model or computational model that is inspired by the structure and functional aspects of biological neural networks (Bertsekas & Tsitsiklis, 1996). A neural network consists of an interconnected group of artificial neurons, and it processes information using a connection approach to computation. In most cases an ANN is an adaptive system that changes its structure based on external or internal information that flows through the network during the learning phase. Modern neural networks are non-linear statistical data modeling tools. They are usually used to model complex relationships between inputs and outputs or to find patterns in data. The original inspiration for the term ANN consists of centre nervous systems and their neurons, axons, dendrites, and synapses, which constitute the

processing elements of biological neural networks investigated by neuroscience. In an ANN, simple artificial nodes, which are called neurons are connected together to form a network of nodes mimicking the biological neural networks.

There are several ways to inspire from the brain, in which there is no single formal definition of what an artificial neural network is. Generally, it involves a network of simple processing elements that exhibit complex global behavior determined by connections between processing elements and elemental parameters. While an artificial neural network does not have to be adaptive, its practical use comes with algorithms designed to alter the weights of the connections in the network to produce the desired signal flow (Bertsekas & Tsitsiklis, 1996). These networks are similar to the biological neural networks in the sense that functions are performed collectively and paralleled by the units, without clear delineation of subtasks to which various units are assigned. Currently, the term ANN tends to refer mostly to neural network models employed in statistics and artificial intelligence.

2.3 Types of artificial neural network

The types of neural network are sectioned into various categories based on the structure of the network including their connections and arrangements. The overall behavior of the network is determined by adjusting the connection weights to achieve the desired output based on its learning algorithm. There are various types of neural network that can be used. However since this work involves dynamic processes, the suitable neural networks that can be used are the feed forward, recurrent and NARX type model (Demuth et al., 2007)

2.3.1 Feed forward network

The feed forward network consists of more than one hidden layer. Multiple layers of neurons using non-linear transfer function will allow the network to recognize non-linear relationship between the outputs and inputs. The input layer is the first layer, while the second layer is the hidden layer and the output layer is the third layer. The layer is consisting of weights and biases. The weights could be adjusted to achieve the target values using appropriate training algorithms (Demuth et al., 2007).

2.3.2 NARX network

The nonlinear autoregressive network with exogenous inputs is a recurrent dynamic network. The feedback connections will enclose the layers of the network. The NARX model consists of feed forward neural network. There are various examples for the NARX network. It can be used as a predictor. It will predict the next value of the inputs. The use of the network can be applied for an important application to model the nonlinear dynamic system (Demuth et al., 2007). The output of the NARX network is to be an estimate of the output of nonlinear dynamic system. The output is fed back to the input of the feed forward neural network. The true output is available during training and it can also create a series of parallel architecture in which the true output is used instead of feeding back the estimated output.

2.4 Learning paradigms learning task

There is one major learning paradigm, each corresponding to a particular abstract learning task which is used in this work that is supervised learning.

2.4.1 Supervised learning

In supervised learning, we are given a set of example pairs x and y and the aim is to find a function $y=f(x)$ in the allowed class of functions that matches the examples. In other words, we need to infer the mapping implied by the data; the cost function is related to the mismatch between our mapping and the data and it implicitly contains prior knowledge about the problem domain. A commonly used cost is the mean-squared error, which tries to minimize the average squared error between the network's output, $f(x)$, and the target value y over all the example pairs. When one tries to minimize this cost using gradient descent for the class of neural networks called multilayer perceptions, one obtains the common and well-known back propagation algorithm for training neural networks. Tasks that fall within the paradigm of supervised learning are pattern recognition (also known as classification) and regression (also known as function approximation). The supervised learning paradigm is also applicable to sequential data. This can be thought of as learning in the form of a function that provides continuous feedback on the quality of solutions obtained.

2.4.2 Learning algorithms

Training a neural network model refers to selecting one model from the set of allowed models that minimizes the cost criterion. There are numerous algorithms available for training neural network models (Demuth et al, 2007). Most of them can be viewed as a straightforward application of optimization theory and statistical estimation. Most of the algorithms used in training artificial neural networks employ some form of gradient descent. This is done by simply taking the derivative of the cost function with respect to the network parameters and then changing those parameters in a gradient-related direction. The supervised learning in a feed forward multilayer perceptron (MLP) is normally used is the back-propagation method. Given two sets of

data, that is input/output pair, the MLP can have its weights adjusted by the back-propagation algorithm to develop a specific nonlinear mapping. The MLP with fixed weights after the training process can provide an association task for prediction. During the training phase of the MLP, the weights are adjusted to minimize the disparity between the actual and desired outputs of the MLP.

2.4.3 Levenberg-Marquardt method

The purpose of using the Levenberg-Marquardt (LM) algorithm method is to train the neural network in the NARX network. The LM is designed for second order training speed without the Hessian matrix to be computed. The performance function consists of sum of square as similar to feed forward training. The Hessian matrix can be derived as

$$G = H^T H \quad (2.1)$$

The gradient can be derived as

$$I = H^T e \quad (2.2)$$

where H is the Jacobian matrix that consists of first derivatives of the network error with respect to biases and weights values and e is the network error. The Jacobian matrix can be defined as a standard back-propagation technique.

The LM algorithm uses almost similar to the Hessian matrix as

$$x_{k+1} = x_k + [H^T H + \mu F]^{-1} H^T e \quad (2.3)$$

When μ is zero, the equation simplifies to Newton's method. When μ is large, the equation will become gradient descent. So the target is to shift the Newton method as fast as possible. When there is a reduction in the the performance function the μ is decreased and it increases when the performance function increases. The effect of the performance function is reduced at each iteration of the algorithm (Demuth et al, 2007). This LM algorithm method is used in this work.

2.5 Neural network design

The greatest advantage of ANN is its ability to be used as an arbitrary function approximation mechanism that learns from observed data (Demuth et al., 2007). However, its usage is not very straightforward. A relatively good understanding of the underlying theory is required which includes the following;

- Choice of model: This will depend on the data representation and the application. Complex models tend to lead to problems with learning.
- Learning algorithm: There is numerous trade-offs between learning algorithms. Almost any algorithm will work well with the correct parameters for training on a particular fixed data set. However selecting and tuning an algorithm for training on unseen data requires a significant amount of experimentation.
- Robustness: The right selection of cost function and learning algorithm ensure the robustness of the resulting ANN.

With the correct implementation, ANN can be used naturally in online learning and large data set applications.

2.5.1 Procedure for obtaining the neural network models

The neural network is complex and it is a crucial and major concern to the system developer. To design the neural network architecture is important and the networks are allowed to learn the data set using appropriate training data set. The detail procedures to obtain a suitable neural network model are outlined below:

1. The data set are partitioned into three categories. The first category is training all the data set. The second category is training and validation. The third category is training, validation and testing.
2. Selecting suitable input and output for the neural network. The inputs can be large data sets that are used in training to predict the output of the network.
3. Selection of suitable neural network architecture. There are several neural network architecture available such as feed forward, recurrent network and radial basis function network. The proposed neural network is the NARX series parallel.
4. Initialize the weights and biases value for training the network.
5. Train the neural network with suitable training algorithm. The selected algorithm is the LM method. The objective is to reduce the error between the observed and predicted value. The training will eventually stop until the training parameter goal is reached.
6. Validate the trained neural network with validation data set. Testing the trained neural network with testing data set.
7. If the validation and testing are not satisfactory, it indicates that the neural network is not properly trained and it requires more training. This is because there is insufficient number of neurons in the hidden layer and improper use of transfer function.

8. To reconfigure the neural network architecture by increasing or decreasing the number of hidden nodes and layer.

The procedure is summarized in Figure 2.1

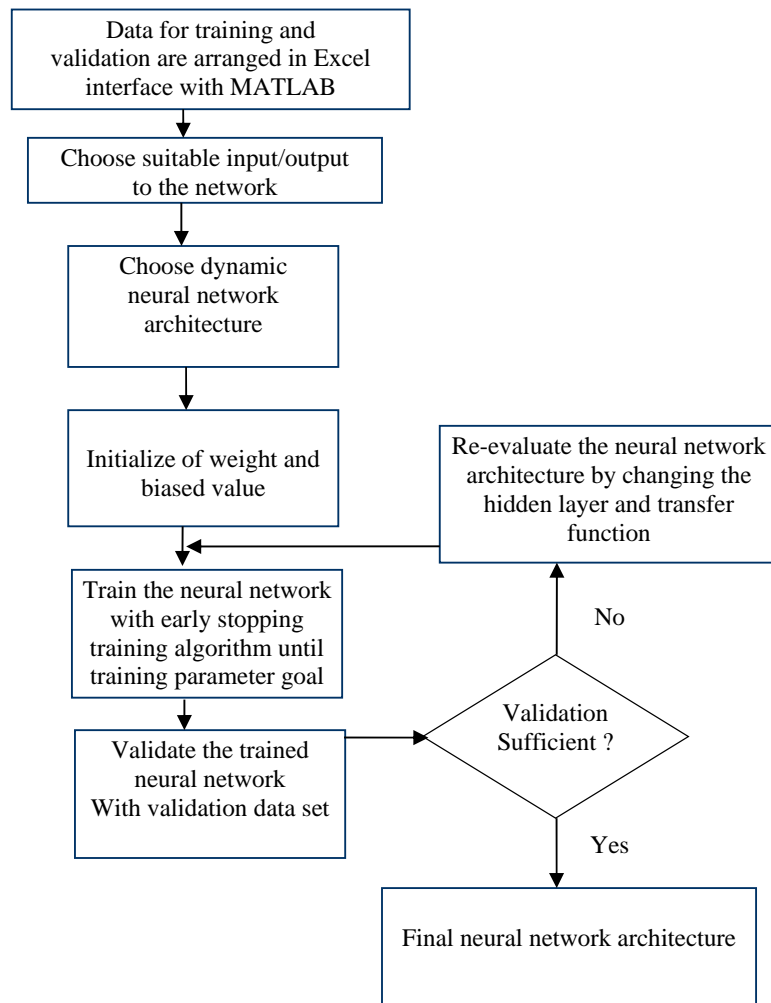


Figure 2.1. General procedure in obtaining the suitable neural network model

2.6 Data pretreatment

These data that are available from the actual plant are large and therefore need to be screened by performing principal component analysis (PCA) and partial least square (PLS), where the important variables for the column are obtained and used for monitoring the composition. For each of the step test, PCA is used to determine the important variables surrounding the column. Once we have determined the process variables, the important variables affecting the composition are further analyzed using PLS analysis. The data that have been screened are used to develop the neural network model in order to predict the temperature and composition.

2.6.1 Principal component analysis (PCA)

Principal component analysis (PCA) is one of the most valuable results from applied linear algebra. PCA is used abundantly in all forms of analysis because it is a simple, non-parametric method of extracting relevant information from confusing data sets. With minimal effort, PCA provides a roadmap to reduce a complex data set to a lower dimension (Eriksson et al., 2006). This is to reveal the sometimes hidden, simplified dynamics that often underlie it. The objective of principal component analysis is to compute the most meaningful basis for the data set. The new basis will filter out the noise and reveal hidden dynamics. Determining this fact allows one to discern which dynamics are important and which are just redundant. Let X and Z are $m \times n$ matrices relate by a linear transformation T

$$TX = Z \tag{2.4}$$

where X is the original recorded data set and Z is a re-representation of that data set.

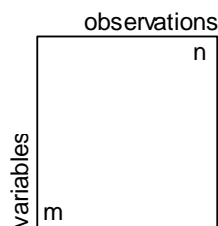


Figure 2.2: Notation used in PCA as extracted from (Eriksson et al., 2006).

The observations (columns) in Figure 2.2 can be analytical samples, chemical compounds or reactions, process time points of a continuous process, and so on. The variables (rows) can be of spectral origins, or be measurements from the sensors and instruments in a process (temperatures, flows, pressures, etc.). Equation 2.4 represents a change of basis and the row vector $T = \{t_1, \dots, t_m\}$ can be interpreted as a new set of basis vectors for representing the columns of X . In this transformation, the rows of T will become the principal components of X . PCA assumes that all basis vectors $\{t_1, \dots, t_m\}$ are orthonormal (i.e. $t_i \bullet t_j = \delta_{ij}$). In linear algebra, PCA assumes T is an orthonormal matrix. Secondly PCA assumes the directions with the largest variances as the most important.

The true benefit of the orthonormality assumption is that it makes the solution amenable to linear algebra (Eriksson et al., 2006). There exists linear algebra decomposition techniques, which can provide efficient, explicit algebraic solutions namely, eigenvectors of covariance matrix (and the more general singular value decomposition) of covariance matrix. Referring to the previous section, the main characteristic of eigenvectors is that all the eigenvectors of a matrix are orthogonal to each other regardless of the number of variables. The second assumption determines the importance of each principal direction. The variances associated with each direction, t_i

quantify the direction of each principal. Hence, we can rank-order each basis vector, t_i according to the corresponding variances.

By the variance assumption, PCA first selects a normalized direction in m -dimensional space in which the variance in X is maximized and it is called as t_1 . Again it finds another direction along which the direction is maximized. However, because of the orthonormality condition, it restricts its search to all directions perpendicular to all previous selected directions. This can continue until m directions are selected. The resulting ordered set of t 's are the principal components (Eriksson et al., 2006).

Performing PCA is quite simple in practice; the following are the steps to perform PCA:

1. Organize a data set as a $m \times n$ matrix, where m is the number of variables (dimensions) and n is the number of trials (observations).
2. Subtract the mean for each measurement type (pre-treatment of data).
3. Calculate the eigenvectors of the covariance matrix. This will give the principal components vector T .

Figure 2.3 gives the geometric illustration of a PCA model with two principal components, t_1 and t_2 in 3 dimensional spaces. The principal component loadings uncover how the PC-model plane is inserted in the variable space. The loadings are used for interpreting the meaning of the scores (Eriksson et al., 2006).

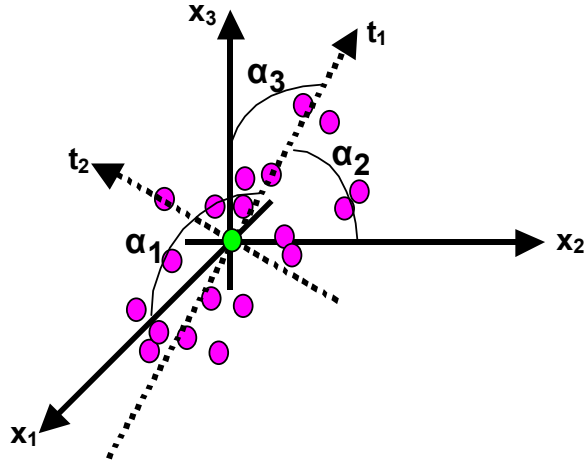


Figure 2.3: A geometric illustration of a PCA model with two principal components t_1 and t_2 .

In Figure 2.3, it can be observed that the direction of the first principal component, t_1 , in relation to the original variables is given by the cosine of the angles α_1 , α_2 and α_3 . These values indicate how the contribution of the original variables x_1 , x_2 , and x_3 is to t_1 , and it is represented by a vector $p_1 = \{\alpha_1, \alpha_2, \alpha_3\}$. Vectors p_1 and p_2 (for principal components t_1 and t_2 respectively) are called principal component loadings or loading vectors. The loading vectors define the orientation of the principal component plane with respect to the original X -variables. The loadings unravel the magnitude (large or small correlation) and the manner (positive or negative correlation) in which the measured variables X contribute to the principal components t_i .

2.6.2 Partial least square (PLS)

PLS is defined as a regression technique for modeling purposes between the input and output variables. It can be used as a building block to detect the regularities of the data in the model under study. It is a method to relate two matrices, X and Y to each other (Eriksson et al., 2006). PLS stands for projections to latent structure by means of partial least squares. It has the ability to analyze data in both X and Y coordinates. The precision of PLS improves by having a large number of X variables that provides more information about the observations. It is a useful regression technique for modeling and can deal with complicated and approximate relationship. It can also be used to check the validity of the model from theory.

It often applies to process modeling. The method used for PLS is to relate two data matrices, for an example variable X as the input and Y is the output. A PLS model will try to find the multidimensional direction in the X space that explains the maximum multidimensional variance direction in the Y space. PLS regression is particularly suited when the matrix of predictors has more variables than observations, and when there is multicollinearity among X values. By contrast, the standard regression will fail in these cases. A linear multivariate model is used to relate between input variable and output variable to each other. PLS has the ability to analyze large data, noisy, collinear and incomplete variable in both input and output. The precision of a PLS model improves with increasing the number of input variables. Large numbers of variables that are analyzed provide better information on the observation (Eriksson et al., 2006). PLS regression is a statistical method that are used for principal component regression; instead of finding hyperplanes of minimum variance between the response and independent variables, it finds a regression model by projecting the predicted variables and the observed variables to a new space. It is used to find the fundamental relations between two matrices, latent variable approach to modeling the covariance structures in

these two spaces. The PLS algorithm is employed in PLS path modeling, a method of modeling a network of latent variables which cannot be determined without experimental or quasi-experimental methods. This technique is a form of structural equation modeling, distinguished from the classical method by being component-based rather than covariance-based.

In PLS, a set of components is determined that performs simultaneously decomposition of X and Y with the constraint that these components explain as much as possible of the covariance between X and Y . It is followed by a regression step where the decomposition of X is used to predict Y . Hence, the first PLS component is a line in Y space, through the average point, such that the lines approximate the data well, and the projections (tl and ul) are well correlated. The projected co-ordinates in the two space (ul and tl in Y and X) are correlated in the inner relation $u_{il}=t_{il}+h_i$ (h_i is a residual). The lines in X space are orthogonal whereas lines in Y space are not orthogonal. The reason being the main objective is to find the maximum correlation between X and Y .

Prediction via PLS model: The output (or dependent) variables are predicted using the multivariate regression formula as:

$$\hat{Y} = TQ^T = XW(P^TW)^{-1}Q^T = X\hat{\beta} \quad (2.5)$$

where $W(P^TW)^{-1}Q^T = \hat{\beta}$ is the correlation/regression coefficient between the input and output variables. It may also be noted that,

1. columns of matrix T contain the latent vectors t
2. weights W are the regression coefficient of columns of X on u

3. P is the loadings for matrix X . The loading vector p is the regression coefficient of columns X onto t . The loading vector p is only computed at the convergence of latent vector t and used to calculate the residuals at each stage

Correlation coefficient and dimension reduction in the PLS model is expressed as a set of X -score vectors, Y score vectors, X -weight and Y weight vectors, as a set of PLS model dimensions. One of the analysis tools available using PLS is the coefficient plot. In the coefficient plot, the sizes and the signs of the coefficient relating to centered and scaled variables indicate the influence of each input variable term. The statistical significant of each coefficient is indicated as 95% confidence intervals.

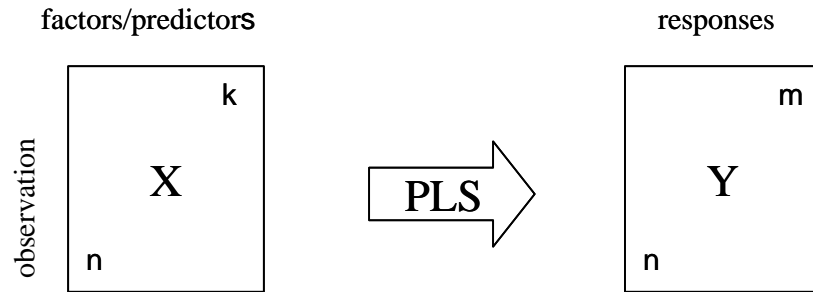


Figure 2.4: The X variables are defined as factors and Y variables are called responses (Eriksson et al., 2006).

2.6.3 Literature review for principal component and partial least square analysis for distillation column

PCA describes a remarkably simple approach to multivariate analysis based on projection methods. The projection approach can be adapted to a variety of data analytical objectives such as summarizing and visualizing a data set, multivariate classification and discriminate analysis and, finding quantitative relationship among the variables. Projection methods can be made robust to outliers, deal with non-linear

relationship and adapt to drift in multivariate process data. Dynamic PCA considers the dynamic process by introducing time lagged variables into the inferential models (Liu et al., 2009). The dynamic methods are suitable for processes with long time delays and varying throughputs on process variables. Secondary variables are sensitive to primary variables when implementing inferential estimator in achieving the column optimum performance (Zamproga et al, 2005). As there are many possible locations of the temperature sensors for a column, the selection of the secondary variables as inputs becomes difficult. PCA properties are measured by extracting a matrix and using input variable for the online implementation (Chen et al, 1998). Many approaches have been studied to build a secondary variable model from readily available measurements such as tray temperatures to replace the quality measurements. A secondary variable approach has been studied for use when quality measurements are not available.

Partial Least Square (PLS) is an extension of PCA, which is used to connect information of variables (Eriksson et al., 2006). In order to understand and interpret the acquired regression model, PLS provides model parameters with other diagnostic tools where by increasing the number of X variables, it can improve the precision of a PLS. In the literature there exists some modelling work of a debutaniser column using PLS. For example, dynamic partial least square regression is used for inferential model for composition prediction in a multicomponent distillation column (Kano et al, 2000). Past sampling times measurements are used as input variables to interpret the dynamic process. PLS is also used to predict the composition profile in a simulated batch distillation column (Zamproga et al., 2004). The inputs are temperature measurements and the output is the composition in the distillate and bottom streams. The estimator performance is evaluated based on the pre-processing of the calibration and validation data sets, number of measurements used as sensor inputs, presence of noise in the input measurements, and use of lagged measurements. A simple augmentation of the

conventional PLS regression approach is proposed, which is based on the development and sequential use of multiple regression models. In this work, PCA is used to analyze all the variables surrounding the column. PLS analyses are performed to decide the variables that are related to composition.

The debutaniser column is an important unit operation in the petroleum refining industries. The objective of this work is to perform principal component analysis (PCA) of the debutaniser column and to study correlation between the variables, to detect critical and moderate outliers, to identify the importance of the variables and loading of variables surrounding the column. The results prove the proposed approach is important for optimum configuration of the column (M Ramli, Hussain & Mohamed Jan, 2011).

2.6.4 Literature review for modeling for distillation column especially debutaniser column

A nonlinear adaptive state estimator/observer (ASE/ASO) is developed based on a simple observer model structure that mainly consists of only two component balance equations around the condenser-cum-reflux drum and the re-boiler-cum-column base (Jan et al., 2009). In this approach, vapor flow rate of component n-pentane (heavy key) leaving top tray, liquid flow rate of component n-butane (light key) leaving bottom tray and distribution coefficient of component nC4 in the re-boiler are considered as extra states with no dynamics. Despite process/model mismatch, the proposed state observer estimates the required states of a simulated debutaniser column precisely. Mainly because of the design simplicity, negligible computational effort and fast convergence, the observer is recommended for online implementation (Jan et al., 2009). In the subsequent part, the globally linearizing control (GLC) structure, which consists of a nonlinear transformer (input–output linearizing state feedback), a linear external controller and an adaptive state observer, has been synthesized. The hybrid GLC–ASO control algorithm provides promising performance compared to the

proportional integral (PI) controller that has been thoroughly investigated on the complex refinery debutaniser column. For example, dual temperature control method is achieved by combining the middle and top temperature change to control the state switch of the total reflux and withdrawal during the operation (Peng et al., 2007)..

The steady state and dynamic process can be characterized for product variability prediction. These characteristics are used to generate a linear dynamic tray-to-tray model for a distillation column (Enagandula & Riggs, 2006). In order to derive low-order dynamic models from detailed models of staged processes, compartmental and aggregated modelling is used.

The debutaniser column is an important unit operation in the petroleum refining industries. The debutaniser column used in this study consists of 35 trays valve type with a partial condenser, and with column diameter and the column length of 1.3 m and 23.95 m respectively. The objective of this work is to study the dynamic behavior of the debutaniser column using HYSYS and to study different types of control strategy applications for the debutaniser column. A comparison of process variables for controller setting based on PID has been made. Set point changes and Internal Model Control (IMC) tuning method is also presented in this paper with acceptable result (M Ramli & Hussain, 2009).

2.6.5 Literature review using neural network for distillation column

NN have the ability to learn from their environment and to adapt to it in an interactive manner similar to their biological counterparts. Indeed this is an exciting prospect of the vast possibilities that exist for performing certain functions with ANN can emulate the comparable biological function. Applications of neural network include prediction and forecasting, associative memory, functional approximation, clustering, data compression, speech recognition, nonlinear system modelling, nonlinear control

and solution of differential equation. In this respect, ANN offers a powerful tool to model non-linear processes and be utilized as an efficient soft sensor. ANN has the ability to learn a relationship between the outputs and the inputs for a system. To develop a process using ANN, it requires suitable network architecture and appropriate data training (Singh et al., 2005). The neural network architecture makes use of many hidden layers for the column and the inputs only consider temperature surrounding the column.

To improve product quality in a debutaniser column, soft sensor design has been used by Fortuna and co-workers (Fortuna et al., 2005). The dynamic neural model that has been implemented used three steps predictions to evaluate its top product concentration. The output from the first dynamic network are fed to input of the second dynamic network and the output from the second dynamic network are fed to the third dynamic network to obtain the desired product. The approach uses appropriate lagged values inputs including composition to the neural network. Real time estimation of plant variables and the composition are used for monitoring purposes and the number of neurons in the hidden layer for the neural network is determined by trial and error method.

The LM algorithm for neural network training has been used because it is suitable for binary as well as multi-component mixture (Singh et al., 2007). The LM algorithm is more suitable compared to Steepest Descent Back Propagation (SDBP) algorithm in both cases and give more accurate and sensitive results. The LM approach has worked efficiently in complex chemical plants, having hundreds of parameters. ANN has also been applied in a crude fractionation section (Zilochan & Bawazir, 2001). Back propagation algorithm is used on real time data and the output of the neural network prediction is the naphtha temperature and not the composition prediction.

A nonlinear state space model has been proposed by (Prasad and Wayne Bequette, 2003). Singular value decomposition (SVD) is used to remove redundant nodes and model reduction. The network is trained in order to provide empirical state space model for the system. Partial least square regression (PLSR) together with ANN with back propagation (BP) algorithm also been proposed by Xuefeng,(2010). The neural network architecture consists of an input layer, a single hidden layer and an output layer. The number of neurons in the hidden layer are considered large for ANN. The neural networks were trained to extract the quantitative information from the training samples using BP.

Neural network techniques have been increasingly used for a wide variety of applications where statistical method has been traditionally employed. Neural network is able to give better prediction of important parameters and be applied to a wide range of problems. The paper presents the prediction of composition in debutaniser column using neural network. The main objective of the work is to identify the important variables for debutaniser column using principal component analysis (PCA), projection to latent structure (PLS) analysis and to implement artificial neural network approach for the prediction of product quality on debutaniser column. A comparison between neural network and PLS is also presented for better prediction of the composition for the column. It shows that neural network gives lower Root Mean Square Error (RMSE) value than PLS (Mohd Ramli et al., 2010).

A decision system has been developed for optimizing the energy efficiency of a petrochemical plant (Monedero et al., 2012). The system has been developed after a data mining process of the parameters registered in the past. The designed system carries out an optimization process of the energy efficiency of the plant based on a combined algorithm that uses the energy efficiency of the operation points occurred in the past and, on the other hand, a module of two neural networks to obtain new

interpolated operation points. The work includes a previous discriminant analysis of the variables of the plant in order to select the parameters most important in the plant and to study the behavior of the energy efficiency index. This study also helps to ensure an optimal training of the neural networks.

Debutaniser column is an important unit operation in petroleum refining industries. The design of online composition prediction by using neural network will help improve product quality monitoring in an oil refinery industry by predicting the top and bottom compositions of n-butane simultaneously and accurately for the column. The single dynamic neural network model can be designed and used to overcome the delay introduced by lab sampling and can be also suitable for monitoring purposes. The objective of this work is to investigate and implement an artificial neural network (ANN) for composition prediction of the top and bottom product of a distillation column simultaneously. The major contribution of the current work is to develop these composition predictions of n-butane by using equation based neural network (NN) models. The composition predictions using this method are compared with partial least square (PLS) and regression analysis (RA) methods to show its superiority over these other conventional methods. Based on statistical analysis, the results indicate that neural network equation, which is more robust in nature, predicts better than the PLS equation and RA equation based methods (Mohamed Ramli et al., 2014).

2.6.6 Literature review using hybrid modeling for chemical processes

Hybrid models are useful for synthesis and design of separation processes because they indicate how a specified separation can be achieved. The same hybrid model is applicable even though different distillation operations may be necessary to achieve the specified separation. Use of the hybrid modelling approach may result in improved

computational efficiency compared to the single model because it can provide better initialization and flexibility in terms of modelling options.

The uses of artificial intelligence on the scaling of pilot plant fluid catalytic cracking are proposed by Bolas (et al., 2003). The work is focused in order to improve the accuracy of the pilot plant by determining the optimum hybrid model. The hybrid model developed is compared with the plant model to a pure neural network model. Simulations for modelling a batch reactor using hybrid neural network rate function (NNRF) are proposed by Chang (et al., 2007). The mechanistic equation for state variable is incorporated into the NNRF model to form hybrid neural network rate function model. The performance of the model is successful in operating the reactor system.

A framework of modeling and simulation of particulate solid based on fundamental associate with neural network have been presented by Cubillos(et al., 1996). The hybrid model consists of dynamic behavior direct flow and batch fluidized dryer using mass and energy balance. The models are evaluated by comparing simulation and experimental data (Guo et al., 1997). The hybrid neural network approach performs better than the neural network prediction. Goal gasification models incorporating a first principle model with neural network parameter estimator have been developed.

The hybrid neural network is trained using experimental data for two coals and the process modeling gives good performance (Horn, 2001). The overall reactivity of the char has been identified using neural network. The model consists of temperature and gasification time. The nonlinear and complex dynamic batch polymerization by neural network is used for training. The input and output linearization are designed to improve performance of the batch polymerization. Data based model dynamic equation using neural network offers reduction in cost.

An algorithm to decompose the hybrid model into subsets of model equation has been solved by Khars & Marquardt,(2008). The algorithm is solved using data reconciliation, nonlinear equation solving, parameter estimation and neural network training. A simultaneous identification approach is used to correct the estimate of the incremental approach. The case study of the identification of a steady state model of an ethylene glycol production process has been used. The first principle models derived from dynamic mass, energy and momentum balance have been developed. Neural network presented by black box model is used when the process is an unknown part of the first principle model (Madar et al., 2005). The identification and application of the hybrid models are presented by using hybrid model consisting of sensitivity algorithm approach. The total frameworks are based on temperature control of continuous stirred tank reactor where neural network have been used to model the heat released for an exothermic chemical reaction.

A multilayer neural network to model the simultaneously mass transfer and chemical reaction in the liquid-liquid reacting system has been proposed by Molga and Cherbanski (1999). The intrinsic reaction kinetics and diffusive mass transfer are obtained by using neural network where the input-output signals are analyzed. The data used for training are taken from the experimental work using reaction calorimeter. The hybrid, first principle neural network model has been defined to describe batch and semi batch stirred tank reactor. The net topology and the range of data used for training the network are based on accuracy and quality knowledge has been studied.

A dynamic bioreactor system model has also been proposed that combine the first principal model and artificial neural network (Oliverira, 2004). The reactor system using a set of mass balance equations and the cell population is represented using mixture of neural network and mechanistic approach. The bounded input and output are

derived from dynamic hybrid model. The equations are derived using analytical calculation of the Jacobian matrix.

A fixed bed reactor has been modelled which includes combining mass and energy balance with artificial neural network (Qi et al., 1999). The reactors are carried out by using benzene oxidation to maleic anhydride as a reaction for performance of the hybrid models. The hybrid model predicts well by having simple structure and easier for real time requirements and online optimization. The deterministic and stochastic modeling has the better understanding for membrane dynamics (Sen et al., 2011). The effect of dial filtration is used to investigate the effects on the membrane. The model is developed by knowledge based hybrid neural network. The network is trained using LM algorithm. A hybrid model combines mechanistic elements with neural network are used as a basic for generalised online estimation technique (Wilson & Zorzetto, 1997). The balance equation is used to model and define the mechanistic element while the neural network is applied to model the nonlinear relationship. The Kalman filter algorithm is modified to accommodate the hybrid model with stochastic process and noise to handle neural network error. The application of this approach is demonstrated in a simulation case study pilot plant scale for three tanks in series. A hybrid neural network for differential catalytic hydrogenation reactor has also been proposed by Zahedi and et al (2005). The hybrid model consists of a mechanistic model and neural model. The mechanistic model consists of heat transfer; mass transfer and pressure drop equations and calculates the effluent temperature of the reactor by having the outlet mole fractions from the output of the neural network model. The model has successfully been tested with the experimental data. The model is able to respond very fast compared to traditional model for carbon dioxide reduction.

A new technique for nonlinear system, which is based on hybrid neural modelling, is proposed. The hybrid model consists of a combination of residual composition and

residual temperature with first principle in the mass and energy balance. For the neural network training, gradient descent with momentum weight and bias learning function are used. The performance function employed is mean square error. The inputs to the neural network are manipulated variable reflux flow rate, manipulated variable re-boiler flow rate, top and bottom temperatures, top and bottom compositions n-butane. Results show that hybrid neural network performs better than the neural network predictions to estimate composition and temperature for the debutaniser column (Mohamed Ramli et al., 2012).

2.6.7 Literature review for control of distillation column

Several alternative column configurations have been developed, in order to control temperature of the column. The internal heat integration concept has been applied on a commercial refinery debutaniser column for the separation of an eight-component hydrocarbon mixture (Jana, 2010). The thermodynamic feasibility of this process has been identified. An economically interesting partially heat integrated debutaniser column (HIDBC) configuration is explored. A sensitivity test has been conducted to select the compression ratio required to meet the product specification. This study deals with the parametric analysis to investigate the effect of important parameters on product purity and energy consumption. An economic comparison between the conventional debutaniser and the proposed thermally coupled debutaniser scheme is also performed. It proposes a control algorithm that considers the control of the most sensitive tray temperatures. The singular-value decomposition (SVD) method is used for selecting the sensitive trays.

The binary distillation columns are controlled by using a nonlinear aggregated model with the objective of deriving computationally efficient models for real-time control and optimization applications. The resulting DAE models are converted into ODE models,

which are the key step to increase the simulation speed (Linhart & Skogestad, 2009). The performances of several full and reduced distillation models, with and without base-layer controllers, are compared using different numerical integrators. It is concluded that the reduced ODE models are able to decrease the simulation time (Linhart & Skogestad, 2009).

Adaptive feedback linearization controller for high purity binary distillation column having uncertain parameters and input saturation has been designed by Biswas et al.(2009). The controller is used to control the top and bottom compositions of a binary distillation column. Both structured and unstructured uncertainty is present. An adaptive control strategy is used for estimating uncertain parameters in the process model. Process input saturation could lead to nonlinearity to the process and become uncontrollable. A cascade reduced order nonlinear adaptive controller is designed and implemented for the column.

Performance comparison of evolutionary algorithms (EAs) such as real coded genetic algorithm (RGA), modified particle swarm optimization (MPSO), covariance matrix adapted evolutionary strategy (CMAES) and differential evolution (DE) on optimal design of multivariable PID controller design have been proposed (Iruthayarajan & Baskar,2009). Decoupled multivariable PI and PID controller structure for binary distillation column plant having 2 inputs and 2 outputs are considered. EAs simulations are carried with minimization of Integral Absolute Error (IAE) using two types of stopping criteria, which are the maximum number of functional evaluations and tolerance of PID parameters using IAE. The performances for the column are compared using various EAs, statistical measures like mean, standard deviation and computation time are considered.

An analytical design for a proportional-integral derivative (PID) controller cascaded with a first order lead/lag filter is used for first order unstable processes with time delay

(Shamsuzzoha & Lee,2008). The internal model control (IMC) criterion, the design algorithm which has a single tuning parameter is used to adjust the performance and robustness of the controller. In order to diminish the overshoot in the servo response, a setpoint filter is used. In the simulation, the controllers are tuned to maintain the same degree of robustness by measuring the maximum sensitivity. The robustness of the controller is investigated by applying a perturbation uncertainty in all parameters simultaneously to obtain the worst case model mismatch, and the proposed method shows more robustness against process parameter uncertainty.

A control scheme is derived for an ideal heat integrated distillation column in which a temperature difference between two stages is designated as the controlled variable to overcome the side-effect of continuous pressure variations in the rectifying section (Huang et al., 2007). The proposed temperature control scheme can remain a stable operation around the nominal steady state with improved dynamic performance and tolerable steady state discrepancies in comparison with the direct composition control scheme. Temperature control scheme is found to be robust to the selection of temperature measurements. Multivariable generic model control (MGMC) structure has been proposed by Karacan and co-workers to control of the packed distillation column (Karacan et al., 2007). Top and bottom product temperatures of the packed distillation column are selected as the controlled variables and reflux ratio and re-boiler heat duty as manipulated variables, respectively. Feed mole fraction and feed temperature are selected as disturbances variables. Two types of black box models, which are linear and non-linear model are used for generic model control for the control of packed distillation. Non-linear model for MGMC has better performance over linear model.

A nonlinear adaptive control strategy is proposed by Murlidhar & Jana,(2007) for a multicomponent batch distillation column. The hybrid control scheme consists of a generic model controller (GMC) and a nonlinear adaptive state estimator (ASE). An

adaptive observer is designed to estimate the partially known parameters based on the measured compositions in the presence of process and predictor mismatch. The open-loop dynamic behavior of the developed ASE estimator is investigated under initialization error, disturbance, and uncertain parameters. A simulation-based comparative study has been conducted between the derived nonlinear GMC–ASE control algorithm and a gain-scheduled proportional integral (GSPI) law in terms of constant composition control. The adaptive control scheme is shown to perform better as it is due to the exponential error convergence capability of the ASE estimator in addition to the performance of the GMC controller.

The performance of input–output linearizing (IOL) controllers is affected because of the constraints on input and output variables (Biswas et al., 2007). This problem could be addressed by augmenting IOL controllers with quadratic dynamic matrix controller (QDMC). However, this can lead to a constraint-mapping problem for coupled MIMO systems distillation column. A multi-objective optimization problem needs to be solved to map the constraints on inputs. A suitable transformation technique is proposed to convert multi-objective optimization to a single one. The controller is less computationally intensive and easy to apply. The controller (IOL-QDMC) with nonlinear observer is implemented on a binary distillation column for dual composition control. The performance is evaluated using a quadratic dynamic matrix controller (QDMC) and input–output linearization with PI controller (IOL-PI).

An application of linear controller design with convex optimization to a binary distillation column by its limits of performance is proposed by Khaisongkram & Banjerdpongchai,(2006). Disturbances of distillation process are determined as input signals with bounded magnitudes and rates of change. Performance measures of top and bottom control loops are defined as the maximum deviation magnitudes of top and bottom compositions, respectively. The convex optimization and the ellipsoid algorithm

are applied to design linear controllers and determine the best optimum performance of the closed-loop system. A series of convex optimization problems are efficiently solved to give a trade-off curve representing limits of performance between the top and bottom compositions. The trade-off curve provides a practical design specification that cannot be achieved for the distillation column control with dynamic controller configuration. To confirm this, a computer simulation using nonlinear dynamical model of the distillation column is used. Closed-loop responses of optimal linear controller are consistent with the trade-off curve and yields better performance than a conventional decentralized PI controller.

The design of a model-based globally linearizing control (GLC) structure for a distillation process within the differential geometric framework has been proposed by Jana et al, (2005). The model of a non-ideal binary distillation column, where the characteristics are nonlinear in nature and interactive, is used as a real process. The classical GLC law consists of a transformer input-output linearizing state feedback, a nonlinear state observer, and an external PI controller. The tray temperature based short-cut observer has been used as a state estimator within the control structure, in which all tray temperatures were considered to be measured.

A single input single output (SISO) controller was used for a distillation column (Chawankul et al, 2005). A First Order Plus Dead Time (FOPDT) model is to represent the process model where the dynamic parameters are estimated as functions of process design variables. A robust internal model control (IMC) controller is designed based on a nominal linear model assuming model error to account for process nonlinearity. The optimum column design and the closed loop time constant which result in the lowest objective function cost are determined. Nonlinear long range predictive control was applied to a pilot packed distillation column (Karacan, 2003). The use of polynomial nonlinear autoregressive integrated moving average with external input (NARIMAX)

model related with top product temperature and reflux ratio for nonlinear control is emphasized. A dynamic model is based on first chemical engineering principles formulated for a packed distillation column. The actual column response to step changes in the feed mole fraction and temperature agree well with the dynamic model predictions. Recursive Gauss_ Newton prediction error algorithm is used to determine NARIMAX model parameters. This algorithm can be used efficiently for this model and a transfer function model relating the manipulated variable (reflux ratio) to the controlled variable (top product temperature) is obtained. The role of data prefiltering prior to model parameter estimation is examined to overcome the parameter bias problem caused by disturbances. Non-linear long range predictive control algorithm is successfully applied in controlling the packed distillation column.

A nonlinear profile position observer using tray temperature instead of tray compositions is proposed by Shin et al.,(2000). Composition measurement has been one of the major difficulties associated with the composition control of distillation columns because the on-line analyzers still suffer from large measurement delays, high investment/maintenance costs and low reliability. One of the common alternatives to the analyzers is to use the secondary measurement such as tray temperatures which is able to infer the tray compositions. The advanced control of a side-stream distillation column removing benzene from a reformed gasoline stream has also been proposed by Bettoni et al.,(2000). A multivariable control strategy based on two SISO schemes, each controlling the benzene concentration in an outlet stream has been developed. Each SISO loop using a cascade type and consists of a secondary loop devoted to control tray temperature and a primary inferential controller of the benzene composition based on a short-cut physical model. The decoupling between the two single loops is obtained by keeping the internal reflux between the side-stream tray and the bottom tray constant.

A linearizing feedback adaptive control structure which leads to a high quality regulation of the output error in the presence of uncertainties and external disturbances has been developed by Gonzalez and et al for distillation column (Gonzale et al., 1999). The controller consists of three elements: a nominal input-output linearizing compensator, a state observer and an uncertainty estimator, which provides the adaptive part of the control structure. The feedback controller, based on the disturbance observer, compensates for external disturbances and plant uncertainties. A preliminary study of the robustness analysis of pilot-scale distillation column has been developed by Nooraii et al., (1997). Using a combination of plant data and non-linear simulations, both a nominal column model and an associated model uncertainty are identified. This important information is used to carry out a complete analysis of robust stability and performance for the case where a Ziegler-Nichols tuned for a multiloop control scheme is employed. To perform robustness analysis of the control, both structured and highly structured uncertainty characterization approaches are used.

The desired behavior of the control system for both set-point changes and disturbances in the feed flow rate and the feed composition can be specified for a distillation column (Haggbloom, 1996). Both types of specifications can be handled because the disturbances can be inferred from the behavior of the inventory control system. The control system is realized as a combined internal model and inferential control (CIMIC) system. A disturbance rejecting and decoupling (DRD) control structure is obtained. The performance of the control system is demonstrated experimentally on a pilot-scale distillation column. An online identification technique where a process is identified in terms of pseudo impulse response coefficients and subsequently used to update convolution type models to accommodate process-model mismatch (Maiti & Saraf, 1995). Dynamic matrix control has been applied adaptively to control the top product composition of a distillation column for both servo and

regulatory problems. The algorithm automatically detects a large step-like disturbance requiring fresh identification of the process and subsequently adapts the controller to the new model. Simulation studies using an analytical dynamic full order model of a distillation column demonstrated the usefulness of the adaptation scheme.

Elementary nonlinear decoupling (END) is a model based control algorithm intended to decouple and linearize a nonlinear multivariable process in order to achieve better control than can be obtained by conventional decentralized linear feedback control (Balchen & Sandrib, 1995). The application of END to the composition control of a theoretical binary distillation column illustrates that the quality achievable is very high. The control of both product purities of a binary distillation column has been proposed by Trotta & Barolo,(1995). Reflux and boilup flow rates are the manipulated variables, and the corresponding control laws are derived within the Globally Linearizing Control framework. Reduced order models of the column are developed that allow the controller synthesis to be carried out easily. Simulation results indicate that the proposed control strategy performs better than the conventional PI control strategy.

Using a high-purity distillation column, model identification and control issues are addressed by Srinivas et al (1995). The structure of the identified models is that of the polynomial type nonlinear autoregressive models with exogenous inputs (NARX). It is concentrated on linear models (one-time scale and two-time scale models), and is aimed at identifying the inherent nonlinearities. Comparisons are drawn between the identified models based on statistical criteria (AIC) and other validation tests. Simulation results are provided to demonstrate the closed-loop performance of the nonlinear ARX models in the control of the distillation.

In practice, most practical systems considered are nonlinear and multivariable in character. It is of certainty that the control theory for nonlinear multivariable systems will find immediate and wide applications. For multivariable nonlinear systems, the

control problem is very complicated which is due to the couplings among various inputs and outputs. It becomes in general very difficult to deal with when there exist uncertain parameters and unknown nonlinear functions in the input coupling matrix. It is due to these difficulties, it is noticed that in comparison with the feedback control design for SISO (single input single output) nonlinear systems in the control literature, there are relatively fewer results available for the broader class of multivariable nonlinear systems.

A robust stability analysis for a harmonic balance for multivariable non-linear plant has been applied to a neural network controller under generic Lur'e configuration (Fernandez et al., 2010). The neural network controller will be used to describe sinusoidal input while the linearized model has been derived to represent the nonlinear plant dynamics. The proposed work are applied to a multivariable binary distillation column under feedback neurocontrol which illustrate the use of robustness approach to predict the absence of limit cycles subject to restriction of describing function. The use of adaptive neural network for composition prediction starting from secondary variable measurements which are used to control both the composition and inventory for a continuous ethanol water nonlinear pilot plant distillation column has been proposed by Fernandez et al, (2012). A principal component analysis based algorithm has been applied to select the input vector for the soft sensor. The proposed control scheme offers high speed of response change as it is due to set point changes and stationary error for composition and inventory control.

A multiple input and multiple output has been presented under partial least square framework for a multi-loop nonlinear model control strategy for a distillation column (Hu et al., 2012). The proposed work has been developed using an ARX-neural network cascaded structure incorporated into PLS inner model. An optimization is provided to identify the set parameter of the ARX-NN PLS in order to minimize the plant model

mismatch. The approach has been used to demonstrate the control effectiveness because of the tracking and disturbance rejection. Neural network has been applied to handle with nonlinear dynamics of the hydrolyzer (Lim et al., 2010). A mathematical model has been used to simulate the dynamic response of the temperatures when the controller is applied into the system. The two control strategies are implemented which are the direct inverse control and internal model controller. The control strategies are evaluated which are due to setpoint tracking and disturbances. IMC is found to perform better for temperature control during setpoint and disturbance tests. It offers better response as it is much stable than conventional controllers and perform better than DIC controller.

The optimal temperature is used to study the temperature profile as setpoint in the control study. A neural network model based on extended Kalman observer is used to estimate the state of the nonlinear process as not all states are accessible (Deng et al., 2009). The neural internal model control can be used for open loop unstable process with its closed loop stability which is derived analytically. The application of the work shows the effectiveness for suppressing nonlinear coupling and disturbances and the feasibility for the control nonlinear discrete time state space processes.

Neural networks for gain prediction within nonlinear, multivariable and constraint has been developed by Dutta & Rhinerhart., (1999). This strategy is implemented on a lab-scale, non ideal, and methanol-water distillation column for servo, regulatory and constrained control. Experimental results also demonstrate a Generic Model Controller using a neural network as the steady-state model inverse that is developed earlier. A study has been conducted for these two neural network model-based controllers with other advanced controllers which are nonlinear process-model based control; model predictive control using dynamic matrix control and an advanced classical control. A control system using a neural net is applied for product composition control of a

distillation plant (Stenanovic, 1996). The neural network controller design is based on the process inverse dynamic modeling. Once the inverse dynamic model is available then it can be used for control. The back propagation algorithm of the Generalized Delta Rule is used to train the network minimizing the sum of squares of the residual. The algorithm is applied to dynamic nonlinear relationship between product composition and reflux flow rate

Neural network models are used for steady state inverse of a process which is then coupled with a simple reference system synthesis to generate a multivariable controller (Ramchandran & Rhinehart, 1995) The control strategy is applied to dynamic simulations of two methanol-water distillation columns that express distinctly different behavior from each other (one simulates a lab column, while the second simulates an industrial-scale high-purity column). A steady-state process simulation package is used to generate all the neural network training data. An efficient training algorithm based on a nonlinear least-squares technique is used to train the networks. The neural network model based controllers show better performance for both set-points and disturbances, and performed better than conventional feedback proportional-integral (PI) controllers. Neural network gives better performance than the conventional control loop and inferential control by developing a model based on neural control for single composition (Baratti & Corti, 1997). The strategy is used to compensate the upsets in the operating pressure, feed flow rate, and feed composition. To keep the content of the key component in the distillate stream, the performance of the neural network has to be precise.

In this study, column information is obtained from the actual industry. There is a huge amount of data set collected from the oil refinery industry over a period of 4 years. Hence an adequate multivariate characterization is necessary as a first step for the data

to be analyzed and expressed in a comprehensible way as will be shown in the next chapter. Literature review has been conducted to screen the methodology for the research and to highlight the novelties and the contributions for this work.

CHAPTER 3: PLANT DESCRIPTION AND CASE STUDY OF THE DEBUTANISER COLUMN

3.1 Introduction

A debutaniser column in PPTSB is a distillation column that produces Liquefied Petroleum Gas (LPG) as the main product. The quality of the LPG is the main concern by PPTSB, one of the national oil refineries. However, the PPTSB's debutaniser column is a challenging process as it deals with non-linearity, is highly multivariable process, and involves a great deal of interaction between the variables. It has lags in many of the control system, all of which makes it a difficult system to be modeled by linear techniques. To control the quality will also be as challenging since the process will be affecting the quality.

3.2 Plant description

The crude oil processing plant as seen in Figure 3.1 consists of a refinery process, condensate fractionation and reforming aromatics section. The feedstocks of the refinery process are mainly crude oil while the products are petroleum products, liquefied petroleum gas, naphtha and low sulphur waxy residue. The refinery has two main process units, which are Catalytic Reforming Unit (CRU) and Crude Distillation Unit (CDU). The Crude Oil Terminal provides the feedstock and the crude oil is preheated using heat exchangers within the range of 190°C – 210°C. It is then further heated in a furnace to 340°C – 342°C before being routed to the CDU. The crude oil is separated into a number of fractions, which are heavy Straight Run Naphtha as overhead vapor, untreated kerosene, straight run kerosene and straight run diesel. From the crude tower, there are 3 sides cut streams, which are drawn to a stripper column and the stripper consists of a kerosene stripper, naphtha stripper and diesel stripper.

From the CDU, the pretreated feed Heavy Straight Run Naphtha (HSRN) is mixed with hydrogen from the reformer and is heated up to the reaction temperature using a heater and fed into the pretreated catalytic reactor. The reactions involved are denitrification and desulphurization, which will protect the reformer catalyst from poisoning. The product from the reactor is transferred to the pretreated stripper while the feed to the reforming unit is the bottom product of the stripper and the feed to the reformers reactors is the treated naphtha, which is heated to the reaction temperature. Effluent from the reactor is collected in a reformer separator where it is cooled. Some portion of the gas, which is separated is recycled to the reactor feed stream while the other is transferred to an absorber. In the absorber, at the raw naphtha feed, hydrogen gas is purged and recycled to the pretreated heater. The feed into the LPG absorber is liquid phase where it is drawn off and the liquid fraction is pumped into a stabilizer. Before being sent to storage, reformat is withdrawn from the stabilizer bottom for cooling. From the stabilizer reflux drum, overhead vapor from the stabilizer are cooled, condensed and recovered. The raw LPG of the refinery LPG recovery unit consists of fraction of the liquid stabilizer.

Debutaniser column is the main column for producing the main product, which is the liquefied petroleum gas. The column is also important as feedstock is transformed to petroleum products, naphtha and low sulphur wax residue. The debutaniser column is located at the CDU section depicted top left in Figure 3.1. The unit is used to recover light gases and LPG from the overhead distillate before producing light naphtha. The light gases mainly C₂ are used to refine fuel gas and mixed with LPG. The feed to the debutaniser column which has 35 valve trays is from the Deethanizer bottom product. The debutaniser condenser condenses the overhead vapor and the debutaniser overhead pressure control valves with two split ranges controls the overhead system. The reflux from the top of the debutaniser consists of the collected condensed hydrocarbon while

re-boiler section is used to strip lighter hydrocarbon. There are four manipulated variables for the column which are the feed flow rate, reflux flow rate, bottom product flow rate and re-boiler flow rate. The feed flow rate controls the feed to the column, the debutaniser re-boiler control valve controls the re-boiler temperature while the debutaniser bottom flow rate controller controls the bottom product level. The debutaniser reflux control valve controls the top temperature of the column. Table 3.1 outlines the column specification while Table 3.2 describes in detail all the variables surrounding the column. The measured variables are the Feed flow, Pressure 1 (Debutaniser receiver overhead pressure), Flow 2 (LPG flow to storage), Flow 1 (Light Naphtha flow to storage), Level 2 (Debutaniser condenser level), Level 1 (Debutaniser level) and Temp 5 (Re-boiler outlet temperature to column). The top and bottom compositions of the column are currently measured using laboratory sampling by gas chromatography. Figure 3.2 shows the column configuration for the debutaniser column. Based on Figure 3.2, the variables used for control are the top and bottom temperatures for the column. So therefore there are no cascade loops.

Table 3.1: Debutaniser column specification

No	Parameter	Value
1	Number of tray of the column	35
2	Feed tray - stage number	23
3	Type of tray used	Valve
4	Column diameter	1.3 meter
5	Column height	23.95 meter
6	Condenser type	Partial
7	Feed mass flow rate	44106 kg hr^{-1}
8	Feed temperature	113 $^{\circ}\text{C}$
9	Feed pressure	823.8 kPa
10	Overhead vapor mass flow rate	11286 kg hr^{-1}
11	Liquid mass flow rate	32820 kg hr^{-1}
12	Condenser pressure	823.8 kPa
13	Re-boiler pressure	853.2 kPa

Table 3.2: Tag name description of the column

No	Tag	Description	Units
1	Temp 1	Debutaniser top temperature	°C
2	Temp 2	Debutaniser bottom temperature	°C
3	Temp 3	Debutaniser receiver bottom temperature	°C
4	Temp 4	Light Naphtha temperature after condenser E 3	°C
5	Temp 5	Re-boiler outlet temperature to column	°C
6	Temp 6	Debutaniser feed temperature	°C
7	Flow 1	Light Naphtha flow to storage	m ³ /hr
8	Flow 2	LPG flow to storage	m ³ /hr
9	Pressure 1	Debutaniser receiver overhead pressure	kPa

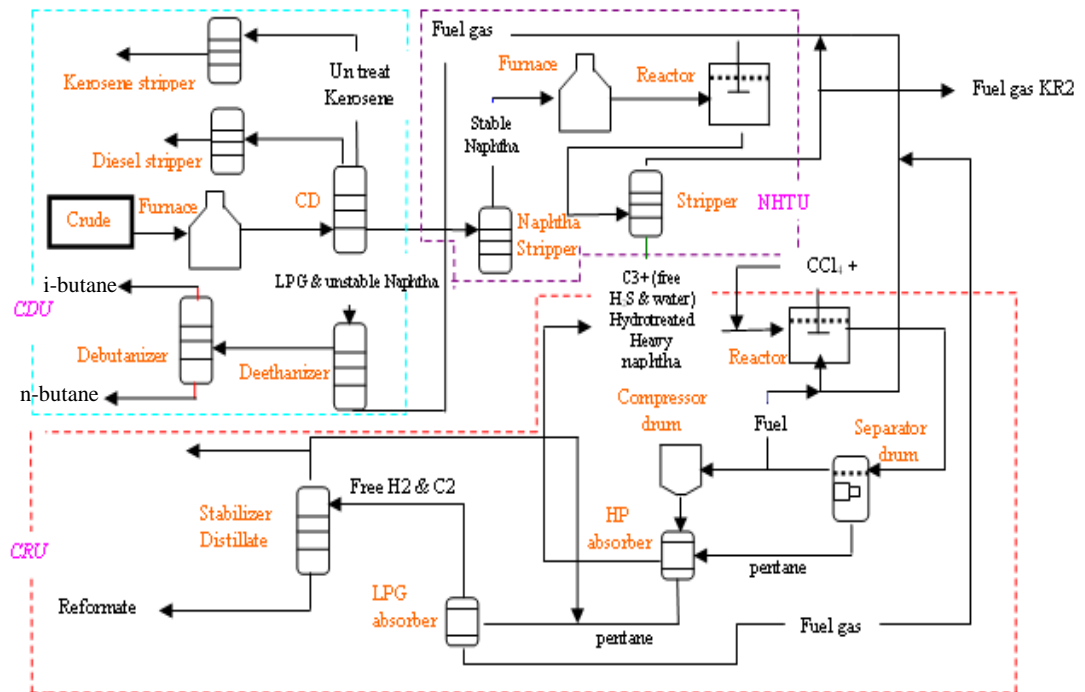


Figure 3.1: Flow chart for the refinery process

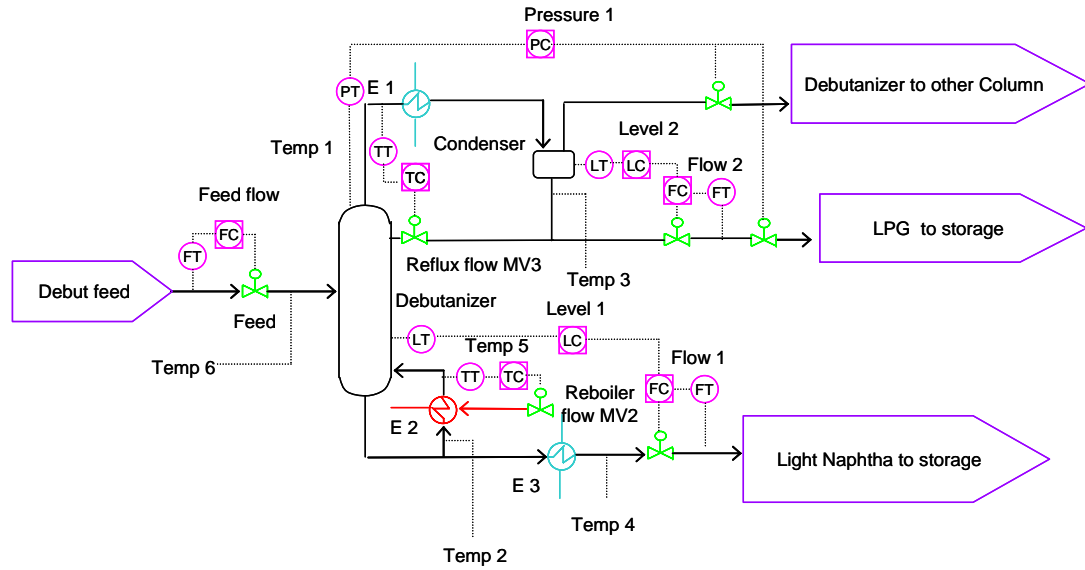


Figure 3.2: Debutaniser column configuration

3.3 Data generation: open loop, closed loop, extract from close loop

High purity of composition in a distillation column requires a large number of stages which are to be monitored for correct operation of the column. By nature, the process industries are dynamic and process plants rarely run at a steady state condition. For the debutaniser column, proper control techniques are selected and implementing them is very important. This is because the controller will affect the product quality, production rate, and energy usage (Gupta et al, 2009). Control of the debutaniser column is very challenging as it is due to the inherent nonlinearity, composition control and the effect as a result of disturbances.

The process model characterizes the dominant features of the process dynamics. The real process may differ from the process model which is characterized as parametric mismatch and structure mismatch. The term parametric mismatch is where the structure of the process model is the same as the true process, but with different parameters. Secondly, the term structure mismatch, where the structure of the process model differs from the true process (Karacan et al., 2007). A dynamic simulation for debutaniser

column is performed using a plant process simulator, HYSYS. The controller settings based on actual and simulation are analyzed. It will be used to check the overall performance of the column as well as to improve the quality of the product and maximize profitability.

There are three sets of important data that are used. There are open loop data which is obtained from industry based on the step test of overhead pressure, reboiler and reflux flow rates. The second set of data is the closed loop data obtained from industries which are used to extract from closed loop to open loop. The third set of data is the simulated data obtained in HYSYS and it is validated with the closed loop data in order to check the accuracy. These data are used for data generation. The data need to be screened because the available are available are large.

Data generation is an important step to identify the responses of all the variables surrounding the column to obtain the neural network model. Some of the variables in the open loop conditions surrounding the column in the real plant are not available. Conventionally most online open loop responses from the plant surrounding the column such as reboiler flow rate, reflux flow rate, overhead pressure flow rate, feed temperature, top temperature and bottoms temperature can be retrieved. Hence plant process simulators are used to obtain the unavailable open loop data sets from the plant and therefore dynamic simulation using ASPEN of the debutaniser column has been performed to obtain Temp 5, Pressure 1 and top and bottom composition of the column, variables that are not available online. The Process Flow Diagram (PFD) and Piping and Instrumentation diagram (P&ID) are used as a guide to perform the simulation where the information on each flow and heat stream involved in the simulation is used in the worksheet.

The type of data that is available from the real plant consists of open loop, closed loop and extract from close loop. The overhead pressure flow rate, reflux flow rate and

reboiler flow rate are measured. The numbers of data used are 301. The control cycle is measured in 1 minute interval with similar interval for the process data.

3.4 Steady state and dynamic state

HYSYS is used to design a steady-state modeling for the debutaniser column before the transition of the steady-state to the dynamic state. Within HYSYS, steady state simulations can be cast easily into dynamic simulations by specifying additional engineering details, including pressure/flow relationships and equipment dimensions. The dynamic mode is selected and converted once the steady state model has been developed. The HYSYS consists of simulation platform. The basic platform is used to select the chemical components that are involved in the simulation, as well as the thermodynamic property suitable for the components.

The simulation environment consists of the worksheet and PFD. The worksheet contains the information on every flow and heat stream involved in the simulation. Some of these streams require input in HYSYS, which are dependent on the degree of freedom that will be able to calculate the output streams. The necessary information such as feed conditions, feed compositions, reflux ratio, condenser pressure, reboiler pressure and etc. have to be provided for the chosen unit operation in order to be able to design the unit automatically.

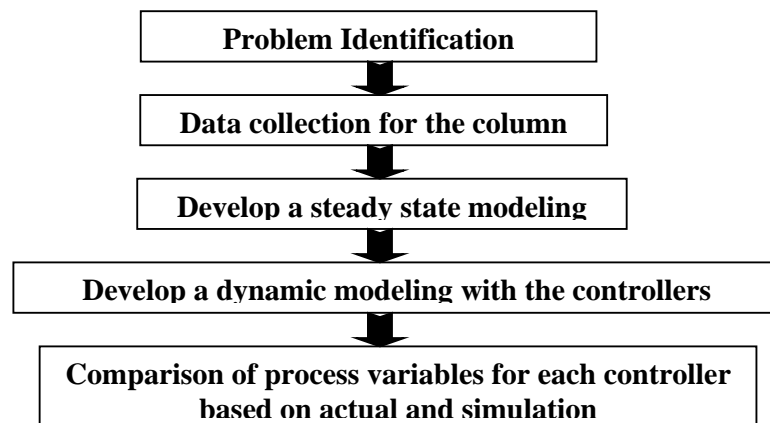


Figure 3.2a Simulation flow chart

Compositions in the feed in mass fraction including components in the feed are given in Table 3.3.

Table 3.3: Composition at the feed

Composition	Mole Fraction
Propane	0.120
i-Butane	0.167
n-Butane	0.215
i-Pentane	0.086
n-Pentane	0.115
Heavy residue	0.296

Table 3.4: Properties of the compounds (Yaws, 1999)

Component	Boiling Temp at STP ($^{\circ}\text{C}$)	Critical P (kPa)	Critical T ($^{\circ}\text{C}$)	Critical Volume (m^3/kgmol)	Molecular Weight	Viscosity 50°C (cSt)	TVP (kPa)
Propane	-42	4249	96.8	0.202	44.09	0.73	1000
i-Butane	-12	3648	135.1	0.262	58.12	1.38	373
n-Butane	-0.35	3797	152.1	0.254	58.12	1.32	258
i-Pentane	28	3381	187.4	0.305	72.15	2.98	98
n-Pentane	36	3369	196.6	0.312	72.15	2.07	73.3

Comparison between the close loop responses in simulation to the actual plant performance from the laboratory sample is conducted to evaluate the deviation between the simulated and actual compositions. This step is taken in order to ensure that the simulation data generated to predict the data not available online closely resemble the actual online industrial data. Furthermore the top and bottom compositions of n-butane including top and bottom temperatures in terms of close loop online data are available for the column. These close loop compositions are obtained from the laboratory sample (gas chromatographs) while the temperatures are obtained from plant data. The time interval to obtain the compositions data 1 minute sampling. These closed loop data are also used to generate further open loop data in addition to the existing open loop data in order to extract more data for use with the model identification step using neural networks. To extract the data in closed loop is when the error of the process variable is

determined, and then the output change of the manipulated variable is calculated. After this the output of the process variable is obtained using the values of the controller setting and hence the data can be extracted to obtain the open loop. Table 3.5 shows the set point and controller settings for Flow 1 and Temp 5. It also shows the PID values and set point for the variables under control (closed loop response) for the debutaniser column. The number of data used is 301.

Table 3.5: Controller setting and set point

Controlled Variable	Manipulated Variable	K_c	T_i	T_d	Set point	Action
Temp 5	Reboiler flow rate	0.4	80	20	135.7 °C	Reverse
Flow 1	Light naptha flow rate	0.5	30	0	24.64 m ³ /hr	Reverse
Flow 2	LPG flow rate	0.5	12	0	7.55 m ³ /hr	Reverse
Level 1		1	660	0	60%	Reverse
Level 2		0.4	550	0	65%	Reverse
Pressure 1	Split range control	2	42	0	784.42 kPa	Reverse
Temp 1	Reflux flow	0.285	50	0	24 m ³ /hr	Direct
Feed flow	Feed flow rate	0.357	25	0	35.9 m ³ /hr	Reverse

Based on the controller setting outline in Table 3.5, the error for each of the process variable can be obtained and incorporated in equation 3.3 to determine the controller output which is the ΔMV . The PID equation is used to determine the controller output (manipulated variable) derived from reference (Seborg et al., 2003) as given below;

$$\Delta MV = K_c \left[e(t) + \frac{1}{\tau_i} \int_0^t e(t) + \tau_D \frac{de(t)}{dt} \right] \quad (3.3)$$

The tuning parameter is used to determine the process gain, K_p (Dwyer, 2003) as shown below;

$$K_p = 3K_c \quad (3.4)$$

By using Equation 3.4, then the output of the process variable can be obtained.

Equations 3.3 and 3.4 are used to extract the close loop data to determine the process variable Temp 5 and manipulated variable of the reboiler and reflux respectively which are MV2 and MV3. The manipulated variable reboiler flow rate can be obtained from Temp 5 which is applied to regulate the particular process variable. Equation 3.4 has been used to determine the process gain from the controller gain, K_c . Process variable for Flow 1, reflux flow and Temp 5 can be determined when the process gain, K_p and the change of the manipulated variable, ΔMV are calculated. Figure 3.2b shows the procedure to extract the close loop data. There are three types of data which comprises actual open loop, data extracted from the close loop and the simulation data.

The purpose to perform the extract from close loop is to obtain the open loop data under close and to compare it with the actual open loop data. The detail procedure to extract close loop are outlined below:

1. First is to determine the error for the particular controller. The equation used is $e = r - y$. r is the set point for specific controller and y is the process variable close loop
2. Determine the values for controller gain K_c , integral T_i and derivative T_d outlined in Table 3.5.
3. Calculate the controller output change of the manipulated variable, ΔMV based on equation 3.3
4. Determine the process gain K_p based on equation.3.4
5. Calculate the change of the process variable, ΔPV and then add with the average process variable
6. Obtain the open loop data from closed loop.

To obtain the change of the ΔMV from DCS is difficult as the operation in the industry is under close loop response. So therefore it is crucial to calculate the ΔMV using PID equation and from there the process variable can be obtained.

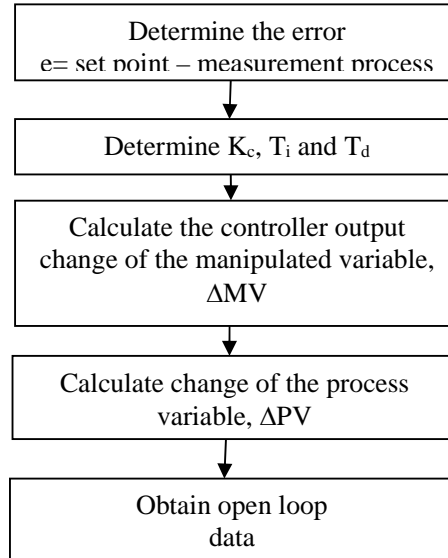


Figure 3.2b Flow chart to extract close loop to obtain open loop data

3.5 Open loop response

There are 3 step tests that are performed for the column which are the step test for the overhead pressure, reflux flow rate and reboiler flow rate. The flow rate is the manipulated variables. To generate the input-output data for the neural network training, various step changes are applied to the inputs to obtain the corresponding outputs. The inputs for the system in this case is the overhead pressure flow rate, reboiler flow rate and reflux flow rate. To obtain the fluctuation of the process the variables surrounding the column by generating step test. The step test is by 5 hour run because it based on actual plant normal operation under open loop response.

3.5.1 Step test for overhead pressure

Figures 3.3 to 3.15 show all the step tests of the overhead pressure. The overhead pressure flow rate is the LPG flow. In order to generate the input-output data for the neural network training, various step changes are applied to the inputs to obtain the corresponding outputs in which the inputs for this system is the overhead pressure flow rate. The step tests of the overhead pressure flow rate which is the manipulated variable are generated by using multi amplitude rectangular pulse. The step test is important to observe the effect and the fluctuations of the process variable when performing changes to the overhead pressure flow rate. However for Temp (see Figure 3.3-3.8) and Pressure 1 (see Figure 3.9), fluctuations are observed and its trend is similar to the step test as performed previously. The number of data used is 301.

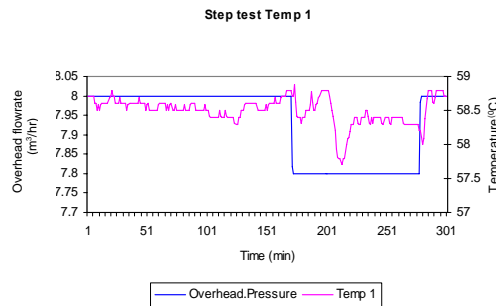


Figure 3.3 top temperature

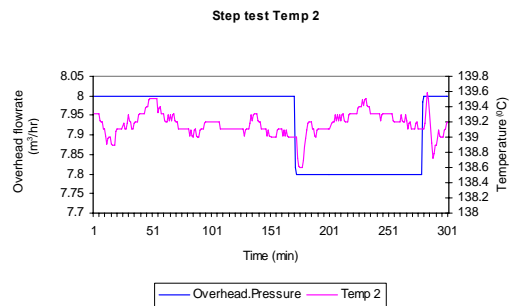


Figure 3.4 bottom temperature

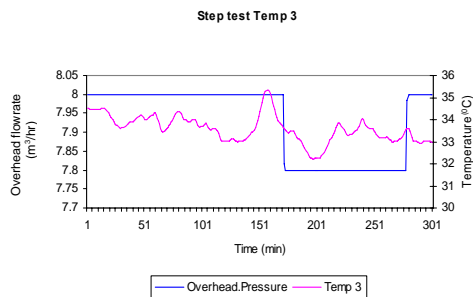


Figure 3.5 receiver bottom temperature

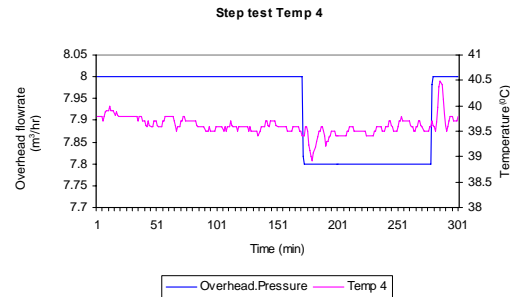


Figure 3.6 light naphtha temperature

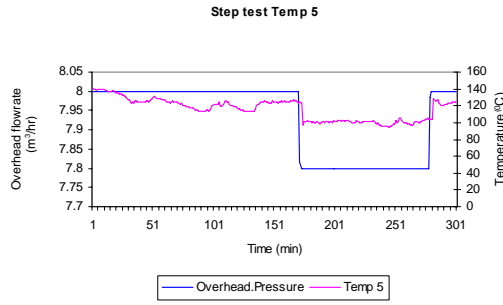


Figure 3.7 reboiler outlet temperature

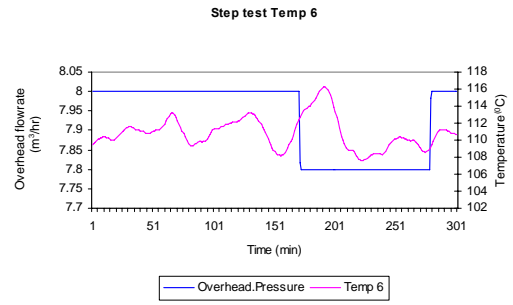


Figure 3.8 feed temperature

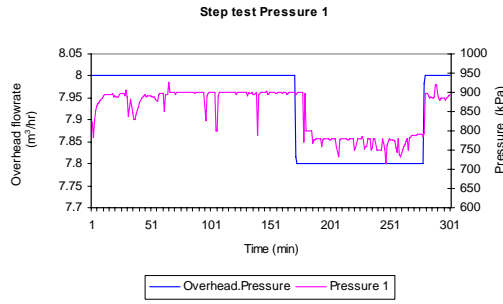


Figure 3.9 receiver overhead pressure

3.5.2 Step test for reflux flow rate

Figures 3.16 to 3.28 show all the step tests of the reflux flow rate data sets. To generate the input-output data for the neural network training, various step changes are applied to the inputs to obtain the corresponding outputs. The inputs for the system in this case are the reflux flow rate. The step test of the reflux flow rate which is the manipulated variable is generated by using multi amplitude rectangular pulse. The step test is important to observe the effect and the fluctuations of the process variable when performing changes to the reflux flow rate. However for Temp (see Figure 3.10-3.15) and Pressure 1 (see Figure 3.16), fluctuations are observed and its trend is similar to the step test was performed previously. The number of data used is 301.

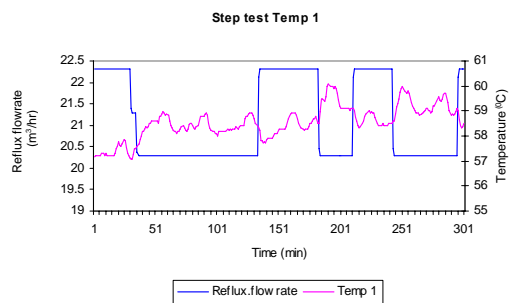


Figure 3.10 top temperature

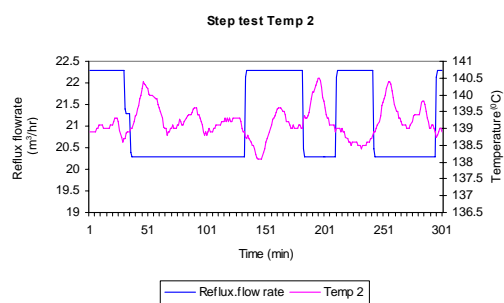


Figure 3.11 bottom temperature

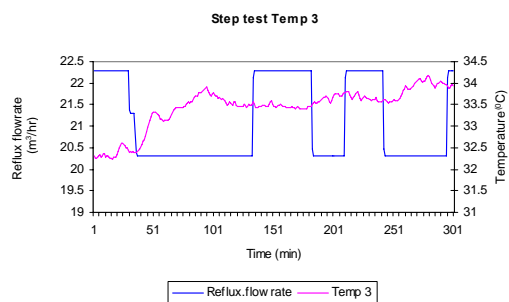


Figure 3.12 receiver bottom temperature

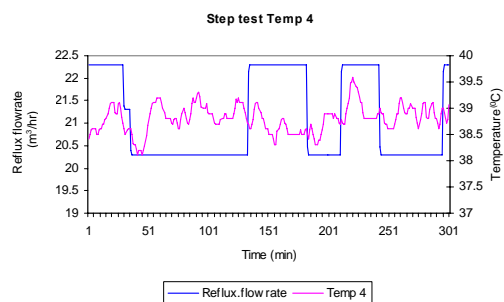


Figure 3.13 light naphtha temperature

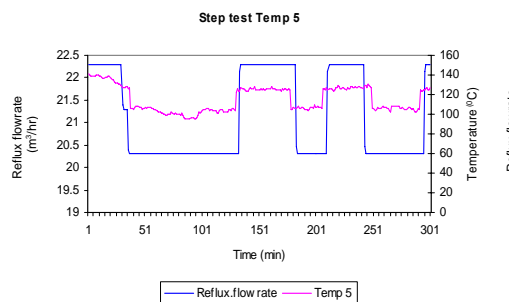


Figure 3.14 reboiler outlet temperature

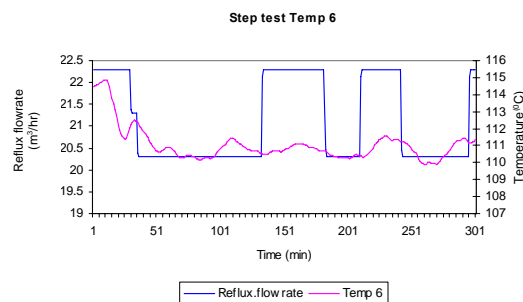


Figure 3.15 feed temperature

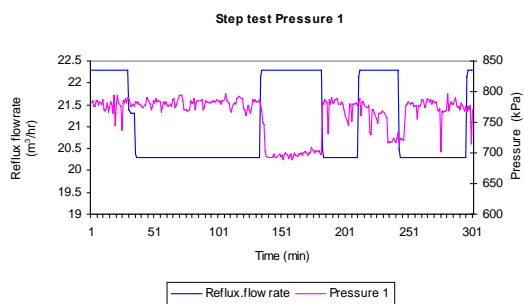


Figure 3.16 receiver overhead pressure

3.5.3 Step test for reboiler flow rate

Figures 3.29 to 3.41 show all the step tests of the reboiler flow rate data sets. In order to generate the input-output data for the neural network training, various step changes are applied to the inputs to obtain the corresponding outputs in which the inputs for this system is the reboiler flow rate. The step test of the reboiler flow rate which is the manipulated variable is generated by using multi amplitude rectangular pulse. The step test is important to observe the effect and the fluctuations of the process variable when performing changes to the reboiler flow rate. However for Temp (see Figure 3.17-3.22), and Pressure 1 (see Figure 3.23), fluctuations are observed and its trend is similar to the step test as performed previously. The number of data used is 541.

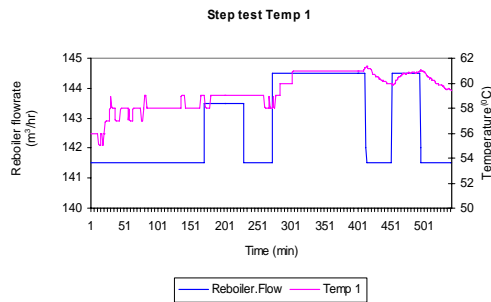


Figure 3.17 top temperature

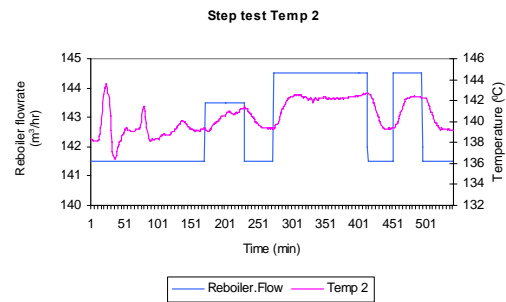


Figure 3.18 bottom temperature

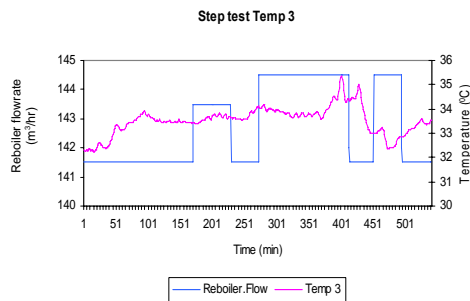


Figure 3.19 receiver bottom temperature

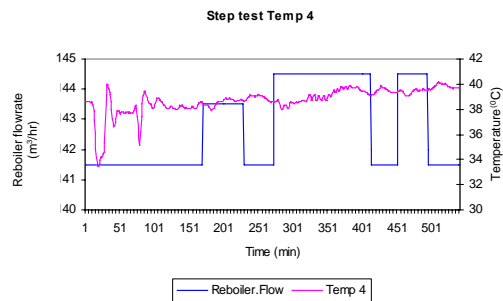


Figure 3.20 light naphtha temperature

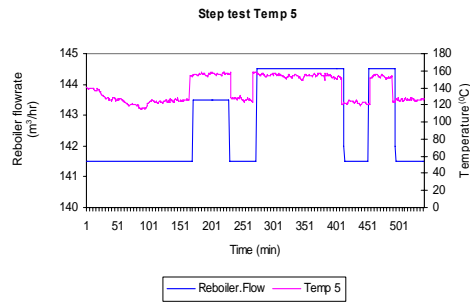


Figure 3.21 reboiler outlet temperature

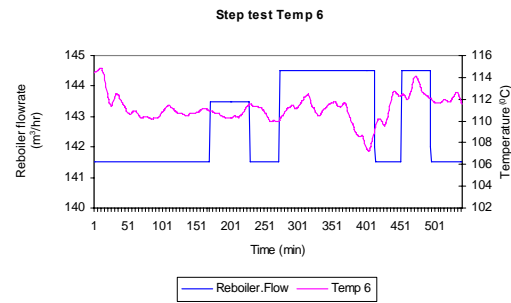


Figure 3.22 feed temperature

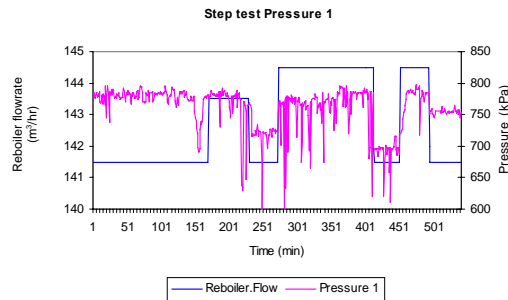


Figure 3.23 receiver overhead pressure

3.5.4 Close loop response

The purpose to perform the close loop is to validate between the simulation and actual plant for variables under control surrounding the column. It indicates that there is a small deviation between the online and simulation data. This implies that the simulation and close loop data agree well with each other including the variables that are not available from the open loop response for the plant. Once the close loop has been verified, then the open loop response for variable that is not available from plant can be obtained. The same step size for the manipulated variable for reboiler and reflux from plant are performed as inputs to obtain the fluctuation of the process variable as outputs in the simulation. Figure 3.24 represents the process variables for outlet temperature controller settings based on simulation, actual plant and different set point values. The response of PV5 is the set point made at 135.3 °C reaches the settling time faster than PID, plant and other set point. PV5 exhibits more stable response with small

oscillation and fluctuates within its set point. Meanwhile, PID shows rapid oscillation and it deviates largely compared to actual plant data which is due to process model mismatch for the column. The temperature profile is affected by the changes of the composition. The deviation of the temperature will effect the fluctuation of the composition. The number of data used is 18000.

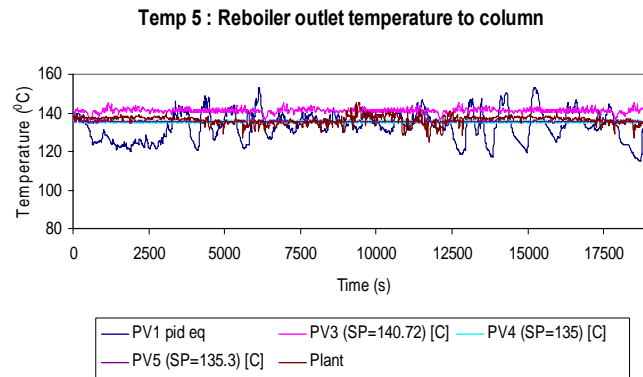


Figure 3.24 Process variables of Temp 5 for controller settings based on PID, plant and different set point

Figure 3.25 represents the process variables for light naphtha flow controller settings based on PID, actual plant and different set point values. The response of PID, PV3 and PV4 is the change of set point made at 19.3 and 20 m³/hr exhibit stable response as the flow rate fluctuates very small. PV4 reaches the settling time faster than PID, plant and other set point. PV4 exhibits more stable response with small oscillation and fluctuates within its set point. Meanwhile, PV2 shows rapid oscillation. The changes of set point have been performed to see the effect of the fluctuation of the level to be controlled and how much is deviated between the actual plant data. By changing the set point of the process is unfavorable for the column although it gives better response; it can upset the performance of the column. The number of data used is 5800.

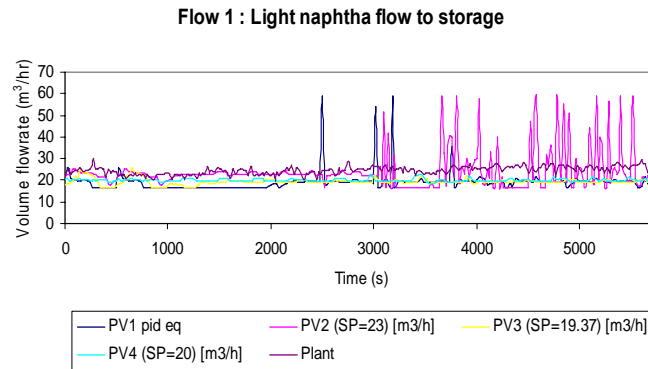


Figure 3.25 Process variables of Flow 1 for controller settings based on PID, plant and different set point

Figure 3.26 represents the process variables for LPG flow controller settings based on PID, actual plant and different set point values. The response of PID, PV3 and PV4 is the change of set point made at 8.5 and 9 m³/hr exhibit stable response as the flow rate fluctuates at a very small rate. PID reaches the settling time faster than plant and other set point. PID exhibits more stable response with small oscillation and fluctuates within its set point. Meanwhile, PV2 shows rapid oscillation. It can be concluded that the simulation data resemble closely with the actual plant data and match the process model of the column for Flow 1. The number of data used is 5800

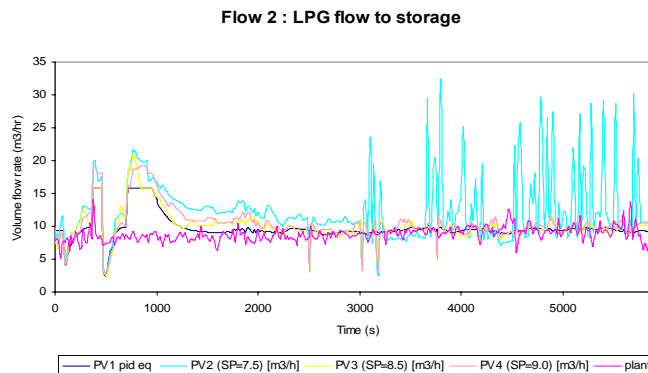


Figure 3.26 Process variables of Flow 2 for controller settings based on PID, plant and different set point

Figure 3.27 represents the process variables for receiver overhead pressure controller settings based on PID, actual plant and different set point values. The response of PID and PV4 (the change of set point made at 815 kPa) exhibit unstable response as the pressure fluctuates are small. Actual plant exhibits more stable response with small oscillation and fluctuates within its set point. Meanwhile, PV4 shows rapid oscillation. The simulation data deviate large compared to actual plant due to process model mismatch. The pressure profile is affected by the changes of the composition. The deviation of the compositions with respect to actual and simulation will effect the fluctuation of the pressure. The number of data used is 18000.

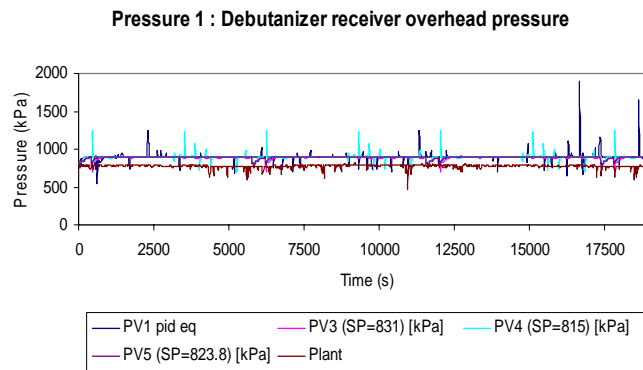


Figure 3.27 Process variables of Pressure 1 for controller settings based on PID, plant and different set point

3.5.5 Validate online and simulation composition in close loop

Once simulation composition and actual composition close loop data agree well with each other the online and simulated close loop response of the composition at the top and bottom of the column is also established to obtain the unmeasured data. Comparison between the close loop responses in simulation to the actual plant from laboratory sample is performed to evaluate the deviation between the simulated and actual composition, to ascertain that the simulation data available closely resemble the actual online industrial data. The composition of interest is the n-butane and i-butane. Figures

3.28 and 3.29 represent the composition at the top and bottom of n-butane. The calculated Root Mean Square Error (RMSE) for top composition is 0.10 and bottom composition is 0.008184 respectively. It indicates that there is small deviation between the online and simulation data. The interval of composition analysis is under 1 minute sampling.

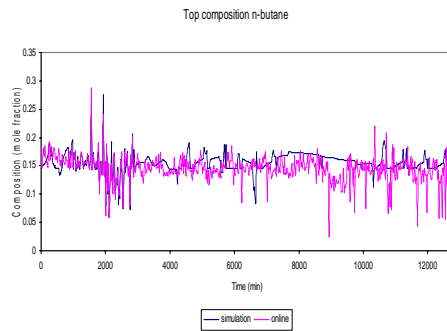


Figure 3.28 Top composition n-butane

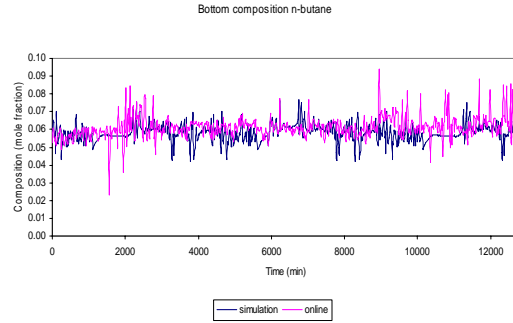


Figure 3.29 Bottom composition n-butane

Figures 3.30 and 3.31 represent the composition at the top and bottom of i-butane. The calculated Root Mean Square Error (RMSE) for top composition is 0.027199 and bottom composition is 0.016554 respectively. It indicates that there is small deviation between the online and simulation data. This implies that the simulation and close loop data agree well with each other. The number of data used is 12100.

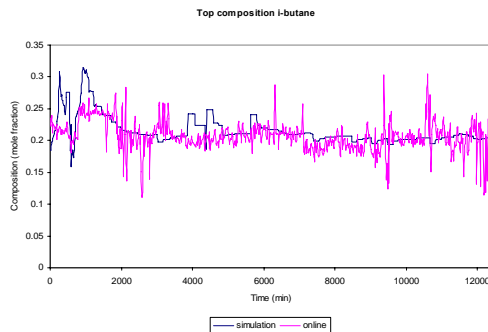


Figure 3.30 Top composition i-butane

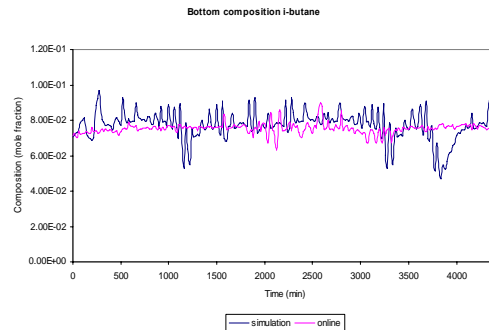


Figure 3.31 Bottom composition i-butane

This is important to show that the simulation and close loop data agree well with each other including the variables that are not available from the open loop response for the plant. Once the close loop has been verified, then the open loop response for variable that is not available from plant can be obtained. The same step size for the manipulated variable for overhead pressure, reboiler and reflux from plant are performed as inputs to obtain the fluctuation of the process variable as outputs in the simulation. For each of the step test are performed individually in the simulation environment to obtain the process variables. All the process variables that are performed in the simulation are under automatic close loop control. The measured data that are used in the simulation is Temp 5, Pressure 1, Flow 1 and Flow 2. From the simulation performed using HYSYS, the simulation and actual data are compared.

3.5.6 Extract from close loop data

Figures 3.32 and 3.33 show the fluctuations of the two process variables that are in close loop response compared to the extracted closed loop. The fluctuations of the variables show a large variation between under control which is the close loop and not under control which is the extract close loop. Pressure 1 and Temp 5 is controlled using PI. The move of the manipulated variable (MV) for Temp 5 is larger than Pressure 1. This is because Temp 5 has small error (0.00025) with respect to time. Pressure 1 has a large error because the variation between the fluctuations of the process variable and its set point is large compared to Temp 5. The controller setting for the plant will affect the error to bring the process variables close to its set point.

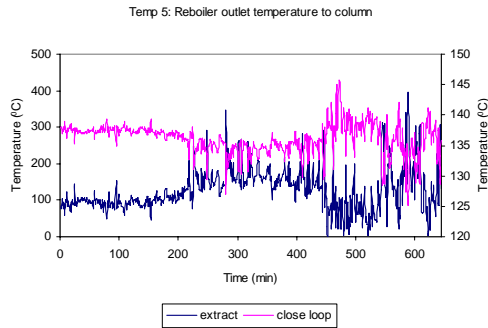


Figure 3.32 Temperature 5

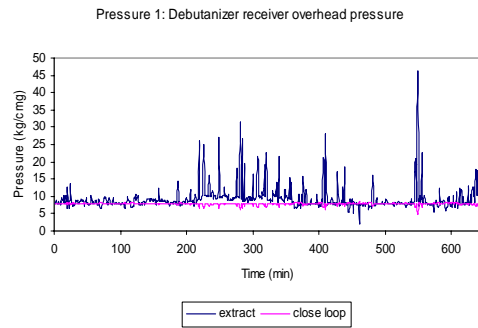


Figure 3.33 Pressure 1

Figures 3.34 and 3.35 show the fluctuations of the two process variables that are in close loop response compared to the extracted closed loop. The fluctuations of the variables show a large variation between under control which is the close loop and not under control which is the extract close loop. Debutaniser feed and reflux flow rate is controlled using PI. The move of the manipulated variable (MV) for reflux flow rate is larger than debutaniser feed. This is because reflux flow has small error with respect to time. Debutaniser feed has a large error because the variation between the fluctuations of the process variable and its set point is large compared to reflux flow. The controller setting for the plant will affect the error to bring the process variables close to its set point.

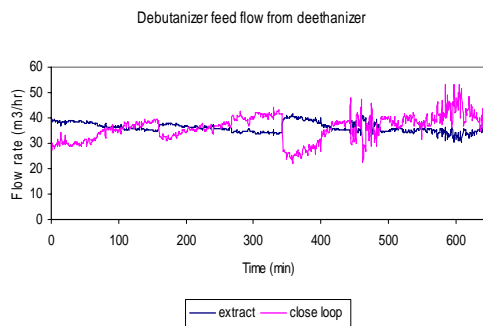


Figure 3.34 Debutaniser feed

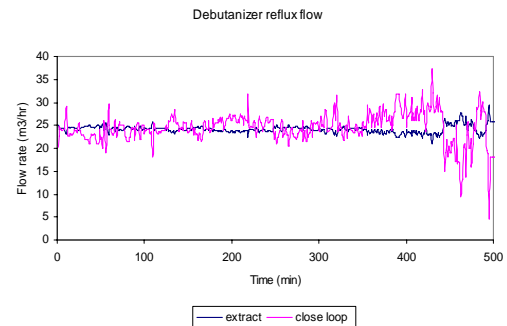


Figure 3.35 Debutaniser reflux flow

Figures 3.36-3.39 show the fluctuations of the four manipulated variables that are extracted from closed loop. The overhead pressure flow rate shows small fluctuations compared to the rest of the fluctuations. The fluctuations of the manipulated variable are

important to see the response under close loop and how it deviate with the actual open loop step response for the overhead pressure, reboiler and reflux flow rate. The number of data used is 650.

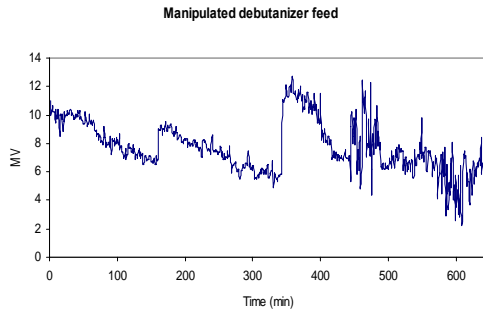


Figure 3.36 Manipulated variable
Debutaniser

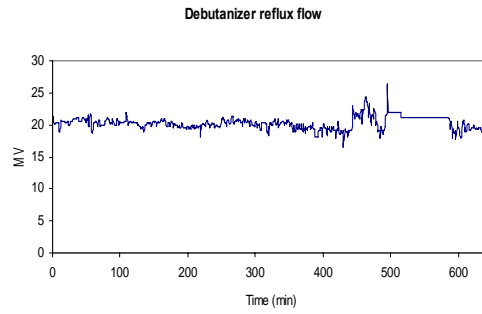


Figure 3.37 Manipulated variable
reflux flow rate

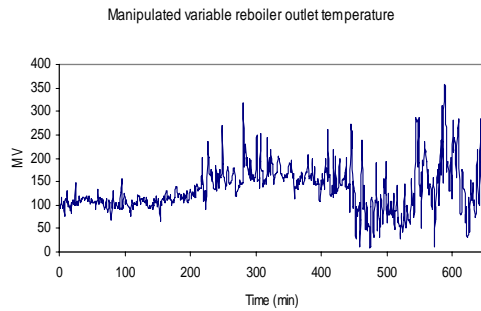


Figure 3.38 Manipulated variable
reboiler flow rate

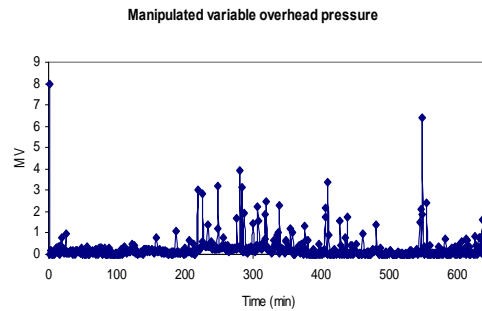


Figure 3.39 Manipulated variable
overhead pressure flow rate

3.6 Data pretreatment using principal component analysis and partial least square

Multivariate data are measured accurately on observations and variables. Hence an adequate multivariate characterization is a necessary first step. Using a multivariate data set, the data must be analyzed so that the information in the data is expressed in a comprehensible way. PCA and PLS analysis are used prior to utilizing neural network

to determine the important variables to be analyzed for composition prediction as this is crucial since there is a large number of variables surrounding the column. The PCA and PLS analyses will also determine the inputs to the neural network. The projection approach can be adapted to a variety of data analytical objectives such as summarizing and visualizing a data set, multivariate classification and discriminant analysis and finding quantitative relationship among the variables. Projection methods can be made robust to outliers, deal with non-linear relationship and adapt to drift in multivariate process data.

Methods used are PCA for projecting X down onto a few latent variables. SIMCA-P is used for classification. The latent variables models are different in objectives and formulation from traditional multivariate models with independent variables. Megavariate analysis models data in terms of multiple latent variables to give results that are multivariate. The projection method is useful for analysis and modeling complicated data. These methods are increasingly used in a wide range of industrial application. The method used is to provide a practical approach to multivariate data analysis. The method approach here is how extensive information contained in multivariate data can be expressed in terms of plots and lists of parameters resulting from a multivariate analysis. Figure 3.40 shows the model window to perform PCA. The simulation data in Excel could be imported to SIMCA-P environment. There are 2 important variables which are the primary variable and observation. Once the work set has been developed, the PCA model has to be fitted. The important analyses are component contribution plot, and variable important plot. The number of data used is 301.

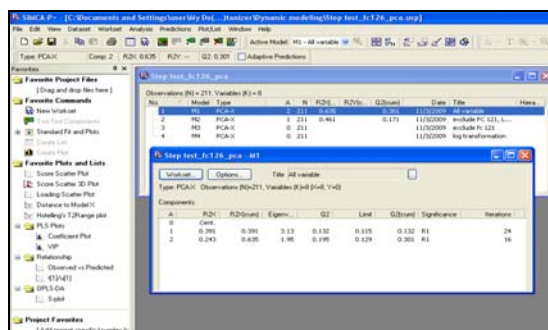


Figure 3.40. Model window for PCA in SIMCA-P environment

Table 3.6 shows the 23 variables involved in the PCA analysis

Table 3.6: Important variables for PCA model

Variable	Symbol	Description
Temp 1	a	Debutaniser top temperature
Temp 2	b	Debutaniser bottom temperature
Temp 3	c	Debutaniser receiver bottom temperature
Temp 4	d	Light Naphtha temperature after condenser E121
Temp 5	e	Reboiler outlet temperature to column
Temp 6	f	Debutaniser feed temperature
Level 1	g	Debutaniser level
Level 2	h	Debutaniser condenser level
Level 3	i	Debutaniser level indicator
Level 4	j	Condenser level indicator
Flow 1	k	Light Naphtha flow to storage
Flow 2	l	LPG flow to storage
Pressure 1	m	Debutaniser receiver overhead pressure
Component 1	n_top	Top composition propane
	n_bot	Bottom composition propane
Component 2	o_top	Top composition i-butane
	o_bot	Bottom composition i-butane
Component 3	p_top	Top composition n-butane
	p_bot	Bottom composition n-butane
Component 4	q_top	Top composition i-pentane
	q_bot	Bottom composition i-pentane
Component 5	r_top	Top composition n-pentane
	r_bot	Bottom composition n-pentane

3.6.1 PCA and PLS analysis

PCA is used to analyze all variables surrounding the column outlined in Table 3.6. If a correlation exists between the variables, small number of principal components will summarize a majority of the variation in X . To analyze the changes in the original data space, changes occurring within the principal components should be used. From the PCA, the important variables surrounding the column are determined. PLS is used to relate the important variables from PCA with respect to the top and bottom composition of n-butane and i-butane. PLS regression is a method that generalizes and combines features from principal component analysis and multiple regressions.

It is normally useful to predict a set of dependent variables (Y) from a large set of independent variables or predictors (X). The data set which obtained from open loop online and simulation are combined together. SIMCA-P is used to perform PCA and PLS analysis for the debutanizer column. There are 2 important variables, which are the primary and observation variables. The primary variable consists of 23 variables surrounding the column while the observation variables are the top and bottom n-butane compositions. The observation variable is the number of observations established once the worksheet has been developed. Then PCA model is fitted to these data.

From the PCA, variables which are not important are excluded while the important variables are analyzed again with respect to the top and bottom composition n-butane and i-butane using PLS. For PCA, component contribution plot are used to analyze all the important variables surrounding the column. For PLS analysis, variable important plot are used to determine variables which are important with respect to the n-butane and i-butane composition. From the PCA and PLS analyses, component contribution plot and variable important plot are used to identify the variables that are important to be selected the right inputs for neural network.

Step test for overhead pressure

Component contribution plot shows all of the important components of the step test overhead pressure flow rate for the top liquefied petroleum gas product and bottom light naphtha product. The variables are outlined in Table 3.6. The values of R^2 (variation explained) and Q^2 (variation predicted according to cross validation) are also shown for each variable. The R^2 indicate the fraction of the Sum of Squares (SS) of all the X 's variables explained by the current component. Q^2 indicate the fraction of the X 's variables that can be predicted by a component.

Q^2 is computed as:

$$Q^2 = \left[1 - \frac{PRESS}{SS} \right] \quad (3.5)$$

The prediction error sum of squares ($PRESS$) is the sum of the squared difference between the observed and predicted values computed as:

$$PRESS = \sum_i \sum_m (Y_{im} - \hat{Y}_{im})^2 \quad (3.6)$$

The variables with high values of R^2 have large loading values for the selected component. The Q^2 values indicate the reliability of these R^2 and loading values. The component is considered less important if all of the variables have low values of R^2 and Q^2 in a component. This is applicable to variables a, b, d, g, h, i, j and k as depicted in Figure 3.41. The highest value of R^2 and Q^2 for variable e is 0.12 and 0.31 respectively. From the plot, it could be concluded that variables c, l, e, f and m have high values for R^2 and Q^2 indicating that these components are important for composition prediction with respect to the overhead pressure flow rate. Large R^2 value indicates that fraction

sum of square is high and large Q^2 value indicates that the sum of square and prediction of sum of square is small.

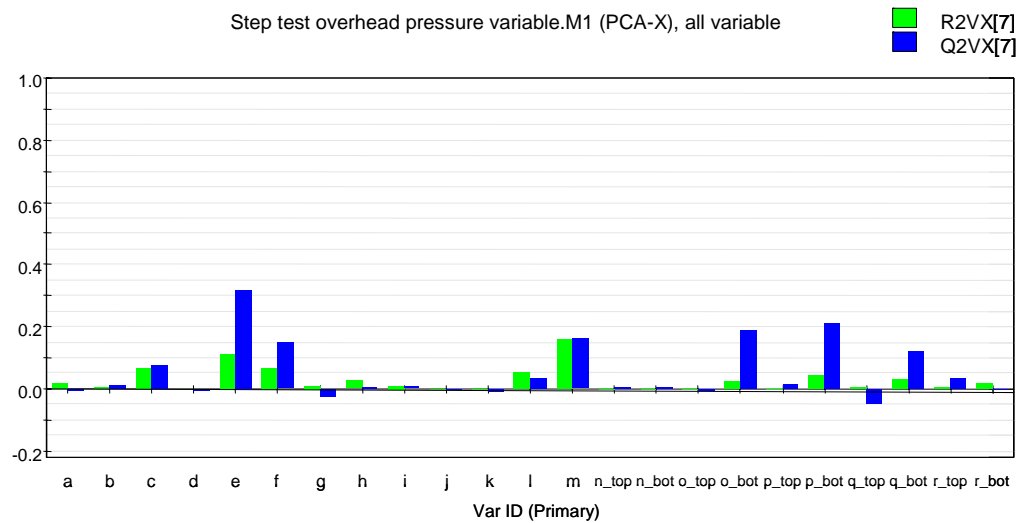


Figure 3.41 Component contribution plot overhead pressure flow rate

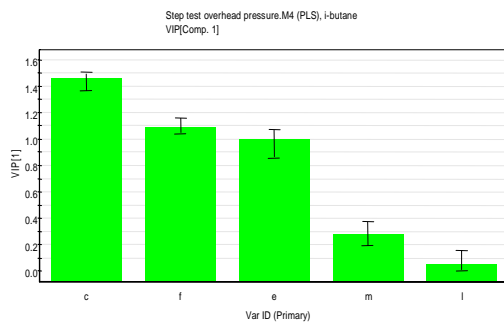


Figure 3.42 PLS i-butane

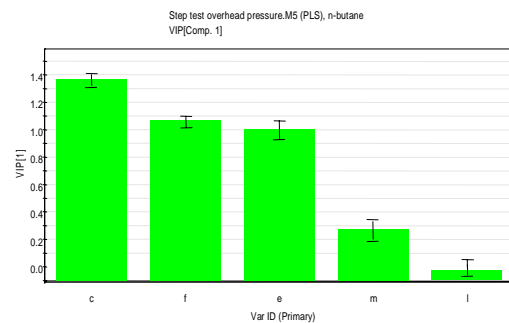


Figure 3.43 PLS n-butane

From Figure 3.42 and 3.43, the output variable of the PLS analysis is the i-butane and n-butane composition. The input variables are the variable Temp 3, Temp 5, Temp 6, Pressure 1 and Flow 2. All of the variables for level have been excluded from the analysis, since level will not affect the fluctuations in the top and bottom composition.

The principal component shows the important variable to be analyzed. From the figure importance of variables is determined by having the y axis value which is the Variable

Important Plot (VIP) more than 0.5. If the value of the bar chart for the particular variable is less than 0.5, the variable is not important and it could be excluded from the analysis i.e. l and m.

Step test for reboiler flow rate

Component contribution plot shows all of the important components of the step test reboiler flow rate for the top liquefied petroleum gas product and bottom light naphtha product. The variables are outlined in Table 3.6. The values of R^2 (variation explained) and Q^2 (variation predicted according to cross validation) are also shown for each variable. The variables with high values of R^2 have large loading values for the selected component. The Q^2 values indicate the reliability of these R^2 and loading values. The component is considered less important if all of the variables have low values of R^2 and Q^2 in a component. This is applicable to variables c, d, f, g, h, i, j, l and m as depicted in Figure 3.44. The highest value of R^2 and Q^2 for variable b is 0.48 and 0.44 respectively. From the plot, it could be concluded that variables a, b, e and k have high values for R^2 and Q^2 indicating that these components are important for composition prediction with respect to the reboiler flow rate.

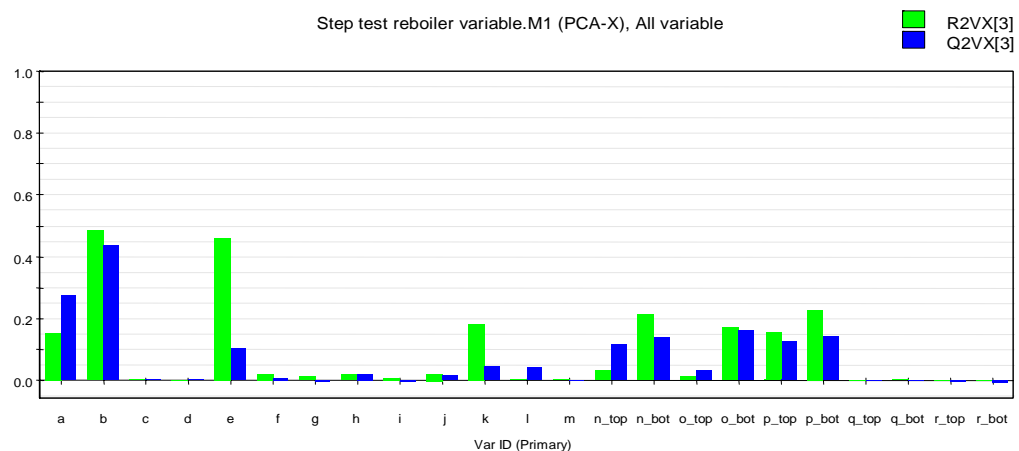


Figure 3.44 Component contribution plot reboiler flow rate

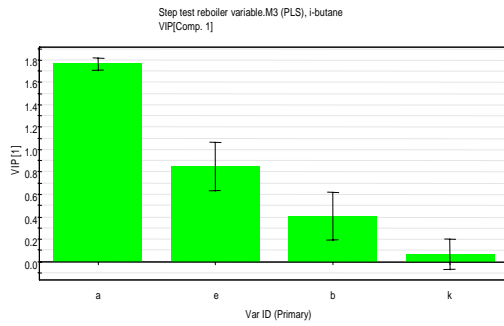


Figure 3.45 PLS i-butane

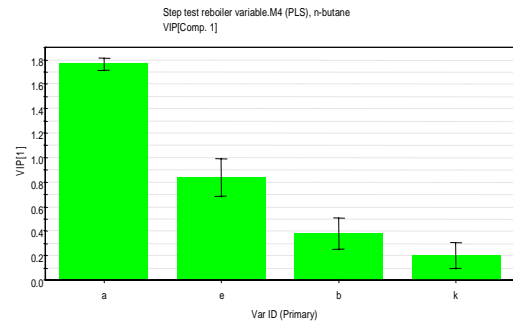


Figure 3.46 PLS n-butane

From Figure 3.45 and 3.46, the output variable of the PLS analysis is the i-butane and n-butane composition and the input variables is the variable Temp 1, Temp 2, Temp 5 and Flow 1. All of the variables for level have been excluded from the analysis, since level will not affect the fluctuations the top and bottom composition of n-butane. The variables which are not important shown in figure, the variables are k and b.

Step test for reflux flow rate

Component contribution plot shows all of the important components of the step test reflux flow rate for the top liquefied petroleum gas product and bottom light naphtha product. The variables are outlined in Table 3.6. The values of R^2 (variation explained) and Q^2 (variation predicted according to cross validation) are also shown for each variable. The variables with high values of R^2 have large loading values for the selected component. The Q^2 values indicate the reliability of these R^2 and loading values. The component is considered less important if all of the variables have low values of R^2 and Q^2 in a component. This is applicable to variables are c, d, f, g, h, i, j and k as depicted in Figure 3.47. The highest value of R^2 and Q^2 for variable e is 0.1 and 0.28 respectively. From the plot, it could be concluded that variables b, e, n_top, o_top and q_top have high values for R^2 and Q^2 indicating that these components are important for composition prediction with respect to the reflux flow rate.

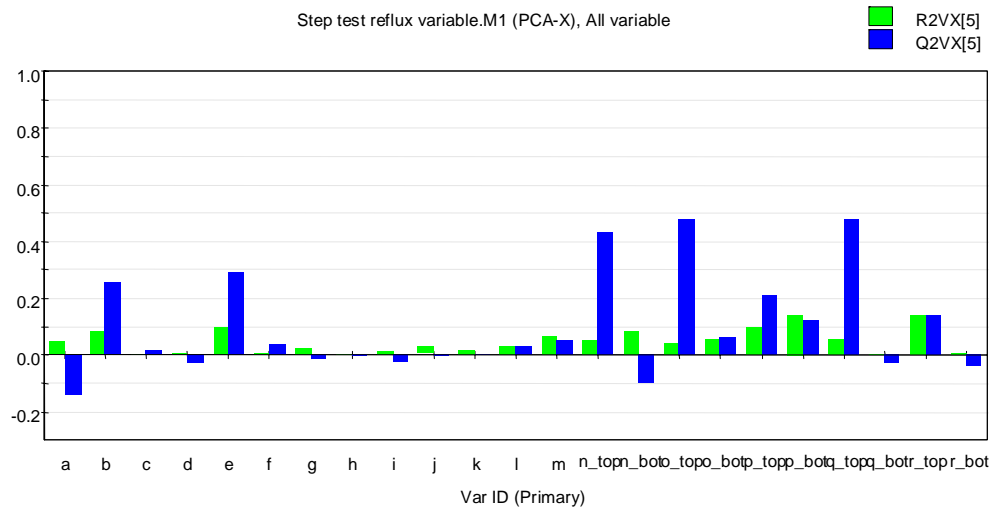


Figure 3.47 Component contribution plot reflux flow rate

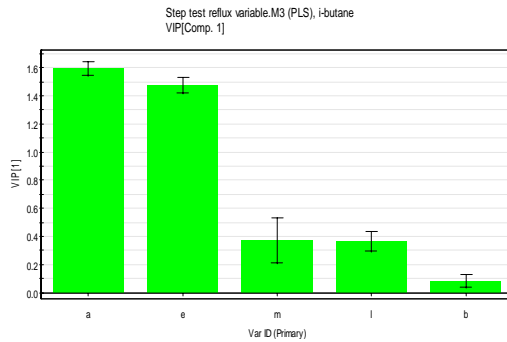


Figure 3.48 PLS i-butane

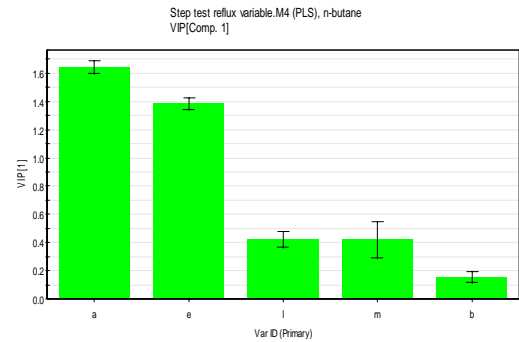


Figure 3.49 PLS n-butane

From Figure 3.48 and 3.49 the output variable of the PLS analysis is the i-butane and n-butane composition and the input variables is the variable Temp 1, Temp 5, Temp 2, Pressure 1 and Flow 2. All of the variables for level have been excluded from the analysis, since level will not affect the fluctuations the top and bottom composition of n-butane. The variable is not important and it could be excluded from the analysis i.e. l, m and b. Table 3.7 shows the important variables involve prediction of i-butane combined for overhead pressure, reboiler and reflux flow rate data set. The number of data used is 301.

Table 3.7 Data pretreatment after PCA and PLS for i-butane

Variable	Symbol	Description
MV1	mv1	Manipulated overhead pressure flow rate
MV2	mv2	Manipulated reboiler flow rate
MV3	mv3	Manipulated reflux flow rate
Temp1	a	Debutaniser top temperature
Temp 3	c	Debutaniser receiver bottom temp
Temp 5	e	Reboiler outlet temperature to column
Temp 6	f	Debutaniser feed temp
Component 2	o_top	Top composition i-butane
	o_bot	Bottom composition i- butane
	o_top+1	Future predictions top composition i- butane
	o_bot+1	Future predictions bottom composition i- butane

Since there a number of variable outlined in Table 3.7, the variables is further reduced by analyzing the variables again using PCA and PLS

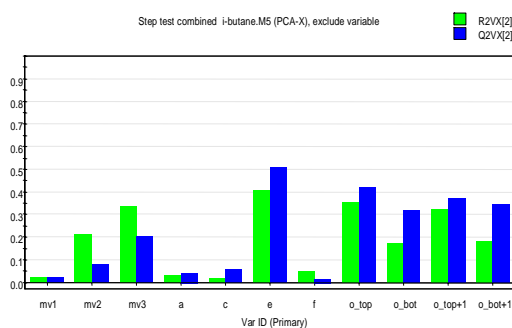


Figure 3.50 Component contribution i-butane

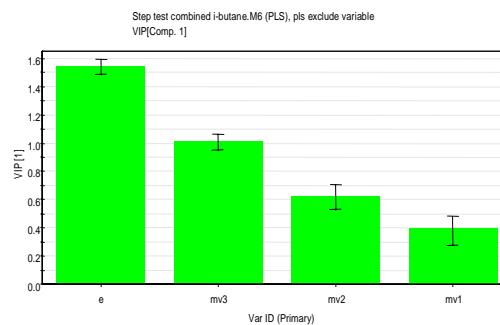


Figure 3.51 PLS i-butane

The purpose to perform the component contribution plot is to determine again the variables that are important for composition prediction i-butane. It could be concluded that mv1, a, c and f is not important and the variables could be excluded. After performing PCA, the important variables are analyzed again using PLS. The important variables based on Variable Important Plot (VIP) are namely variable mv2, mv3 and e.

Table 3.8 shows the important variables involve prediction n-butane combined for overhead pressure, reboiler and reflux flow rate data set. The number of data used is 301.

Table 3.8 Data pretreatment after PCA and PLS n-butane

Variable	Symbol	Description
MV1	mv1	Manipulated overhead pressure flow rate
MV2	mv2	Manipulated reboiler flow rate
MV3	mv3	Manipulated reflux flow rate
Temp1	a	Debutanieer top temperature
Temp 3	c	Debutaniser receiver bottom temp
Temp 5	e	Reboiler outlet temperature to column
Temp 6	f	Debutaniser feed temp
Component 3	p_top	Top composition n-butane
	p_bot	Bottom composition n- butane
	p_top+1	Future predictions top composition n- butane
	p_bot+1	Future predictions bottom composition n- butane

Since there are a number of variables outlined in Table 3.8, the variables are further reduced by analyzing the variables again using PCA and PLS

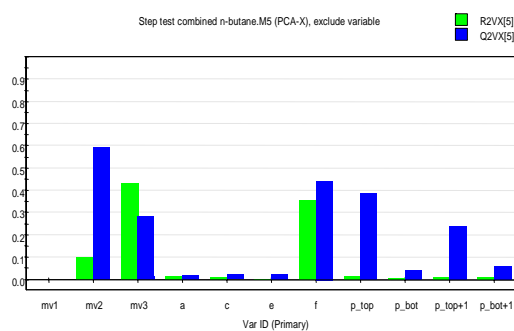


Figure 3.52 Component contribution n-butane

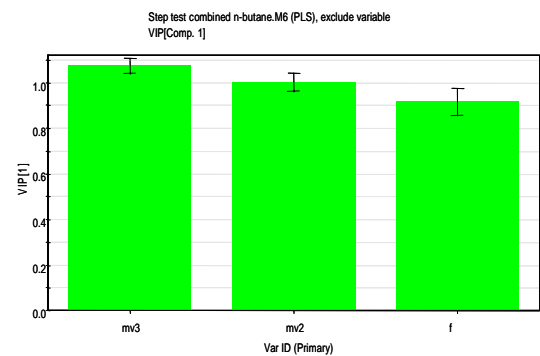


Figure 3.53 PLS n-butane

From the component contribution plot it could be concluded that mv1, a, c and e is not important and the variables could be excluded. After performing PCA, the important

variables are analyzed again using PLS. The important variables based on Variable Important Plot (VIP) are namely variables mv2, mv3, and f.

Table 3.9 Important variables for neural network prediction of n-butane

Variable	Symbol	Description
MV2	mv2 (k)	Manipulated reboiler flow rate
	mv2 (k-1)	Lag MV2
MV3	mv3 (k)	Manipulated reflux flow rate
	mv3 (k-1)	Lag MV3
Temp 6	f (k)	Debutaniser feed temp
	f (k-1)	Lag Temp 6
Component 3	p_top (k)	Top composition n-butane
	p_top (k-1)	Lag composition top
	p_bot (k)	Bottom composition n- butane
	p_bot (k-1)	Lag composition bottom
	p_top (k+1)	Future predictions n- butane top
	p_bot (k+1)	Future predictions n- butane bottom

Table 3.10 Important variables for neural network prediction of i-butane

Variable	Symbol	Description
MV2	mv2 (k)	Manipulated reboiler flow rate
	mv2 (k-1)	Lag MV2
MV3	mv3 (k)	Manipulated reflux flow rate
	mv3 (k-1)	Lag MV3
Temp 5	e (k)	Reboiler outlet temperature to column
	e (k-1)	Lag Temp 5
Component 2	o_top (k)	Top composition i-butane
	o_top (k-1)	Lag composition top
	o_bot (k)	Bottom composition i- butane
	o_bot (k-1)	Lag composition bottom
	o_top (k+1)	Future predictions i- butane top
	o_bot (k+1)	Future predictions i- butane bottom

The summary of this chapter are concluded these data that are available from actual plant are large and therefore need to be screened by performing PCA and PLS, where the important variables for the column are obtained and are used for monitoring the composition of n-butane and i-butane. For each of the step test, PCA is used to determine the important variables surrounding the column. Once we have determined the important process variables, the important variables affecting the composition of

n-butane and i-butane is further analyzed using PLS analysis. The important variables that have been determined by PCA and PLS are used as inputs to the neural network prediction to determine the process model for the column. The important variables for neural network prediction are outlined in Tables 3.9 and 3.10. The time interval for control and time interval for composition is 301 minutes. The interval for (k) and $(k+1)$ is determined that gives the best results with least lag time. This is also based on references from various literatures on dynamic modeling using neural network based models for non-linear chemical process. The time at $t(k)$ and $t(k+1)$ are arranged accordingly in the data set before it is used in the prediction by neural network.

Step test that are analysed previously consist of Temp 6 and Temp 5 that are used as the input variables to predict the composition for n-butane and i-butane. It is also used to predict the top (Temp 1) and bottom temperature (Temp 2).

CHAPTER 4: NEURAL NETWORK PROCESS MODEL FOR COMPOSITION AND TEMPERATURE

4.1 Introduction

The design of neural network for process modeling has often been done in an unorganized fashion. It is important to create a neural network structure by optimizing the weights and biases value to be capable of interpret it in model forms. Thus it is possible to create efficient neural network model which can be understood in physical terms. In our case the network is based on linear transfer functions which are identified with a technique by using equation based method. The architecture of the neural network utilizes trial and error techniques to determine the number of hidden nodes. Finally, the network structure, weights and biases values are the parameters to develop the equation for the process model of the neural network.

4.2 Methodology for modeling

The utility of artificial neural network models lies in the fact that they can be used to infer a function from observations. This is particularly useful in applications where the complexity of the data or task makes the design of such a function by hand impractical. The online composition at the top and bottom of the column in the refinery is currently measured using normal laboratory sampling. This is tedious and the results could not be obtained immediately therefore neural network are used as a benchmark because it is able to predict the composition faster with more accuracy and precision and could also handle non-linearities in the process variable surrounding the column as proposed in this study.

Open loop response of the reboiler and reflux data, which include the compositions, are used to develop the dynamic neural network architecture. The selected input

variables to the network including the composition are time delayed while the outputs are the future predictions of composition. The type of dynamic network used for training, validation and testing the data set are Nonlinear Autoregressive Network with Exogenous (NARX) inputs with series-parallel architecture. The training algorithm used is the Levenberg-Marquardt method is because using dynamic network. Early stopping criteria are implemented to train the network while the performance function used is the mean square error.

These data sets are partitioned into three sets, which are the training, validation and test set. In the network, the number of layers used is 3 with only 1 hidden layer. The number of hidden layer is determined using statistical analysis and it is described in section 4.3. The transfer function to train the network is purelin (linear) for the entire layer and the networks are trained to predict simultaneously the top and bottom composition. Prior to implementing the neural network, the data are arranged by combining the open loop response from the simulation and online data. The data set are then trained until the network reaches its epoch and meet its performance criteria. The data set are also validated and tested after the network is trained. Since the extracted close loop data are available, the data are replaced as inputs to the neural network in the validation and test set by maintaining the actual architecture that are trained for the open loop response. The raw process data generated are scaled down between 0.05 to 0.95 using the following equation:-

$$scaled\ value = \left(\frac{actual\ value - min\ value}{max\ value - min\ value} \right) (0.95 - 0.05) + min\ value \quad (4.1)$$

Hence the actual value is then given by,

$$actual\ value = \frac{(scaled\ value - min\ value) \times (max\ value - min\ value)}{(0.95 - 0.05)} + min\ value \quad (4.2)$$

4.3 Model adequacy test for neural network to determine the hidden layer

Prior to implementing the neural network methodology, the data are arranged accordingly by combining the open loop response from simulation and plant data. The performances need to be measured for its accuracy by determination of the comparison prediction using the Root Mean Square Error method. (RMSE) given by;

$$RMSE = \sqrt{\frac{(x_{measured} - x_{predicted})^2}{N}} \quad (4.3)$$

Correct Directional Change (CDC) measures the capacity of a model to accurately predict the subsequent actual change of a predicted variable. The formula of CDC is defined as:

$$CDC = \frac{100}{N} \sum_i^N D_i \quad (4.4)$$

where formula of D_i is defined as:

$$D_i = y_i \times \overline{y_i}$$

D_i is equal to 1 if the product $y_i \times \overline{y_i}$ is greater than zero. D_i is equal to zero if the product $y_i \times \overline{y_i}$ is negative.

The best known information criteria are the Akaike information criterion (AIC) and Bayesian information criteria (BIC) which is given below:

$$AIC = MSE + \sigma^2 \frac{2K}{T} \quad (4.5)$$

$$BIC = MSE + \frac{\log(N)\sigma^2 2K}{T} \quad (4.6)$$

The Akaike information criteria related to the square of the residual to the number of free model parameters was to weigh the error of the model against the number of

parameters whereby the model with low value of the information criteria gave the best performance. The BIC is similar to the AIC except that it is motivated by the Bayesian model selection principles.

The coefficient of determination is defined as:

$$R^2 = 1 - \frac{\sum_{t=L}^T (y_t - \hat{y}_t)^2}{\sum_{t=L}^T (y_t - \bar{y}_t)^2} \quad (4.7)$$

Mean Absolute Percentage Error (MAPE) is the measure of accuracy in a fitted time series value given as:

$$MAPE = \frac{1}{N} \sum_{t=1}^N \frac{|F_t - A_t|}{A_t} \times 100\% \quad (4.8)$$

Pearson Correlation Coefficient (C_p), measures the goodness of the regression fit (the closer the value to one indicate higher accuracy) as given below:

$$C_p = \frac{\sum_{j=1}^{N_s} (E_{p,j} - \bar{E}_{p,j})(E_{a,j} - \bar{E}_{a,j})}{\sqrt{\sum_{j=1}^{N_s} (E_{p,j} - \bar{E}_{p,j})^2 \sum_{j=1}^{N_s} (E_{a,j} - \bar{E}_{a,j})^2}} \quad (4.9)$$

The number of neurons in the hidden layer is determined from a range of 8 to 40. Using the statistical analysis described above, with the following the deviation between actual and composition prediction by neural network are determined. The following set of criteria; low RMSE, CDC approaching 100, small AIC and BIC, R^2 approaching 1, low MAPE and C_p approaching 1. Equations 4.3 – 4.9 are obtained from reference (Ramli, 2008), (Wan et al, 2011), (Sharma et al., 2004). Based on the set criteria, the best neural network architecture is determined. The hidden nodes are selected by trial and error method. The neural network is trained with an initial guess of the hidden nodes at 8 and the number of hidden nodes is increased by a factor of 2 till the hidden

nodes achieve a value of 40. The RMSE is then monitored and the one with the lowest RMSE value is selected for determining the final number of the hidden nodes.

The difference between the proposed method that it consists of the long equation that contains the input weights and biases values. It could be easily simplified in equation based as the transfer function is linear. The conventional linear least square method is by analyzing the relationship between the inputs and the outputs variables.

4.4 Neural network prediction of n-butane composition (MIMO model)

Table 4.1 shows the important variables in the neural network where the data set are combined from the manipulated variable reboiler flow rate and reflux flow rate for n-butane after performing the PCA and PLS analysis.

Table 4.1 Important variables for neural network prediction

Inputs		
Variable	Symbol	Description
MV2	mv2 (k)	Manipulated reboiler flow rate
	mv2 (k-1)	Lag MV2
MV3	mv3 (k)	Manipulated reflux flow rate
	mv3 (k-1)	Lag MV3
Temp 6	f (k)	Debutaniser feed temp
	f (k-1)	Lag Temp 6
Component 3	p_top (k)	Top composition n-butane
	p_top (k-1)	Lag composition top
	p_bot (k)	Bottom composition n- butane
	p_bot (k-1)	Lag composition bottom
Outputs		
	p_top (k+1)	Future predictions n- butane top
	p_bot (k+1)	Future predictions n- butane bottom

The inputs for the neural network are from mv2 (k) to p_bot (k-1). The outputs are the variable p_top (k+1) and p_bot (k+1), making the neural network as a MIMO based model. The control cycle is 1 minute sampling and the time interval between p_top(k) and p_top(k+1) is by 1 minute ahead prediction.

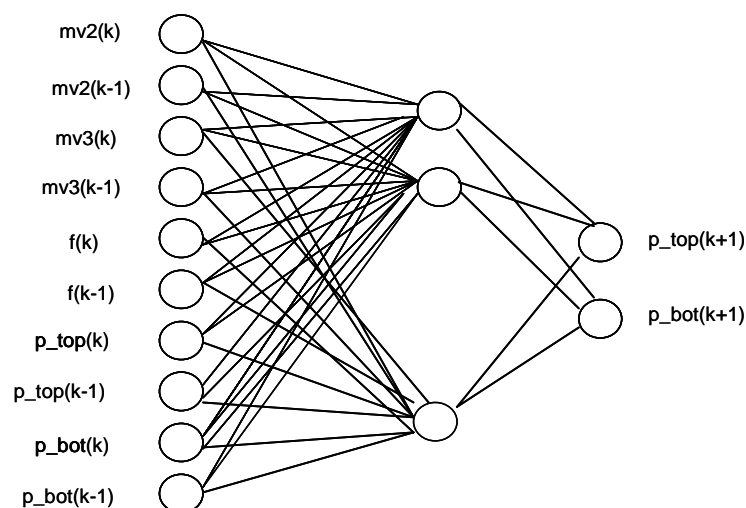


Figure 4.1 Neural network architecture for n-butane

Figure 4.1 shows the neural network architecture of the n-butane composition prediction

Table 4.2. Neural network architecture

Parameters	Description	
Network	NARX series parallel network (newnarxsp)	
Category	With partitioning divided into 2	with partitioning divided into 3
Training function	TRAINLM	TRAINLM
Adaptation learning function	LEARNGDM	LEARNGDM
Performance function	MSE	MSE
Epochs	1000	1000
Goal	1e-6	1e-6
Number of layers	2	2
Layer 1: Number of Neuron	10	34
Transfer function	PURELIN	PURELIN
Layer 2: Number of Neuron	2	2
Transfer function	PURELIN	PURELIN

4.4.1 with partition into 3

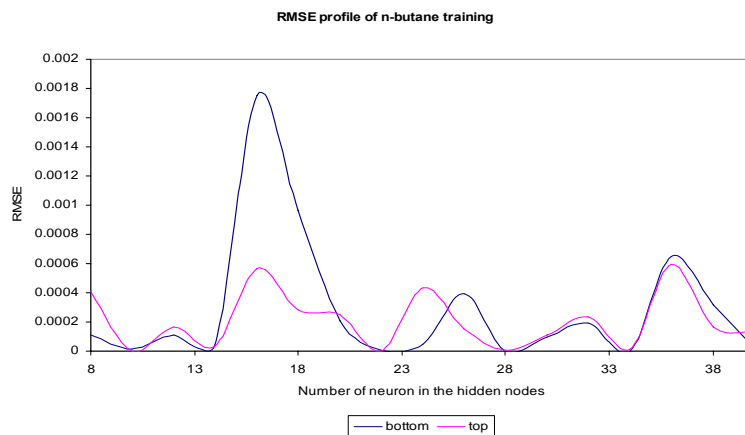


Figure 4.2 Profile of the RMSE of n-butane training

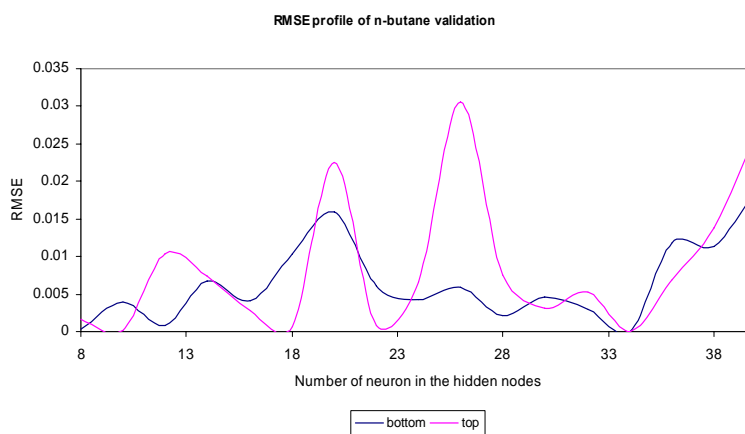


Figure 4.3 Profile of the RMSE of n-butane validation

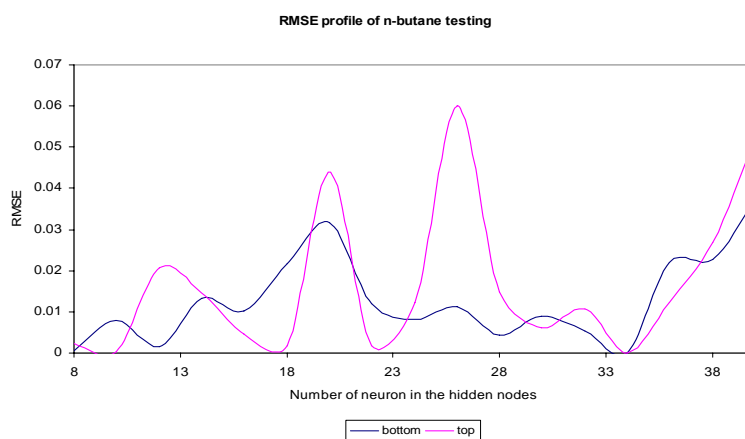


Figure 4.4 Profile of the RMSE of n-butane testing

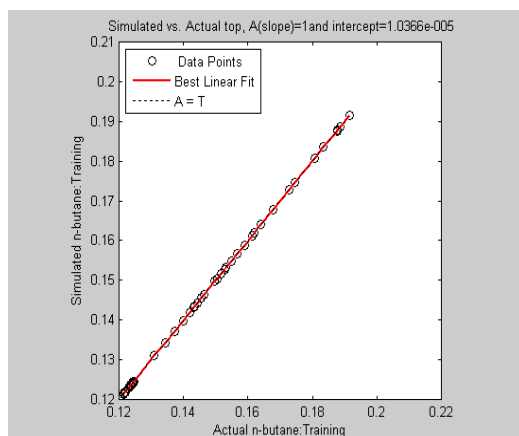


Figure 4.5 Actual and simulated n-butane top composition training

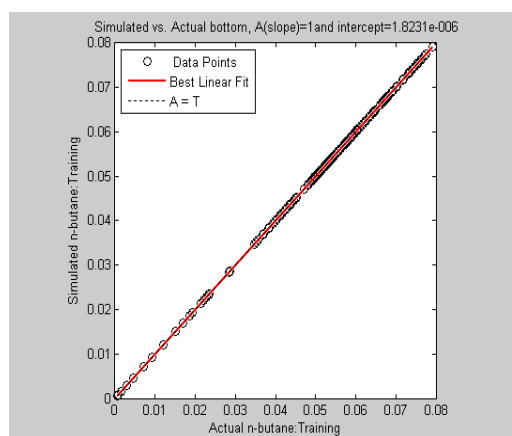


Figure 4.6 Actual and simulated n-butane bottom composition training

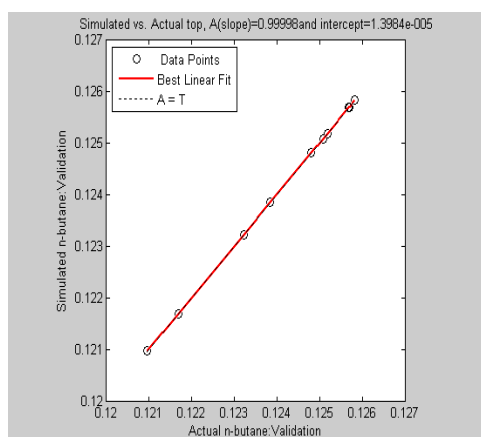


Figure 4.7 Actual and simulated n-butane top composition validation

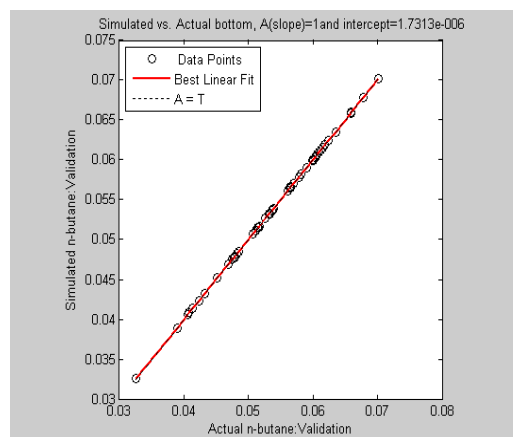


Figure 4.8 Actual and simulated n-butane bottom composition validation

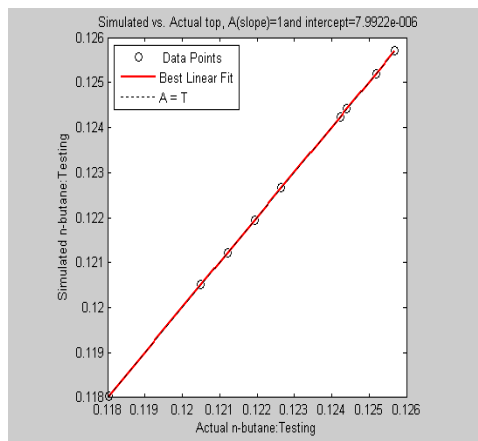


Figure 4.9 Actual and simulated n-butane top composition testing

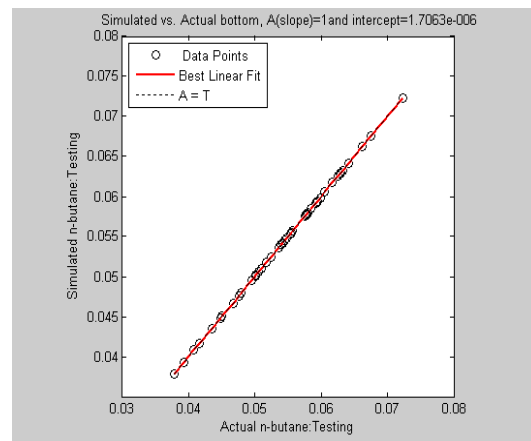


Figure 4.10 Actual and simulated n-butane bottom composition testing

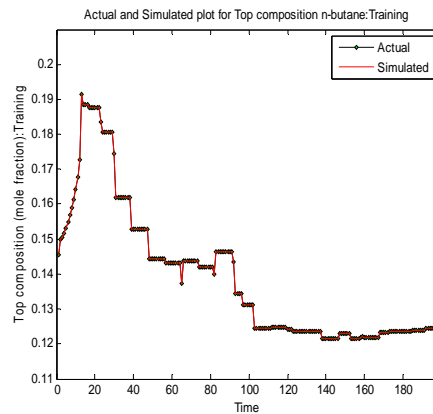


Figure 4.11 Actual and simulated n-butane top composition line plot training

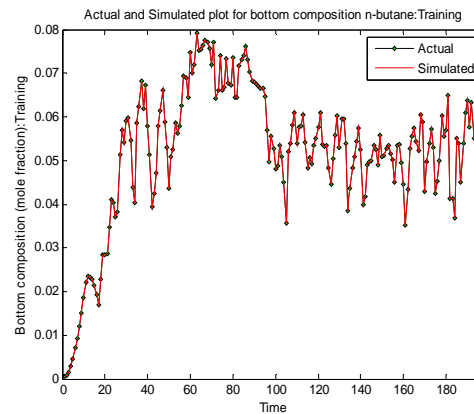


Figure 4.12 Actual and simulated n-butane bottom composition line plot training

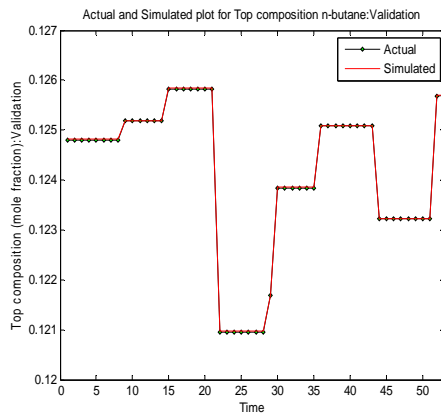


Figure 4.13 Actual and simulated n-butane top composition line plot validation

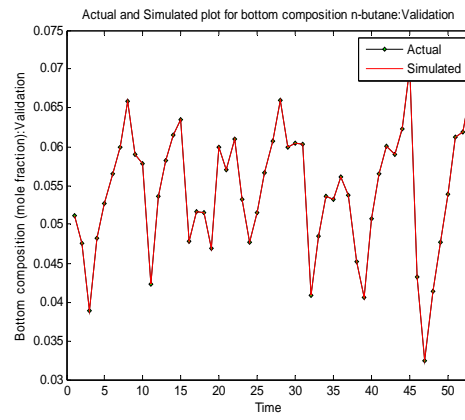


Figure 4.14 Actual and simulated n-butane bottom composition line plot validation

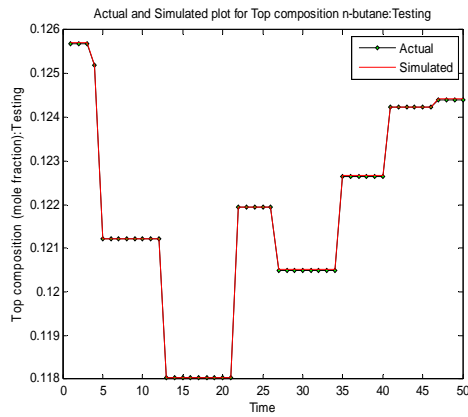


Figure 4.15 Actual and simulated n-butane top composition line plot testing

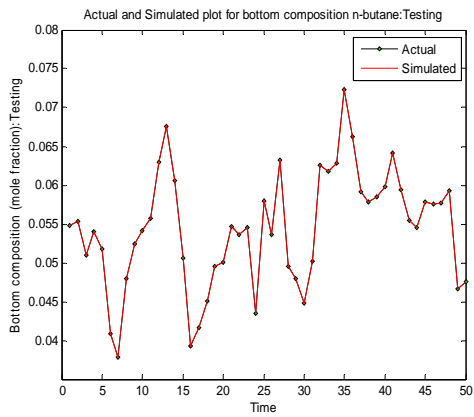


Figure 4.16 Actual and simulated n-butane bottom composition line plot testing

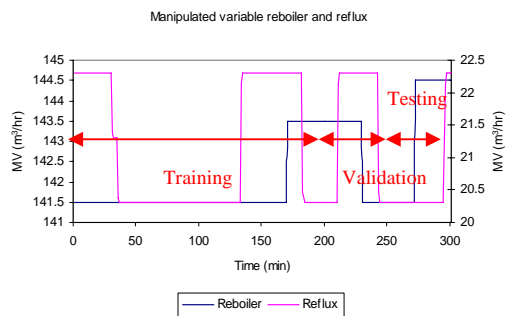


Figure 4.17 Manipulated variable reboiler and reflux flow rate

The data are partitioned according to the training, validation and test set as shown in Figure 4.17. Figure 4.2 to Figure 4.4 shows the RMSE profile with the change in the number of hidden nodes in the hidden layer. Figure 4.5 to Figure 4.16 show the top and bottom composition prediction of n-butane for training, validation and testing. The amount of data that are partitioned according to training is 65%, for validation is 18% and test is 17%. From the result, it could be concluded that the RMSE deviation between the open loop and the extract open loop is 5×10^{-8} for the bottom validation data set and 4×10^{-7} for the top validation. The CDC value for bottom and top composition training, validation and testing are similar. The CDC value for bottom training, bottom validation and bottom testing calculated to be 100. The high CDC value indicate D_i is equal to 1 based on the prediction is larger than D_i which is zero. The CDC value for top training, top validation and top testing calculated to be 30.96, 17.3 and 16.32 respectively. The CDC value is small. This is because D_i which is zero is larger than D_i is equal to 1 and the subsequent actual change of the predicted variable is small. The regression value of R for top and bottom validation and test set is 1. Thus the prediction between the actual and simulated is similar. For the AIC and BIC, low value is preferred as it indicates better prediction. The AIC and BIC values for open loop for top composition validation are 572 and 564 respectively. The AIC and BIC values for open loop for bottom composition validation are 357 and 349 respectively. The AIC and BIC values for open loop for top composition testing are 479 and 471 respectively. The AIC and BIC values for open loop for bottom composition testing are 345 and 337 respectively. For the AIC and BIC, low value is preferred as it indicates better prediction. This is also applied to training data set. Cp value is close to 1. The Cp value for validation and test set for bottom and top are calculated to be 1. The MAPE deviation between the open loop and the extract open loop is 1.02×10^{-4} for the bottom validation data set and 2.63×10^{-4} for the top validation. The MAPE values for top and

bottom composition validation open loop are 8.8×10^{-3} and 3.3×10^{-3} respectively. The MAPE values for top and bottom composition testing open loop are 8.9×10^{-3} and 3.2×10^{-3} respectively. The MAPE values are smaller compared to extract from close loop. The open loop performs better prediction than the extract open loop as the RMSE for bottom and top composition is smaller. Table 4.3 shows the statistical analysis of n-butane with partition compared to the extract close loop. From the analysis it can be concluded that the optimum number of neurons in the hidden layer for the neural network is 34. The prediction error increase as number of hidden nodes increase is because to obtain the optimum nodes is by evaluating RMSE between the actual and predicted values.

Table 4.3 Statistical analysis for n-butane composition prediction

Parameter	Open loop	Extract
rmse_bottom_training	1.75E-06	1.75E-06
rmse_top_training	1.1E-05	1.1E-05
CDC_bottom_training	100	100
CDC_top_training	30.96	30.96
R_bottom_training	1	1
R_top_training	1	1
AIC_bottom_training	1245.61	1245.61
AIC_top_training	1545.78	1545.78
BIC_bottom_training	1232.46	1232.46
BIC_top_training	1532.63	1532.63
MAPE_bottom_training	0.007321	0.007321
MAPE_top_training	0.008065	0.008065
Cp_bottom_training	1	1
Cp_top_training	1	1
rmse_bottom_validation	1.75E-06	1.8E-06
rmse_top_validation	1.1E-05	1.14E-05
CDC_bottom_validation	100	100
CDC_top_validation	17.30	17.30
R_bottom_validation	1	1
R_top_validation	1	1
AIC_bottom_validation	357.77	357.77
AIC_top_validation	572.13	572.13
BIC_bottom_validation	349.89	349.89
BIC_top_validation	564.25	564.25
MAPE_bottom_validation	0.0033	0.0034
MAPE_top_validation	0.0088	0.0091
Cp_bottom_validation	1	1
Cp_top_validation	1	1

rmse_bottom_testing	1.72E-06	1.79E-06
rmse_top_testing	1.09E-05	1.13E-05
CDC_bottom_testing	100	100
CDC_top_testing	16.32	16.32
R_bottom_testing	1	1
R_top_testing	1	1
AIC_bottom_testing	344.94	344.94
AIC_top_testing	479.409	479.408
BIC_bottom_testing	337.29	337.29
BIC_top_testing	471.761	471.76
MAPE_bottom_testing	0.00323	0.003357
MAPE_top_testing	0.0089	0.0092
Cp_bottom_testing	1	1
Cp_top_testing	1	1

4.4.2 Validate based on close loop data for n-butane

Figure 4.18 to Figure 4.29 shows the top and bottom composition prediction of n-butane for train, validation and testing. From the results, they indicate that the RMSE is low at 7.71×10^{-7} for the bottom validation data set and 5.58×10^{-7} for the top validation data set, and the CDC is high for the top and bottom composition for validation at 98.21. The high CDC value indicate D_i is equal to 1 based on the prediction is larger than D_i which is zero. The regression value of R is 1, thus the prediction between the actual and simulated is similar. Low AIC and BIC are preferred as it indicates better prediction. The AIC and BIC values for open loop for top composition validation are 517 and 506 respectively. The AIC and BIC values for open loop for bottom composition validation are 816 and 805 respectively. Cp value is close to 1. The MAPE values for top and bottom composition validation open loop are 3.23×10^{-5} and -1.1×10^{-5} respectively. It also indicate that the RMSE is low at 1.37×10^{-6} for the bottom testing data set and 9.94×10^{-7} for the top testing data set, and the CDC is high for the top and bottom composition for testing at 98.18. The regression value of R is 1, thus the prediction between the actual and simulated is similar. Low AIC and BIC are preferred as it indicates better prediction. The AIC and BIC values for open loop for top composition testing are 471 and 460 respectively. The AIC and BIC values for open

loop for bottom composition testing are 765 and 754 respectively. Cp value is close to 1 and the MAPE should be close to 0. The MAPE values for top and bottom composition testing open loop are 4.5×10^{-4} and -1.3×10^{-3} respectively Table 4.4 shows the statistical analysis for the n-butane online implementation

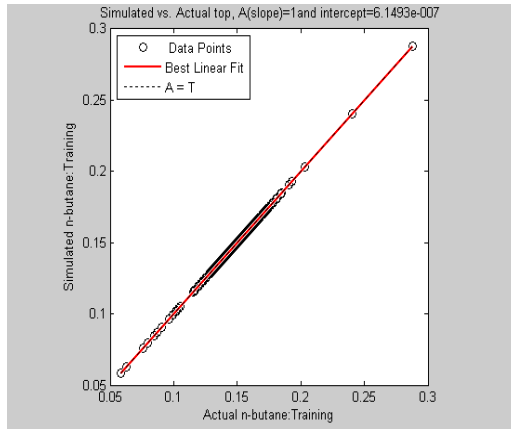


Figure 4.18 Actual and simulated n-butane top composition training

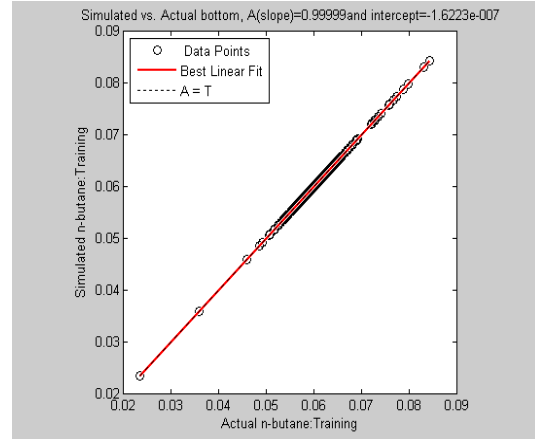


Figure 4.19 Actual and simulated n-butane bottom composition training

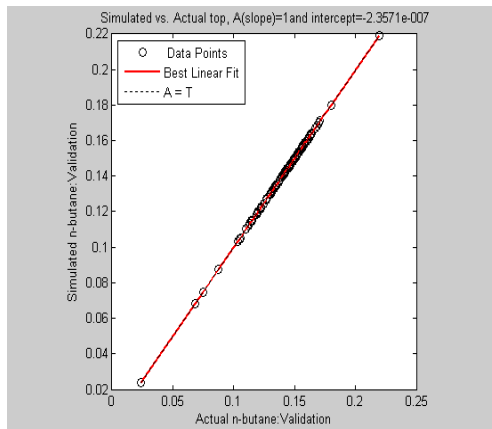


Figure 4.20 Actual and simulated n-butane top composition validation

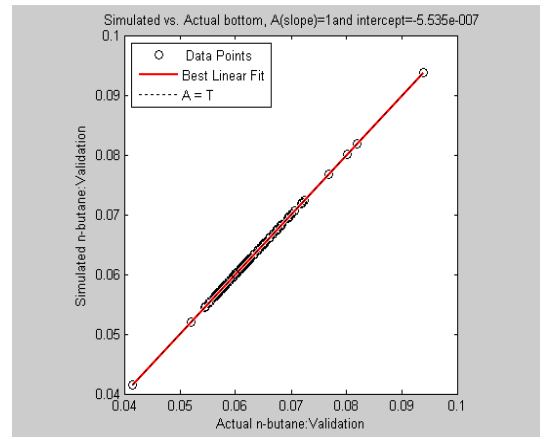


Figure 4.21 Actual and simulated n-butane bottom composition validation

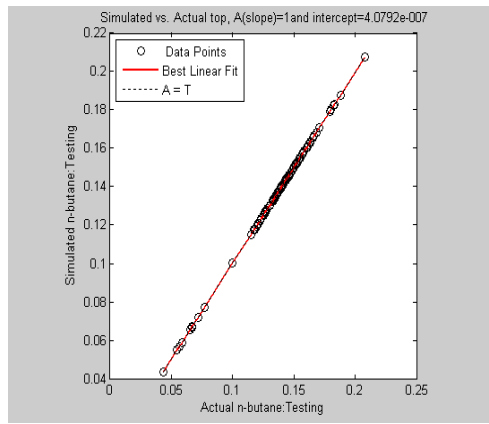


Figure 4.22 Actual and simulated n-butane top composition testing

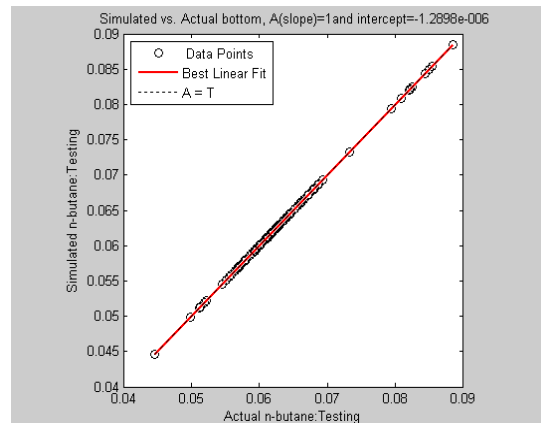


Figure 4.23 Actual and simulated n-butane bottom composition testing

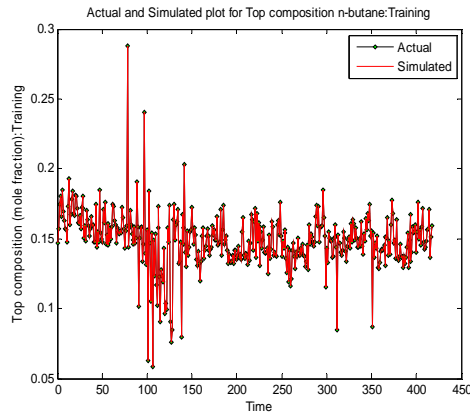


Figure 4.24 Actual and simulated n-butane top composition line plot training

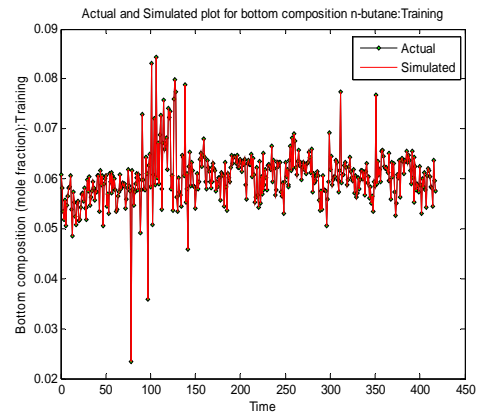


Figure 4.25 Actual and simulated n-butane bottom composition line plot training

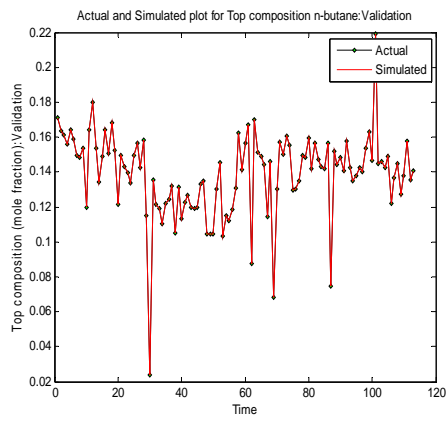


Figure 4.26 Actual and simulated n-butane
top composition line plot validation

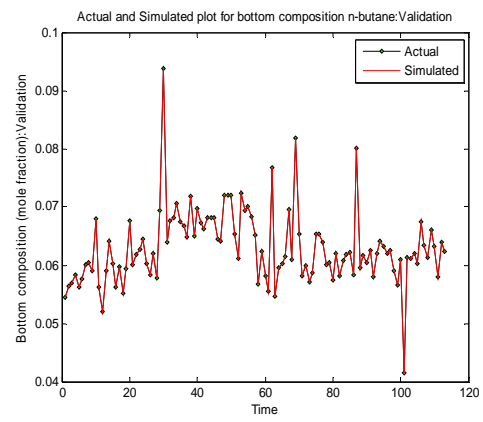


Figure 4.27 Actual and simulated n-butane
bottom composition line plot validation

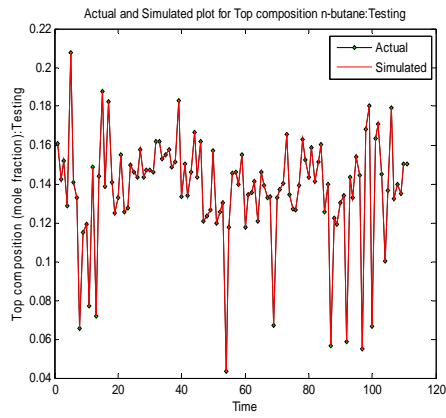


Figure 4.28 Actual and simulated n-butane
top composition line plot testing

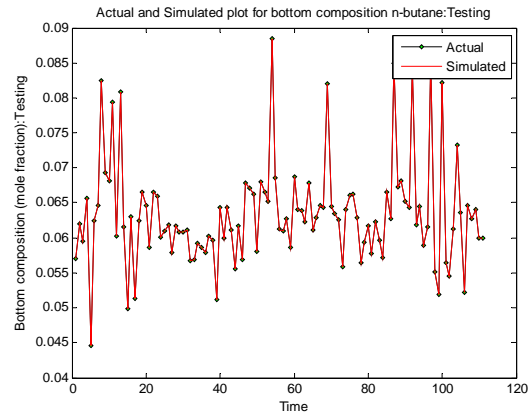


Figure 4.29 Actual and simulated n-butane
bottom composition line plot testing

Table 4.4 Statistical analysis for online n-butane composition prediction

Parameter	Online
rmse_bottom_training	8.05E-07
rmse_top_training	5.83E-07
CDC_bottom_training	98.79
CDC_top_training	98.79
R_bottom_training	1
R_top_training	1
AIC_bottom_training	3239.61
AIC_top_training	2137.29
BIC_bottom_training	3223.48
BIC_top_training	2121.16
MAPE_bottom_training	0.00
MAPE_top_training	0.000285
Cp_bottom_training	1
Cp_top_training	1
rmse_bottom_validation	7.71E-07
rmse_top_validation	5.58E-07
CDC_bottom_validation	98.21
CDC_top_validation	98.21
R_bottom_validation	1
R_top_validation	1
AIC_bottom_validation	816.26
AIC_top_validation	517.54
BIC_bottom_validation	805.35
BIC_top_validation	506.63
MAPE_bottom_validation	0.00
MAPE_top_validation	3.23E-05
Cp_bottom_validation	1
Cp_top_validation	1
rmse_bottom_testing	1.37E-06
rmse_top_testing	9.94E-07
CDC_bottom_testing	98.18
CDC_top_testing	98.18
R_bottom_testing	1
R_top_testing	1
AIC_bottom_testing	765.01
AIC_top_testing	471.58
BIC_bottom_testing	754.17
BIC_top_testing	460.74
MAPE_bottom_testing	0.00
MAPE_top_testing	0.00045
Cp_bottom_testing	1
Cp_top_testing	1

Artificial Neural Network (ANN) is a popular and reliable tool when dealing with problems involving prediction of variables in engineering problems at the present age (Fortuna et al., 2005). It comprises a great number of interconnected neurons ANN that consists of a series of layers with a number of nodes. Every node receives a signal from the network link. The signal is added together before being applied to a specific transfer function to produce the output. The signal from the output will be sent to other node until it reaches the network output. Nodes called neuron are the basic processors of neural network. Each connection between two nodes with a real value is called weight and the values of the weights are obtained by training a set of input and output correlations. The weights are adapted by the learning rule and it has long-term memory for the network.

However the main argument against the widespread use of the neural network is that it is a black box model and can only be represented by the NN structure and cannot be represented by algorithmic equations which are cumbersome in nature. In this work, it can be shown that by the appropriate use of activation functions and with proper pruning of the weights, an equation based neural network model can be obtained to be used in the prediction for the column compositions.

The general equation for the output from the neural network can be given as (for a 3 layer network)

$$y = f^i \left(LW^{3,i} f^i \left(LW^{2,i} f^i \left(IW^{1,i} p + b^1 \right) + b^2 \right) + b^3 \right) \quad (4.10)$$

$IW^{1,i}$ = input weight at layer 1 (input layer)	b^l = bias values at layer 1
$LW^{2,i}$ = layer weight at layer 2 (hidden layer)	b^2 = bias values at layer 2
$LW^{3,i}$ = layer weight at layer 3 (output layer)	b^3 = bias values at layer 3
p = vector inputs to the neural network	y = vector outputs from the neural network
f^i = activation function at layer i	

This equation based neural network model is more robust and stable as compared to the black box model, frequently used by researchers and practitioners and will be the highlight of our research work.

PLS regression is a method that generalizes and combines features from principal component analysis and multiple regressions. This is very useful in data analyses, which are collinear and have incomplete variables. The precision of PLS model is a function of the number of input variables. This is often useful in predicting a set of dependent variables (Y) from a large set of independent variables or predictors (X). PLS has been proven reliable in process monitoring and optimization prediction. PLS interpretation could indicate matrix vector multiplication to a set of bivariate regression. It provides the connection between two operations in algebra matrix and statistics. PLS has the ability to provide the foundation of a multivariable system. It could also demonstrate projection models as long as there is a similarity between the variables (Eriksson et al, 2006).

Based on PLS, the general regression equation (Eriksson et al, 2006) is given as

$$Y = 1 * \bar{y} + XW * C + F \quad (4.11)$$

where $\bar{1} * \bar{y}$ are the variable averages, $W * C$ are the loading weights and F is the residual in Y .

The disadvantages of PLS with further increase in the size of the data sets is that we will start to see inadequacies in the multivariate methods, both in their efficiency and interpretability. PLS coefficients are of interest because it could be simplified when there are several components in the model. The disadvantages of the coefficients for the PLS equation is that information regarding the correlation structure among the response is unknown.

Multivariate regression is the conventional method used to obtain the relationship between the input variables, X and the output variable, Y . It is assumed that the regression analysis is multivariate normal distribution for the entire set of variables and uniform error variance exists across the X variable. The residuals namely have a linear relationship with the predicted variables and the variance of the residuals is the same for all the predicted scores. Regression analysis provides an equation that predicts raw data on the predicted output Y variable from the X variables. The Y can be predicted as a function of X by using an equation in the following form given as,

$$Y' = a + b_0 X_0 + b_1 X_1 + \dots + b_n X_n \quad (4.12)$$

where Y' is the predicted variable on the Y variable, a is the slope represents the predicted change in Y for a one unit increase in X_0 . The slope for each individual predictor is calculated for all other predictors. Then the equation in terms of X with respect to Y' could be obtained (Warner, 2008). The performance of regression analysis methods in practice depends on the form of the data generating process, and how it relates to the regression approach being used. Since the true form of the data-generating process is generally not known, regression analysis often depends to some extent on

making assumptions about this process. These assumptions are sometimes testable if a large amount of data is available. Regression models for prediction are often useful even when the assumptions are moderately violated, although they may not perform optimally. However, the disadvantage in many applications of these regression methods is that it could give misleading results when causality exists on the observation data.

4.5 Model data generation

The manipulated variables are reboiler and reflux flow rate. Once the data set are available, the data set are partitioned in 2 sets and 3 sets which are training and validation, other set training, validation and testing. The percentages of the partition are 65% for training and 35% for validation. For the other set, the percentages of the partition are 65% for training, 18% for validation and 17% for testing.

4.5.1 Neural network, Partial least square (PLS) and Regression Analysis (RA) data sets

One of the objectives of this work is to develop composition predictions online using neural network, partial least square and regression analysis. The composition at the top and bottom for the column in the refinery currently is measured using normal laboratory sampling. Therefore neural network, PLS and RA are used as alternate online methods to predict the composition as they are expected to produce more robust, stable and precise results.

Open loop responses of the reboiler and reflux data set, which include the composition, are used to develop the dynamic neural network architecture. The selected input variables to the network are time delayed including the composition since the models are dynamic in nature and the outputs are the future predictions of composition. The type of dynamic network used for the data set training, training algorithm, adaption learning function, performance function, the data set that are partition, the network

training, the transfer function used is similar as outlined in the previous section. The networks are trained and validated, trained, validated and tested to simultaneously predict the top and bottom composition for the column. The architecture consists of 3 layers which are the input, hidden and output layer. The weights and biases value used in the neural network equation are obtained after training and validation of the neural network. Analysis of variance (ANOVA) for NN is analyzed by using the Statistical Toolbox in MATLAB. From MATLAB, the analysis of variance (ANOVA) using F statistics are produced. The two 'mean square' between groups and within group estimates of the population variance are obtained where the F test statistics is the ratio of the two mean squares.

Table 4.13 shows the important variables involved for the neural network where the open loop responses of the reboiler flow rate and reflux flow rate data set are obtained from plant and simulation. The simulated data is the composition and the rest of the variables are obtained from actual plant data.

Multivariate data are measured based on observations and variables and the data generated for PLS is similar to the data generated in NN. The data used for PLS analysis are performed using multivariate software called SIMCA-P. There are 2 important variables classified which are the primary variable and the observation variable. The primary variable consists of 23 variables surrounding the column and the observation variables are the top and bottom composition. Once the work set has been developed, the PLS model will be fitted with the Partial Least Square equation and it involves the loading weight and residual in terms of the composition of n-butane and average value of the composition of n-butane.

The data generated for Regression Analysis (RA) is also similar to the data generated for NN and PLS. The data for regression are analyzed using the data analysis tool in Excel. The important element of the RA modeling is the range of inputs and

outputs of the data analyzed where the confidence level is set at 95%. Once all the required inputs and outputs are fed to the regression analysis, it will calculate the predicted output, the equation for RA and residual analysis. The regression is based on multivariate linear equation and these input variables are generally shown in equation 3 in terms of the X variable. The combined data consisting of the plant and simulation data are then used to develop the neural network model, represented by the equations as will be shown in the next section. Similar data sets are also used to generate the PLS and regression models for comparison with the neural network predictions for the top and bottom compositions.

4.5.2 Neural network n-butane equation based model

As mentioned in the previous section, the final configuration of the neural network model obtained from the training and validation exercise is given to be of a 10-10-2 network. By applying the general equation (4.10) for this network with the linear activation function, we get the following equation for the top and bottom composition prediction of n-butane where y_1 refers to top composition and y_2 refers to the bottom composition (Mohamed Ramli etc, 2014) ;

$$y = \begin{pmatrix} y_1 \\ y_2 \end{pmatrix} = LW^{2,1} f^1(IW^{1,1} p + b^1) + b^2 \quad (4.13)$$

where the values of the matrix $LW^{2,1}$, $IW^{1,1}$, b^1 and b^2 are given in the appendix

$IW^{1,1}$ = input weight at layer 1 (input layer) b^1 = biases value at layer 1

$LW^{2,1}$ = layer weight at layer 2 (hidden layer) b^2 = biases value at layer 2

p is the inputs to the neural network and for this case study is given by the vector

$$\begin{bmatrix} mv2(k) & mv2(k-1) & mv3(k) & mv3(k-1) & f(k) & f(k-1) & p_{top}(k) & p_{top}(k-1) & p_{bot}(k) & p_{bot}(k-1) \end{bmatrix}^T \quad (4.14)$$

These weights and biases are obtained from the optimum neural network model after validation. On applying the values of the respective weights and biases for the validated model neural network model for equation (4.13) and with further pruning of the values, we get the following equation to represent the neural network model for the composition prediction as in equation below i.e.;

Training, validation and testing

$$y = \begin{bmatrix} y1 \\ y2 \end{bmatrix} = \begin{bmatrix} -0.14 & -0.64 & 0.53 & 0.22 & 0.004 & 0.85 & 0.0047 & -0.19 & -0.27 & -0.96 \\ -0.07 & -0.58 & -0.74 & 0.79 & -1.31 & -0.23 & 2.02 & -1.72 & -0.12 & 0.24 \end{bmatrix} p + \begin{bmatrix} 1.77 \\ 2.50 \end{bmatrix} \quad (4.15)$$

These equations are obtained by simplifying the general equation (4.13) by considering only the hidden layer with inputs weight $IW^{1,1}$ and the output layer with the layer weight $LW^{2,1}$. Initially the matrix input $IW^{1,1}$ is multiplied with the input vector, p and added to biases value b^1 . The activation function of f^1 is determined as unity, the resulting matrix is then multiplied to layer weight 2, $LW^{2,1}$ and added biases value at layer 2, b^2 . By pruning out the small resulting values, the equation is then simplified to the version in Equation 4.15. This equation is a multi input multi output equation based representation of the neural network model for composition prediction of the debutaniser column. This equation is robust in nature and can be easily used as an online estimation for composition in the column, without having to resort to use of complex structure of the neural network, normally difficult to use in an online measurement system.

4.5.3 PLS analysis

After validation, the equation of PLS for prediction of n-butane at top composition is given as

$$Y_{1,PLS} = 0.1335 + \begin{bmatrix} mv2(k) \\ mv2(k-1) \\ mv3(k) \\ mv3(k-1) \\ f(k) \\ f(k-1) \\ p_top(k) \\ p_top(k-1) \\ p_bot(k) \\ p_bot(k-1) \end{bmatrix} \begin{bmatrix} 0.074 \\ -0.075 \\ -0.061 \\ 0.062 \\ -0.067 \\ -0.11 \\ 0.068 \\ -0.017 \\ 0.68 \\ -0.83 \end{bmatrix} + \begin{bmatrix} -0.0034 \\ 0.00071 \\ -0.00065 \\ -0.0017 \\ -0.0011 \\ -0.00076 \\ -0.00043 \\ -7.67e-05 \\ 0.00035 \\ 0.0010 \\ 0.0021 \\ 0.0042 \\ 0.018 \\ 0.0049 \\ \cdot \\ \cdot \\ -0.00032 \end{bmatrix} \quad (4.16)$$

and the equation of PLS for predictions of n-butane at the bottom composition is given as;

$$Y_{2,PLS} = 0.05276 + \begin{bmatrix} mv2(k) \\ mv2(k-1) \\ mv3(k) \\ mv3(k-1) \\ f(k) \\ f(k-1) \\ p_top(k) \\ p_top(k-1) \\ p_bot(k) \\ p_bot(k-1) \end{bmatrix} \begin{bmatrix} 0.0021 \\ -0.0007 \\ -0.0012 \\ 0.0004 \\ -0.0044 \\ 0.0024 \\ 0.062 \\ 0.17 \\ 1.64 \\ -0.073 \end{bmatrix} + \begin{bmatrix} -0.0048 \\ -0.0046 \\ -0.0041 \\ -0.0033 \\ -0.0026 \\ -0.0016 \\ -0.0011 \\ -0.00020 \\ 0.0010 \\ 0.0021 \\ 0.0028 \\ 0.0013 \\ -0.00026 \\ -0.0017 \\ . \\ . \\ 0.00120778 \end{bmatrix} \quad (4.17)$$

The F residual for PLS equation consists of 301 data points for top and bottom composition.

4.5.4 Regression analysis

For the regression model, the equations for the top and bottom prediction n-butane are described below;

$$Y_{1,RA} = 0.0008 \quad mv2(k) - 0.00078 \quad mv2(k-1) + 0.00049 \quad mv3(k) \\ - 0.00061 \quad mv3(k-1) - 0.0011f(k) + 0.0019 \quad f(k-1) + 1.015 \quad p_top(k) \\ - 0.051 \quad p_top(k-1) + 0.0027 \quad p_bot(k) - 0.010p_bot(k-1) - 0.078 \quad (4.18)$$

$$Y_{2,RA} = 0.0019 \quad mv2(k) - 0.0018 \quad mv2(k-1) - 0.0020 \quad mv3(k) \\ + 0.0016 \quad mv3(k-1) + 0.0041f(k) - 0.006 \quad f(k-1) + 0.30 \quad p_top(k) \\ - 0.23 \quad p_top(k-1) + 0.81p_bot(k) - 0.059 \quad p_bot(k-1) + 0.27 \quad (4.19)$$

4.5.5 Analysis of variance (ANOVA) n-butane

Top composition

From Table 4.5, the adjusted R^2 is smaller than R^2 value. This is because the number of cases is relatively small and the number of predictor variables is relatively large. There are a total of 301 samples data observations. The sum of square regression is calculated to be 0.0906 and the total sum of square is calculated to be 0.0917. The multiple R is calculated based on the square root of ratio between these 2 values. The multiple R is proportional to the total variance in the actual and predicted value. The standard error shows the ratio between the standard deviation to the square root of number of observations. The degree of freedom (df) is the variation between the sample size and number of groups with confidence level 95%.

The sum of square (SS) consists of regression, residual and total. It is explained by the difference between each group mean and the overall mean. The value of mean squares (MS) are obtained from the ratio of the sum of the square (SS) to the degree of freedom (df). The F value is obtained from the ratio of MS of regression to MS of residual. From the ANOVA outlined in Table 4.5, the F value obtained is 2562. It indicate that the between estimate groups is more than 2562 times the within group estimate. The F value is very small. In addition the calculated population means are not constant and the F value is bigger than 1.83. Therefore the hypothesis analysis may not be rejected. The standard deviation (s) may also be determined from the MS of residual. The s value is 1.88×10^{-3} . The analysis is used to determine the hypothesis between the actual and predicted value of n-butane composition.

Bottom composition

Table 4.6 also shows that the adjusted R^2 is smaller than the R^2 value. This is because the number of cases is relatively small and the number of predictor variables is relatively large. There are a total of 301 samples data observations. The multiple R is defined and based on the square root of ratio regression sum of square to total sum of square. The multiple R is proportional to the total variance in the actual and predicted value. The standard error shows the ratio between the standard deviation to the square root of number of observations. The confidence level is 95%. From the ANOVA outlined in Table 4.6, the F value is 127. It indicates that the between groups estimate is more than 127 times the within group estimate. The significance F value is relatively very small. Different population mean are recorded. The F value is larger than 1.83. Therefore the hypothesis analysis may not be rejected. The standard deviation s could also be determined from the MS of the residual. The s value is 6.05×10^{-3} . The analysis is used to determine the hypothesis between the actual and predicted value of n-butane composition.

Table 4.5. ANOVA of the n-butane top composition

<i>Regression Statistics</i>					
Multiple R	0.99				
R Square	1.00				
Adjusted R Square	0.98				
Standard Error	0.0018				
Observations	301				

ANOVA					
	<i>df</i>	<i>SS</i>	<i>MS</i>	<i>F</i>	<i>Significance F</i>
Regression	10	0.0906	0.0090	2562	2.34E-276
Residual	290	0.0010	3.53E-06		
Total	300	0.0917			

Table 4.6. ANOVA of n-butane bottom composition

<i>Regression Statistics</i>	
Multiple R	0.95
R Square	1.00
Adjusted R Square	0.93
Standard Error	0.0060
Observations	301

ANOVA					
	<i>df</i>	<i>SS</i>	<i>MS</i>	<i>F</i>	<i>Significance F</i>
Regression	10	0.0467	0.0046	127	5.73E-100
Residual	290	0.0106	3.66E-05		
Total	300	0.0573			

4.5.6. Comparison NN, PLS and RA

Figure 4.30, shows the observed versus predicted values of the top composition of n-butane from NN equation. It is apparent that all the points fall close to the 45 degree line. The calculated RMSE for the NN equation is 6.6×10^{-7} . The R^2 of the regression line indicates the goodness of fit. The value of the R^2 is 1. Figure 4.31, shows the composition line plot of the actual and neural network equation for n-butane top composition.

Table 4.7 the variables involved in the PLS analysis, regression analysis and neural network n-butane

Inputs		
Variable	Symbol	Description
MV2	mv2 (k)	Manipulated reboiler flow rate
	mv2 (k-1)	Lag MV2
MV3	mv3 (k)	Manipulated reflux flow rate
	mv3 (k-1)	Lag MV3
Temp 6	f (k)	Debutaniser feed temp
	f (k-1)	Lag Temp 6
Component 3	p_top (k)	Top composition n-butane
	p_top (k-1)	Lag composition top
	p_bot (k)	Bottom composition n- butane
	p_bot (k-1)	Lag composition bottom
Outputs		
	p_top (k+1)	Future predictions n- butane top
	p_bot (k+1)	Future predictions n- butane bottom

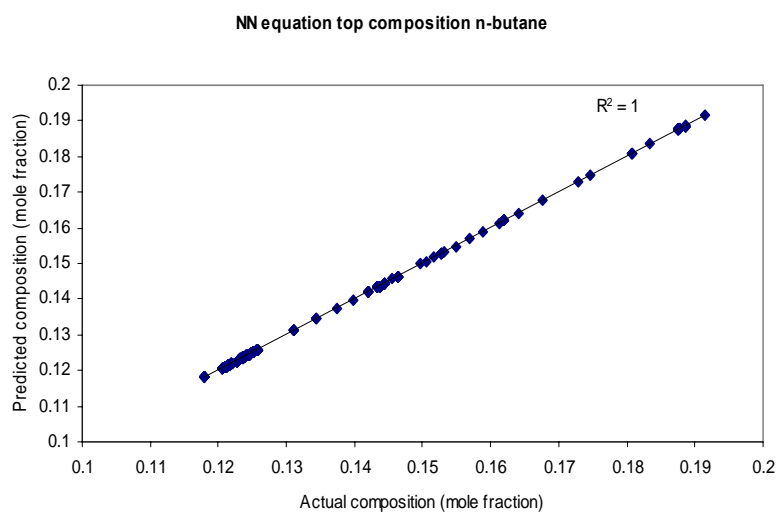


Figure 4.30 Prediction versus actual value neural network equation top composition n-butane

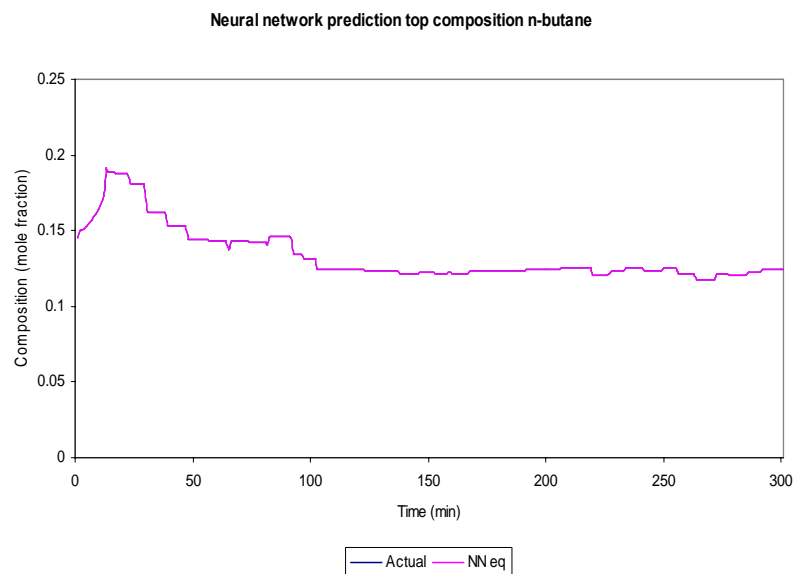


Figure 4.31 Prediction and actual value for top composition n-butane line plot

Figure 4.32, shows the observed versus predicted values of the bottom composition of n-butane from NN equation. It is apparent that all the points fall close to the 45 degree line. The calculated RMSE for the NN equation is 3.88×10^{-7} . The R^2 of the regression line indicates the goodness of fit. The value of the R^2 is 1. Figure 4.33, shows the composition line plot of the actual and neural network equation for n-butane bottom composition. The CDC value for top composition is calculated to be at 26.33 and for bottom composition is calculated to be 100 where the high CDC value indicates better prediction. The regression value of R for top and bottom composition is 1. Thus the prediction between the actual and simulated is similar. For the AIC and BIC, low value is preferred as it indicates better prediction. For the AIC and BIC top composition, low value is preferred and calculated to be 2572 and 2555 respectively. Cp value is close to 1. The Cp value for bottom and top composition are calculated to be 1 and the MAPE close to 0. The MAPE for top and bottom are calculated to be -0.0005 and -0.00132.

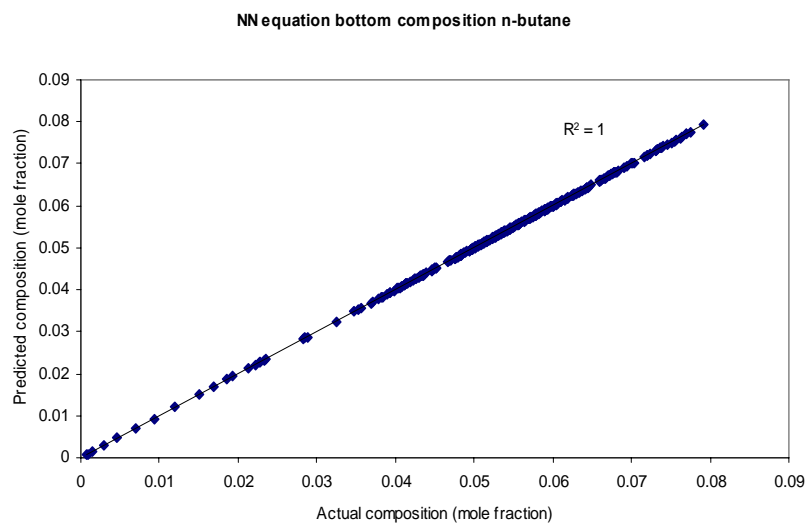


Figure 4.32 Prediction versus actual value neural network equation bottom composition n-butane

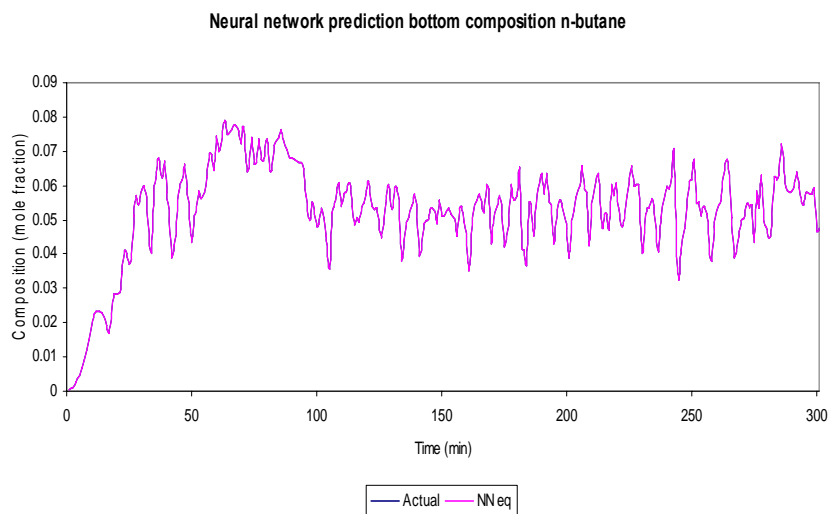


Figure 4.33 Prediction and actual value for bottom composition n-butane line plot

Figure 4.34, shows the observed versus predicted values of the top composition of n-butane from PLS equation. It is apparent that all the points fall close to the 45 degree line. The calculated RMSE for the PLS equation is 0.002004. The R^2 of the regression line indicates the goodness of fit. The value of the R^2 is 0.9851. Scattered data points

around the regression line are an indication of poor prediction. Figure 4.35, shows the composition line plot of the actual and PLS equation n-butane top composition.

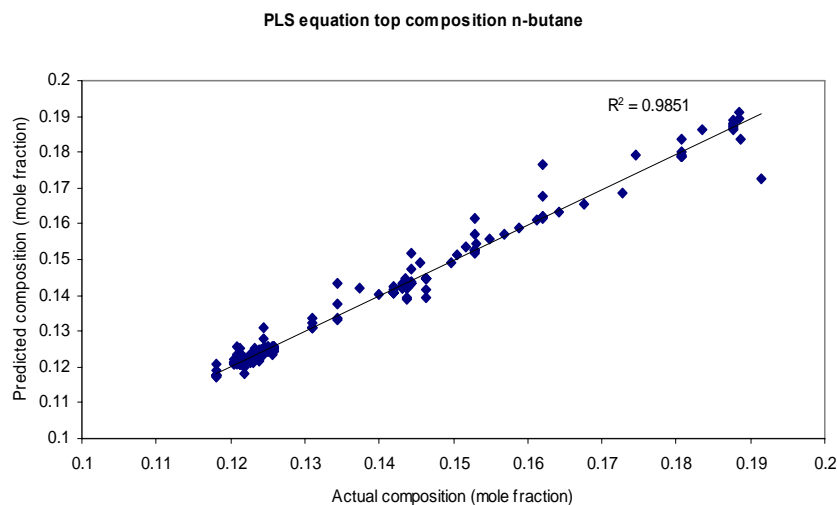


Figure 4.34. Prediction versus actual value PLS equation top composition n-butane

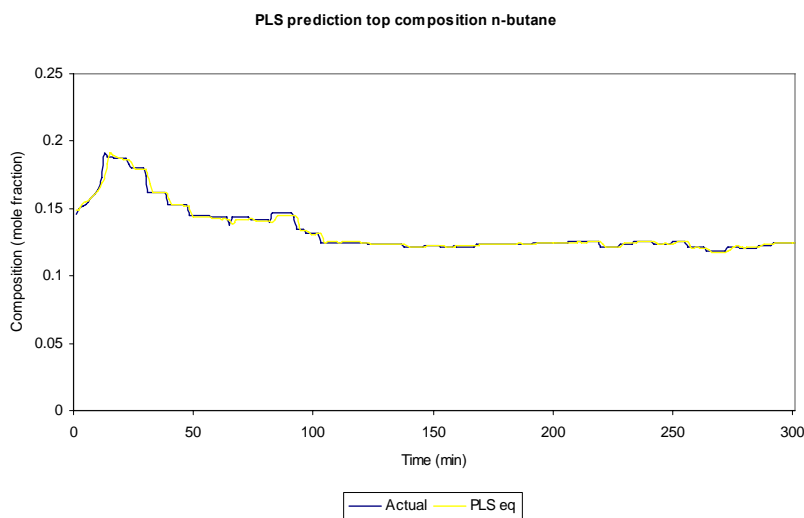


Figure 4.35 Prediction and actual value for top composition n-butane line plot

Figure 4.36, shows the observed versus predicted values of the bottom composition of n-butane from PLS equation. The calculated RMSE for the PLS equation is 0.005989. The R^2 of the regression line indicates the goodness of fit. The value of the R^2 is 0.8117. Scattered data points around the regression line are an indication of poor

prediction by PLS equation. Figure 4.37, shows the composition line plot of the actual and PLS equation n-butane bottom composition. The CDC value for top composition is calculated to 17.66 and for bottom composition is calculated to be 56.66. The CDC value calculated compared to neural network, indicates that NN would be able to predict the composition of n-butane better than PLS. The regression value of R for top and bottom composition is 0.99 and 0.9 respectively. Thus the prediction between the actual and simulated is almost similar but the prediction by NN is much better than PLS. For the AIC and BIC, low value is preferred as it indicates better prediction. For the AIC and BIC for top composition, low value is preferred and calculated to be 2573 and 2558 respectively. For the AIC and BIC for bottom composition, low value is preferred and calculated to be 2073 and 2059. Cp value is close to 1. The Cp value for bottom and top composition are calculated to 0.9 and 0.99 respectively and the MAPE should be close to 0. The MAPE for top and bottom are calculated to be -0.034 and -0.97. Based on this analysis the prediction by NN performs better than PLS.

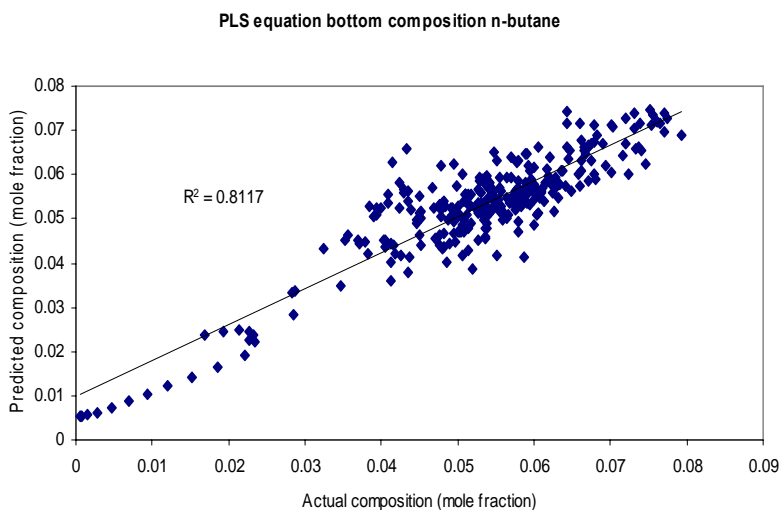


Figure 4.36 Prediction versus actual value PLS equation bottom position n-butane

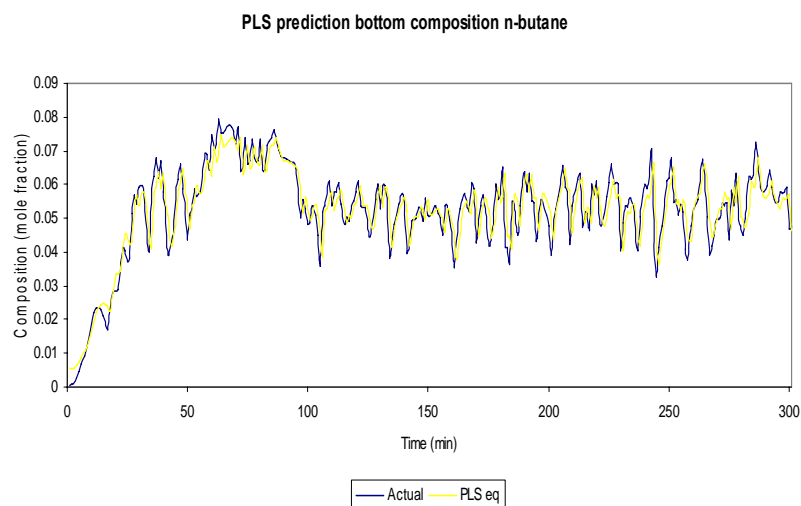


Figure 4.37. Prediction and actual value for bottom composition n-butane line plot

Figure 4.38, shows the observed versus predicted values of the n-butane top composition using regression analysis equation. A good model is identified by having all data points fall close to the 45 degree line. The calculated RMSE for the regression equation is 0.002128. The R^2 of the regression line indicates the goodness of fit. The value of the R^2 is 0.9888. Figure 4.39 shows the composition line plot of the actual and RA equation of the n-butane top composition.

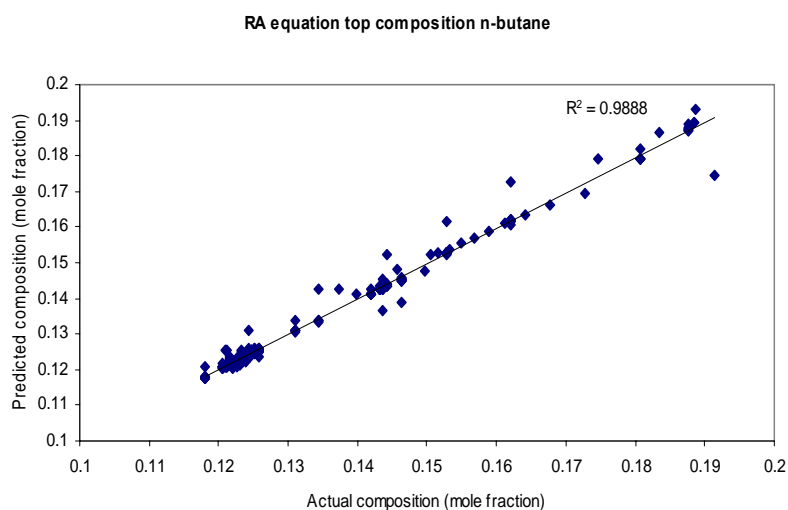


Figure 4.38. Prediction versus actual value RA equation top composition n-butane

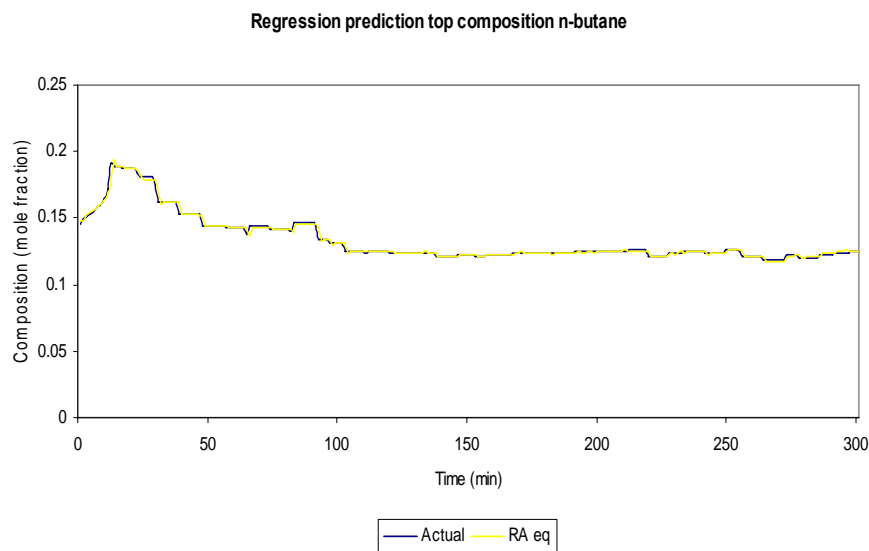


Figure 4.39. Prediction and actual value for top composition n-butane line plot

Figure 4.40, shows the observed versus predicted values of the n-butane bottom composition using regression analysis equation. The points are scattered as shown in the figure by RA equation. This indicates poor prediction by RA equation. The calculated RMSE for the normal regression equation is 0.006433. The R^2 of the regression line indicates the goodness of Fit. The value of the R^2 is 0.8148. Figure 4.41, shows the composition line plot of the actual and RA equation n-butane bottom composition. The CDC value for top composition is calculated to 17.33 and for bottom composition is calculated to be 56.66. The CDC value calculated compared to neural network, indicates that NN would be able to predict the composition of n-butane is better than RA. The regression value of R for top and bottom composition is 0.99 and 0.89 respectively. Thus the prediction between the actual and simulated is almost similar but the prediction by NN is much better than RA. For the AIC and BIC, low value is preferred as it indicates better prediction. For the AIC and BIC for top composition, low value is preferred and calculated to be 2580 and 2560 respectively. For the AIC and BIC for bottom composition, low value is preferred and calculated to be 2074 and 2058. Cp

value is close to 1. The Cp value for bottom and top composition are calculated to 0.89 and 0.99 respectively and the MAPE should be close to 0. The MAPE for top and bottom are calculated to be 0.058 and -2.67. Based on this analysis the prediction by NN performs better than RA.

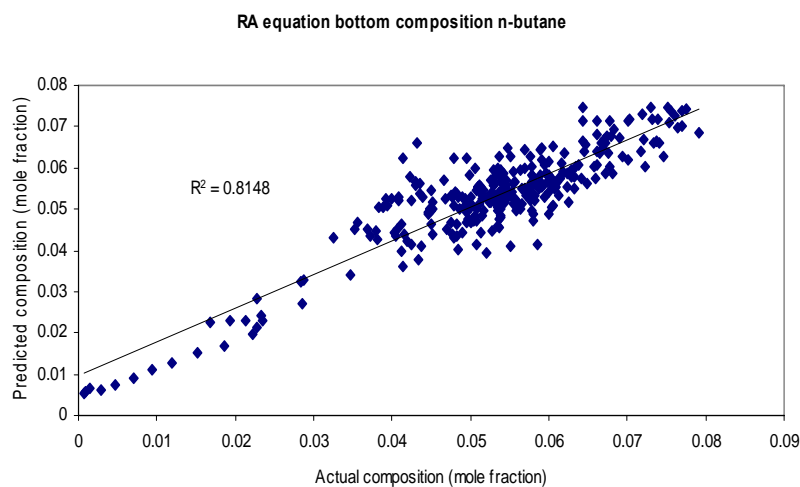


Figure 4.40. Prediction versus actual value RA equation bottom composition n-butane

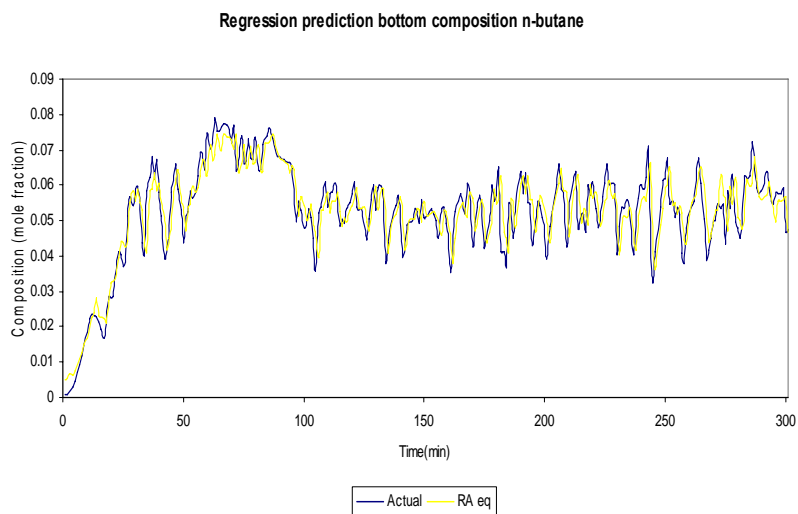


Figure 4.41. Prediction and actual value for bottom composition n-butane line plot

Table 4.8. n-butane statistical analysis of NN equation, PLS equation and RA equation

Parameter	NN eq	PLS eq	RA eq
rmse_bottom	3.88E-07	0.0059	0.0064
rmse_top	6.6E-07	0.0020	0.0021
CDC_bottom	100	56.66	56.66
CDC_top	26.33	17.66	17.33
R_bottom	1	0.90	0.89
R_top	1	0.999	0.993
AIC_bottom	-1957.26	-2073.63	-2074.26
AIC_top	-2572.72	-2573.78	-2580.29
BIC_bottom	-1942.43	-2059.8	-2058.44
BIC_top	-2555.89	-2558.96	-2560.46
MAPE_bottom	-0.0013	0.97	-2.67
MAPE_top	-0.0005	0.034	0.058
Cp_bottom	1	0.90	0.89
Cp_top	1	0.999	0.992

4.5.7 Residual analysis

Figure 4.42 and Figure 4.43 shows the residual of the neural network equation, PLS equation and normal regression equation for top and bottom composition n-butane respectively. From the plot, the residual of the neural network equation is small compared to PLS equation and NR equation. This shows that neural network is able to predict the top and bottom composition n-butane with high accuracy and small error compared to PLS and RA. Residual analysis is very important to evaluate the deviation between actual and prediction for NN, PLS and RA.

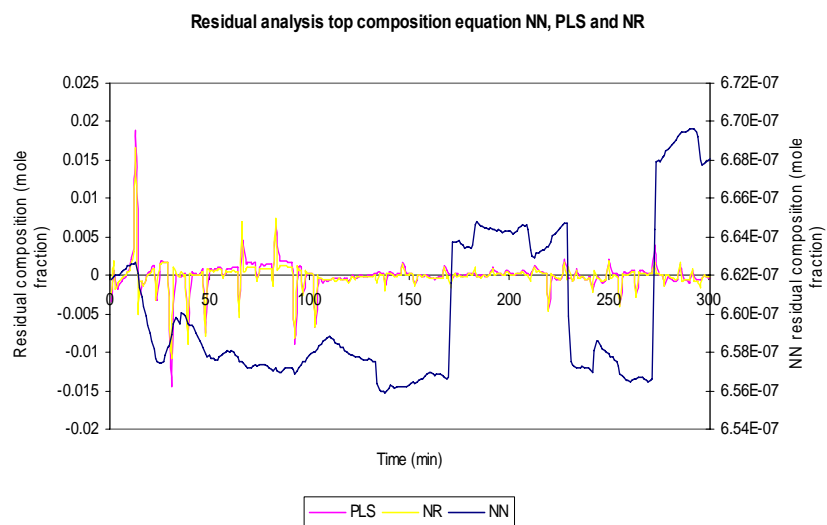


Figure 4.42. Residual analysis for neural network equation, PLS equation and regression analysis equation top composition n-butane

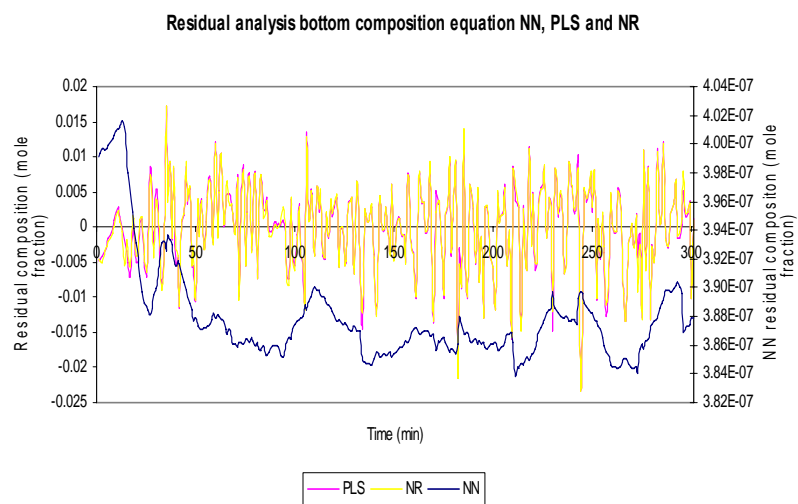


Figure 4.43. Residual analysis for neural network equation, PLS equation and regression analysis equation bottom composition n-butane

The method used to prediction of i-butane is similar as the above and are shown in the appendices.

4.6 Neural network design

The main objective of this work is to develop temperature prediction online using neural network. The temperature at the top and bottom respectively for the column in the refinery is currently measured based on step test. Neural network is used as a benchmark because it is able to predict the temperature with more accuracy and precision. Neural network could also handle non-linearities in the process variable surrounding the column. Neural network comprises a great number of interconnected neurons in a series of layers with a number of nodes. The nodes are the basic processors of neural network. Each connection between two nodes with a real value is called weight.

Open loop response of the overhead pressure, reboiler and reflux data which includes the top and bottom temperature are used to develop the dynamic neural network architecture. The selected input variables to the network including the temperature are time delayed while the outputs are the future predictions of temperature. The type of dynamic network used for training, validation and testing the data set, the training algorithm, early stopping criteria to train the network, the adaptation learning function, and the performance function is similar outlined in the previous section.

The networks are trained to predict simultaneously the top and bottom temperature. Prior to implementing the neural network, the data are arranged by combining the open loop response from the simulation and plant data. The data set are then trained until the network reaches its epoch and meet its performance criteria. The data set are also validated and tested as the network is trained.

4.6.1 Neural network top and bottom temperature (MIMO model)

Table 4.8 shows the important variables in the neural network where the data set are combined from the manipulated variable overhead pressure, reboiler flow rate and reflux flow rate for top and bottom temperature..

Table 4.9 Important variables for neural network prediction

Inputs		
Variable	Symbol	Description
MV1	mv1 (k)	Manipulated overhead pressure
	mv1(k-1)	Lag MV1
MV2	mv2 (k)	Manipulated reboiler flow rate
	mv2 (k-1)	Lag MV2
MV3	mv3 (k)	Manipulated reflux flow rate
	mv3 (k-1)	Lag MV3
Temp 6	f (k)	Debutaniser feed temp
	f (k-1)	Lag Temp 6
Temperature	T_top (k)	Top temp
	T_top (k-1)	Lag top temp
	T_bot (k)	Bottom temp
	T_bot (k-1)	Lag bottom temp
Outputs		
	T_top (k+1)	Future predictions top temp
	T_bot (k+1)	Future predictions bottom temp

The inputs for the neural network are from mv1 (k) to T_bot (k-1). The outputs are the variable T_top (k+1) and T_bot (k+1).

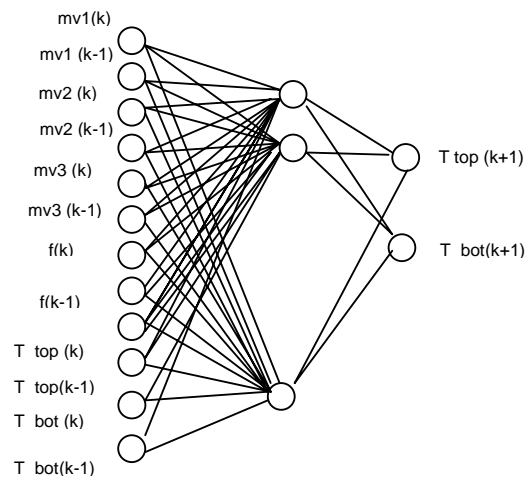


Figure 4.44 Neural network architecture for top and bottom temperatures

Figure 4.44 shows the neural network architecture of the n-butane composition prediction

Table 4.10. Neural network architecture

Parameters	Description	
Network	NARX series parallel network (newnarxsp)	
Category	With partitioning divided into 2	with partitioning divided into 3
Training function	TRAINLM	TRAINLM
Adaptation learning function	LEARNGDM	LEARNGDM
Performance function	MSE	MSE
Epochs	1000	1000
Goal	1e-6	1e-6
Number of layers	2	2
Layer 1: Number of Neuron Transfer function	12 PURELIN	12 PURELIN
Layer 2: Number of Neuron Transfer function	2 PURELIN	2 PURELIN

4.6.2 With partition into 3

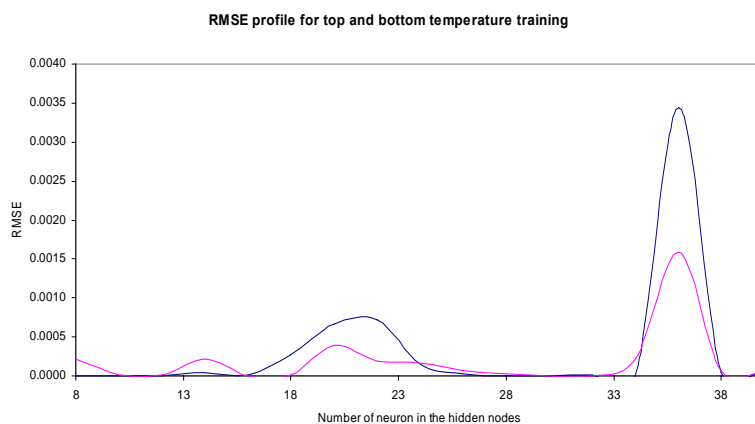


Figure 4.45 Profile of the RMSE training

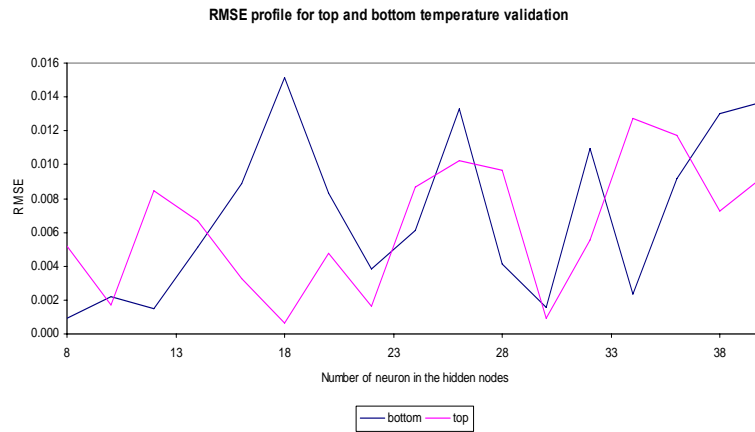


Figure 4.46 Profile of the RMSE validation

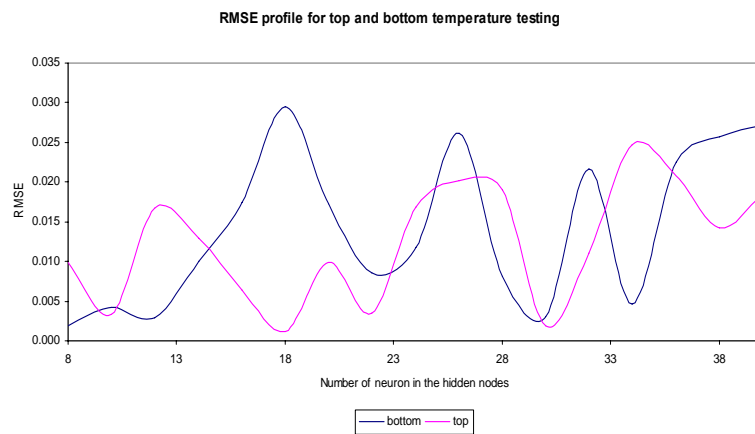


Figure 4.47 Profile of the RMSE testing

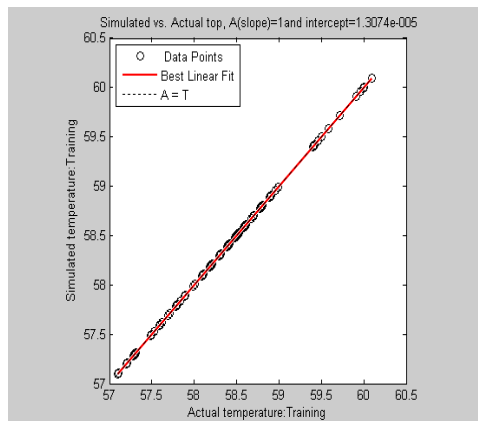


Figure 4.48 Actual and simulated top temperature training

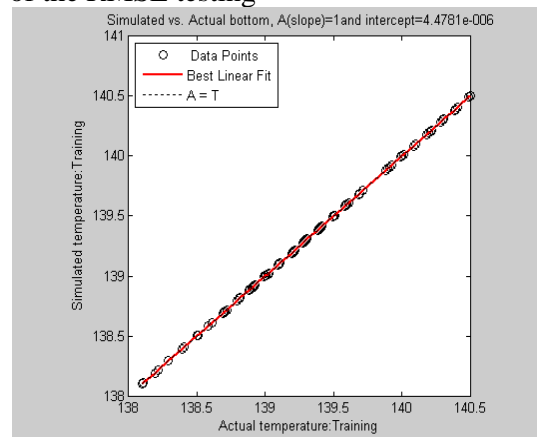


Figure 4.49 Actual and simulated bottom temperature training

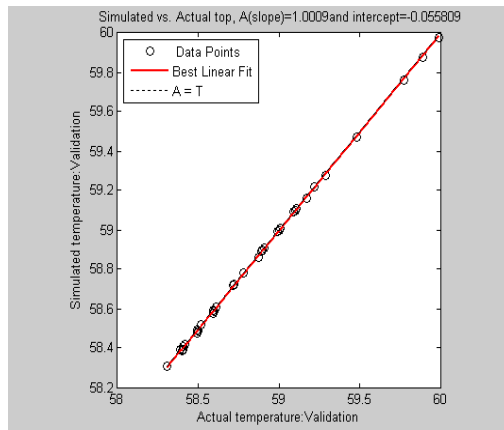


Figure 4.50 Actual and simulated
top temperature validation

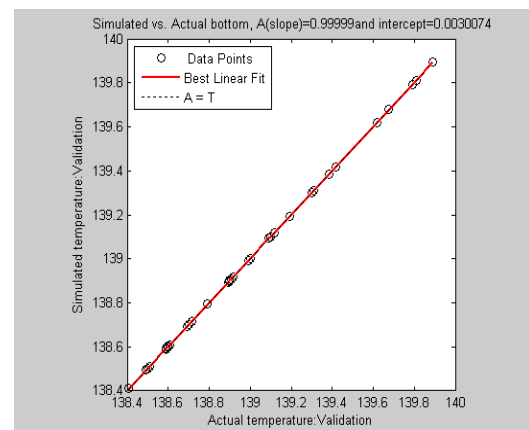


Figure 4.51 Actual and simulated
bottom temperature validation

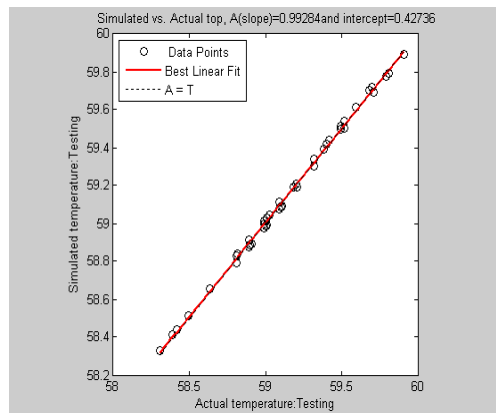


Figure 4.52 Actual and simulated
top temperature testing

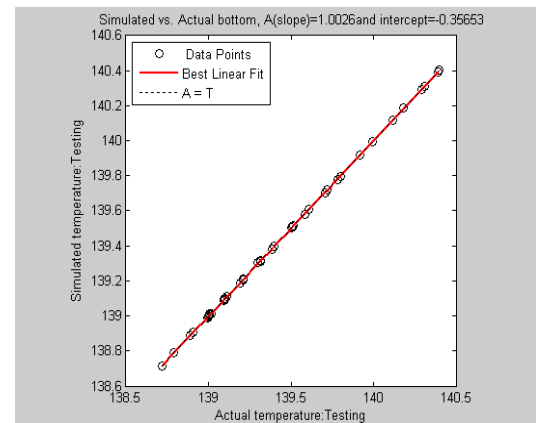


Figure 4.53 Actual and simulated
bottom temperature testing

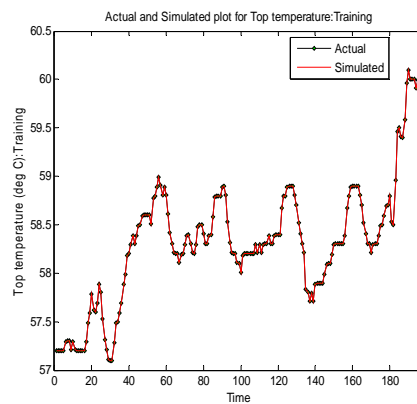


Figure 4.54 Actual and simulated
top composition line plot training

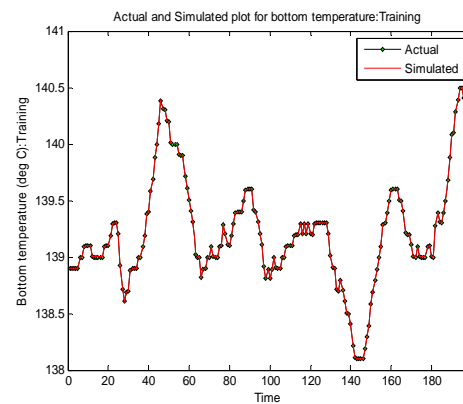


Figure 4.55 Actual and simulated
bottom composition line plot training

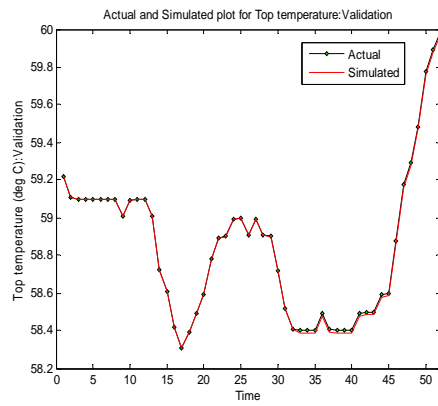


Figure 4.56 Actual and simulated
top temperature line plot validation

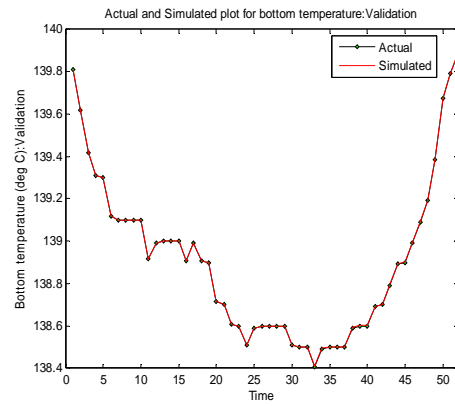


Figure 4.57 Actual and simulated
bottom temperature line plot validation

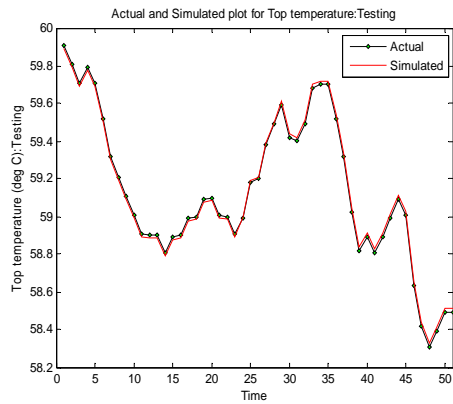


Figure 4.58 Actual and simulated
top temperature line plot testing

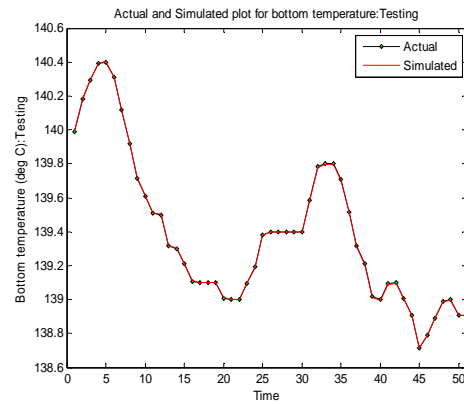


Figure 4.59 Actual and simulated
bottom temperature line plot testing

Figures 4.45 to 4.47 show the profile with the change in the hidden nodes in the hidden layer. Figures 4.48 to 4.59 show the top and bottom temperature prediction for training, validation and testing. The amount of data that are partitioned according to training is 65%, for validation is 18% and for testing is 17%. From the result, it can be concluded that the analysis are similar to previous section. Table 4.11 shows the statistical analysis with partition. From the analysis it can be concluded that the optimum number of neurons in the hidden layer for the neural network is 12

Table 4.11 Statistical analysis for temperature with 3 partitions

Parameter	Open loop
rmse_bottom_training	1.99E-06
rmse_top_training	8.74E-06
CDC_bottom_training	79.69
CDC_top_training	79.18
R_bottom_training	1
R_top_training	1
AIC_bottom_training	30.77
AIC_top_training	135.57
BIC_bottom_training	43.92
BIC_top_training	148.72
MAPE_bottom_training	1.10E-06
MAPE_top_training	-8.67E-06
Cp_bottom_training	1.00E+00
Cp_top_training	1
rmse_bottom_validation	0.0014
rmse_top_validation	0.0084
CDC_bottom_validation	76.47
CDC_top_validation	78.43
R_bottom_validation	0.99
R_top_validation	0.99
AIC_bottom_validation	5.07
AIC_top_validation	32.83
BIC_bottom_validation	12.88
BIC_top_validation	40.64
MAPE_bottom_validation	0.00066
MAPE_top_validation	-0.0089
Cp_bottom_validation	0.99
Cp_top_validation	0.99
rmse_bottom_testing	0.0029
rmse_top_testing	0.016
CDC_bottom_testing	82
CDC_top_testing	94
R_bottom_testing	0.99
R_top_testing	0.99
AIC_bottom_testing	21.07
AIC_top_testing	19.59
BIC_bottom_testing	28.80
BIC_top_testing	27.32
MAPE_bottom_testing	-0.00047
MAPE_top_testing	0.0063
Cp_bottom_testing	0.99
Cp_top_testing	0.99

4.7 Neural network, PLS and RA modeling temperature prediction

The objective of this work is to develop temperature prediction online using neural network, partial least square and regression analysis. The temperature at the top and bottom for the column is available from the open loop response (step test) for overhead pressure flow rate, reflux flow rate and reboiler flow rate. Therefore neural network, PLS and RA are used as a benchmark to predict the temperature as they are expected to produce more accurate and precise results.

Open loop response of the overhead pressure, reboiler and reflux data set, which include the temperature are used to develop the dynamic neural network architecture. The selected input variables to the network are time delayed including the temperature. The outputs are the future predictions of the temperature. The purpose of having lags to the inputs of neural network is to establish a dynamic network. Statistical analysis are also performed for comparison between PLS and RA.

4.7.1 Neural network equation based

The final configuration of the neural network model obtained from the training and validation exercise is given to be of a 12-12-2 network. By applying the general equation (4.10) for this network with the linear activation function, we get the similar equation outlined in the previous section for the top and bottom temperature prediction where $y1$ refers to top temperature and $y2$ refers to the bottom temperature.

p is the inputs to the neural network and for this case study is given by the vector

$$\begin{bmatrix} mv1(k) & mv1(k-1) & mv2(k) & mv2(k-1) & mv3(k) & mv3(k-1) & f(k) & f(k-1) & T_{top}(k) & T_{top}(k-1) & T_{bot}(k) & T_{bot}(k-1) \end{bmatrix}^T \quad (4.20)$$

The equation below represents the matrix for temperature prediction for training, validation and testing data set;

$$y = \begin{bmatrix} y1 \\ y2 \end{bmatrix} = \begin{bmatrix} -0.16 & -0.14 & 0.04 & -0.002 & -0.094 & -0.95 & 1.03 & -0.61 & -0.71 & 0.81 & 0.16 & -0.049 \\ 0.42 & 0.07 & 0.04 & 0.20 & -0.30 & -0.19 & 0.12 & -0.28 & 0.35 & -0.29 & -0.48 & 0.168 \end{bmatrix} p + \begin{bmatrix} -0.28 \\ -0.22 \end{bmatrix} \quad (4.21)$$

4.7.2 PLS model

After validation, the equation of PLS for prediction top temperature is given as

$$Y_{top} = 58.555 + \begin{bmatrix} mv1(k) \\ mv1(k-1) \\ mv2(k) \\ mv2(k-1) \\ mv3(k) \\ mv3(k-1) \\ f(k) \\ f(k-1) \\ T_{top}(k) \\ T_{top}(k-1) \\ T_{bot}(k) \\ T_{bot}(k-1) \end{bmatrix} \begin{bmatrix} -0.57 \\ -0.9 \\ -0.02 \\ -0.02 \\ -0.04 \\ -0.04 \\ -0.19 \\ 0.13 \\ 1.07 \\ 0.7 \\ 0.3 \\ -0.3 \end{bmatrix} + \begin{bmatrix} -0.019 \\ -0.023 \\ -0.024 \\ \cdot \\ \cdot \\ \cdot \\ \cdot \\ \cdot \\ \cdot \\ \cdot \\ \cdot \\ \cdot \\ \cdot \\ \cdot \\ 0.1439 \end{bmatrix} \quad (4.22)$$

and the equation of PLS for predictions bottom temperature is given as,

4.7.4 Analysis of variance (ANOVA) results for neural network model

Top temperature

From Table 4.12, the adjusted R^2 is smaller than R^2 value. The discussion analysis is similar in the previous section 4.5.5 and this is the results shown below.

Bottom temperature

Table 4.13 also show that the adjusted R^2 is smaller than the R^2 value.

Table 4.12. ANOVA of the n-butane top temperature

<i>Regression Statistics</i>					
Multiple R	0.98				
R Square	1.00				
Adjusted R Square	0.97				
Standard Error	0.094				
Observations	301				

ANOVA					
	<i>df</i>	<i>SS</i>	<i>MS</i>	<i>F</i>	<i>Significance F</i>
Regression	12	126.33	10.52	1170.25	2.30E-236
Residual	288	2.59	0.0089		
Total	300	128.92			

Table 4.13. ANOVA of n-butane bottom temperature

<i>Regression Statistics</i>					
Multiple R	0.98				
R Square	1.00				
Adjusted R Square	0.96				
Standard Error	0.087				
Observations	301				

ANOVA					
	<i>df</i>	<i>SS</i>	<i>MS</i>	<i>F</i>	<i>Significance F</i>
Regression	12	66.06	5.50	725.90	2.73E-207
Residual	288	2.18	0.00758		
Total	300	68.24			

4.7.5. Comparison NN, PLS and RA

Table 4.14. The variables involved in the PLS analysis, regression analysis and neural network

Inputs		
Variable	Symbol	Description
MV1	mv1 (k)	Manipulated overhead pressure
	mv1 (k-1)	Lag MV1
MV2	mv2 (k)	Manipulated reboiler flow rate
	mv2 (k-1)	Lag MV2
MV3	mv3 (k)	Manipulated reflux flow rate
	mv3 (k-1)	Lag MV3
Temp 6	f (k)	Debutaniser feed temp
	f (k-1)	Lag Temp 6
Component 3	T_top (k)	Top temperature
	T_top (k-1)	Lag top temperature
	T_bot (k)	Bottom temperature
	T_bot (k-1)	Lag bottom temperature
Outputs		
	T_top (k+1)	Future predictions top
	T_bot (k+1)	Future predictions bottom

Figure 4.60, shows the observed versus predicted values of the top temperature for NN equation. Figure 4.61, shows the composition line plot of the actual and neural network equation for top temperature.

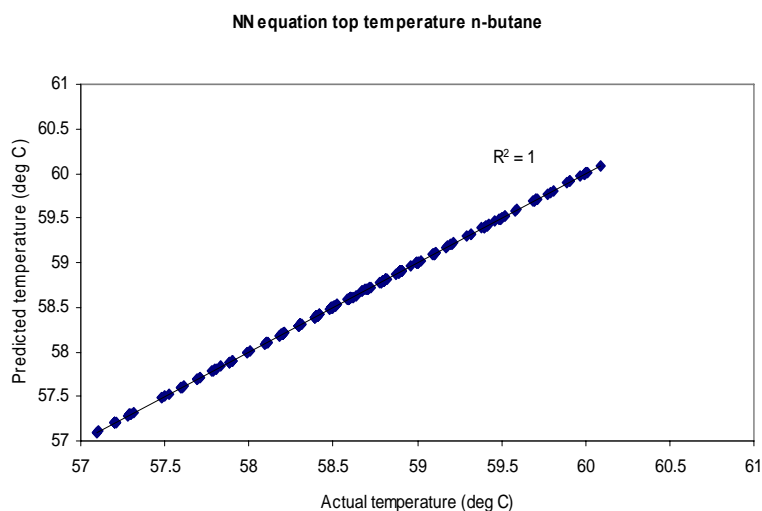


Figure 4.60 Prediction versus actual value neural network equation top temperature

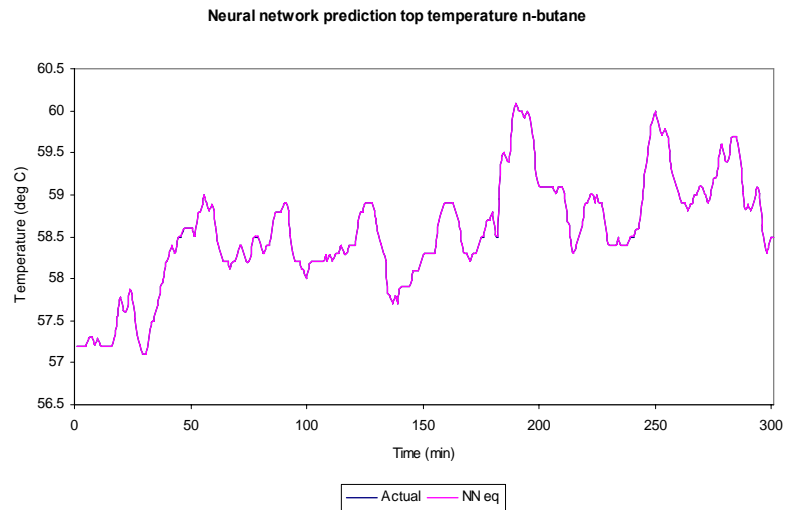


Figure 4.61. Prediction and actual value for top temperature line plot

Figure 4.62, shows the observed versus predicted values of the bottom temperature for NN equation. Figure 4.63, shows the temperature line plot of the actual and neural network equation for bottom temperature.

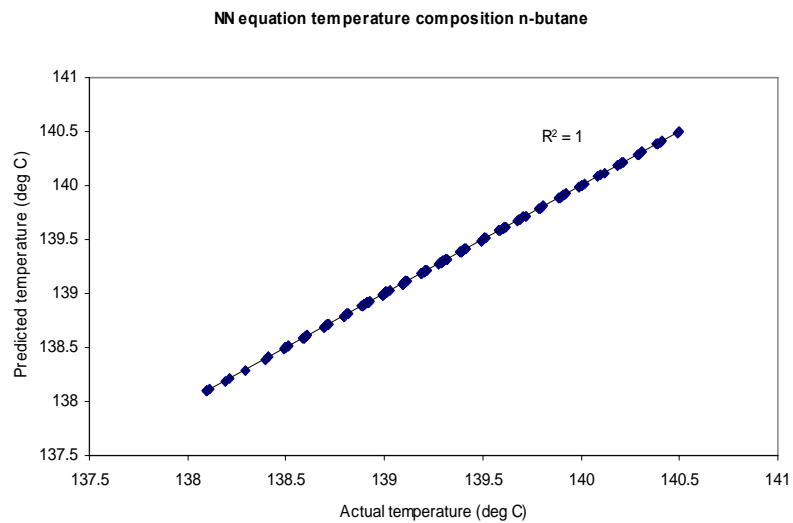


Figure 4.62. Prediction versus actual value neural network equation bottom temperature

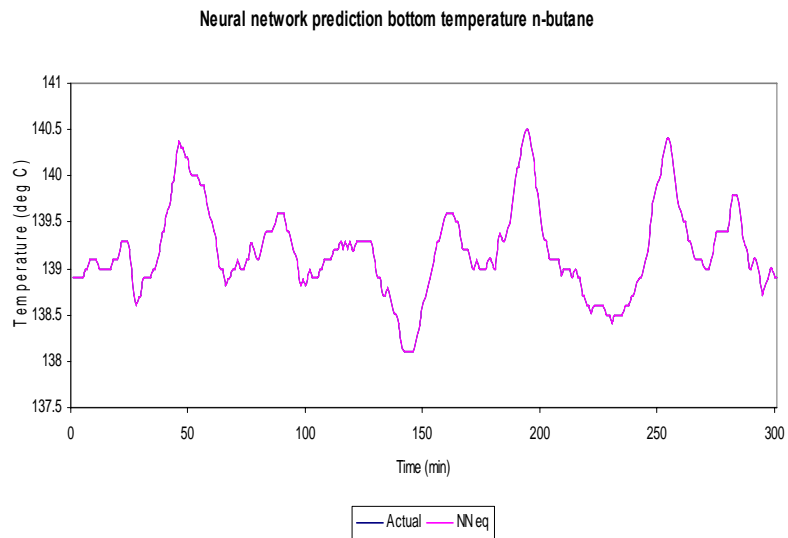


Figure 4.63 Prediction and actual value for bottom temperature line plot

Figure 4.64, shows the observed versus predicted values of the top temperature of n-butane from PLS equation. Figure 4.65, shows the temperature line plot of the actual and PLS equation n-butane top temperature.

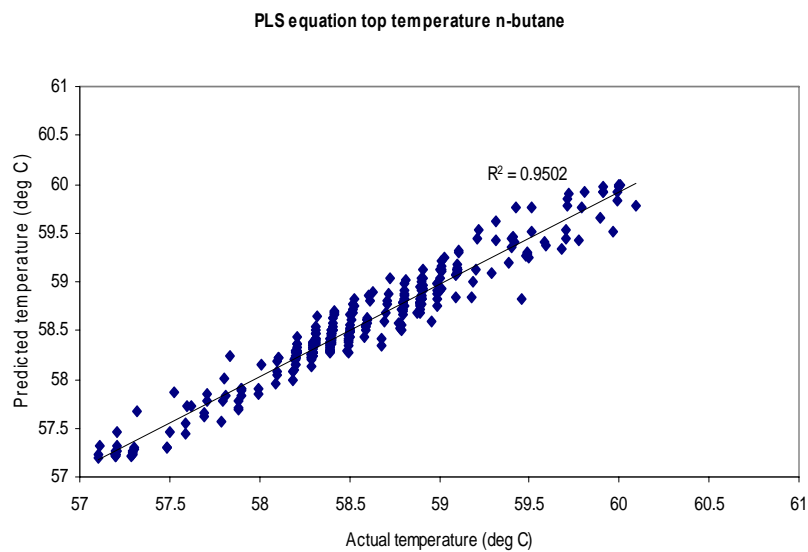


Figure 4.64. Prediction versus actual value PLS equation top temperature

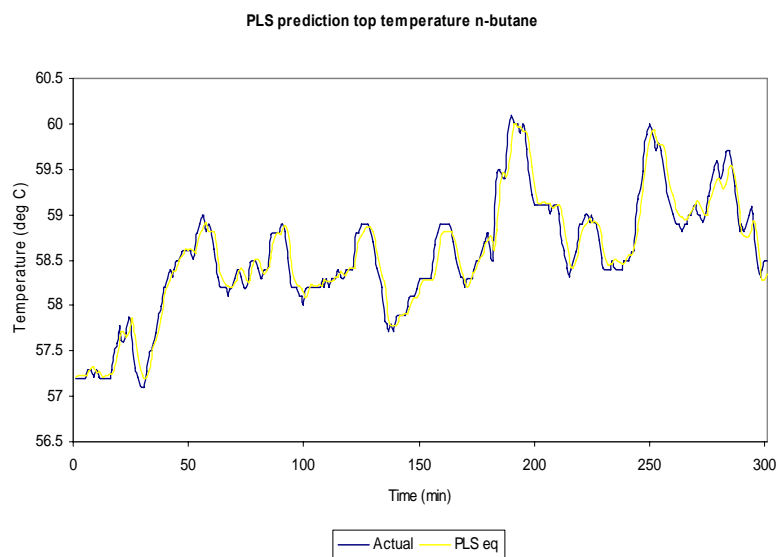


Figure 4.65. Prediction and actual value for top temperature line plot

Figure 4.66, shows the observed versus predicted values of the bottom temperature for PLS equation. Figure 4.67, shows the temperature line plot of the actual and PLS equation temperature

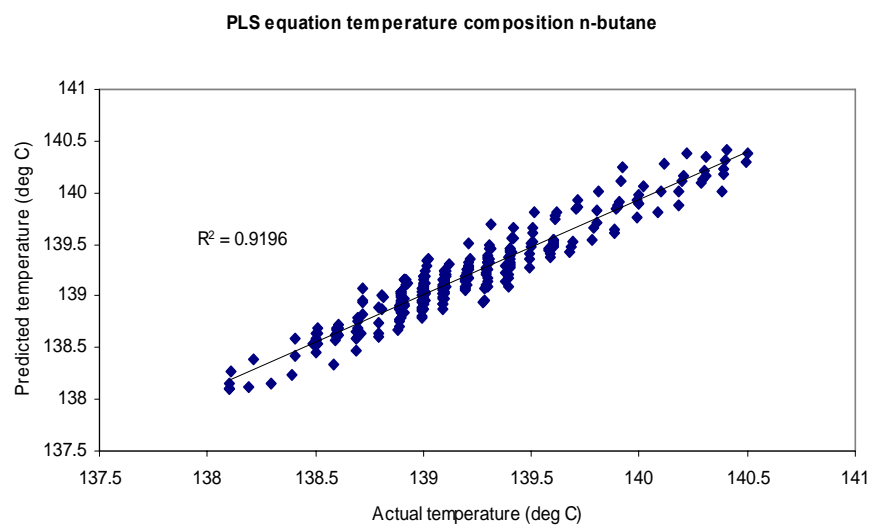


Figure 4.66 Prediction versus actual value PLS equation bottom temperature

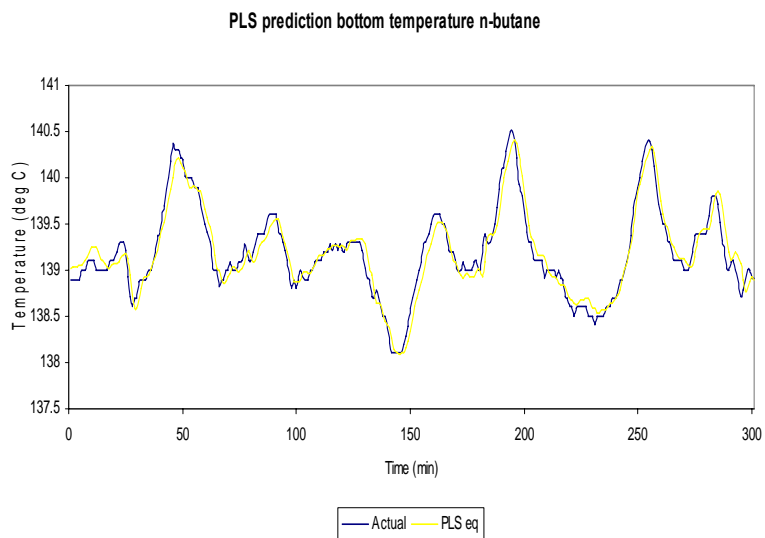


Figure 4.67. Prediction and actual value for bottom temperature line plot

Figure 4.68, shows the observed versus predicted values of the top temperature using regression analysis equation. Figure 4.69 shows the composition line plot of the actual and RA equation for the top temperature.

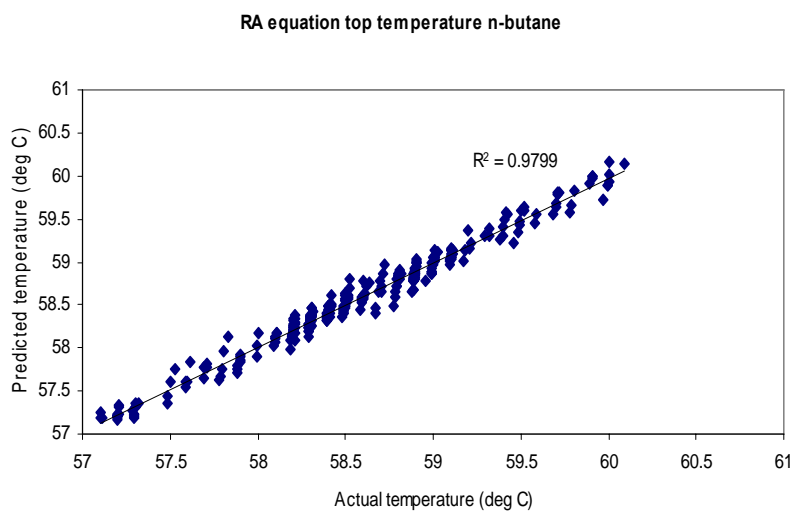


Figure.4.68 Prediction versus actual value RA equation top temperature

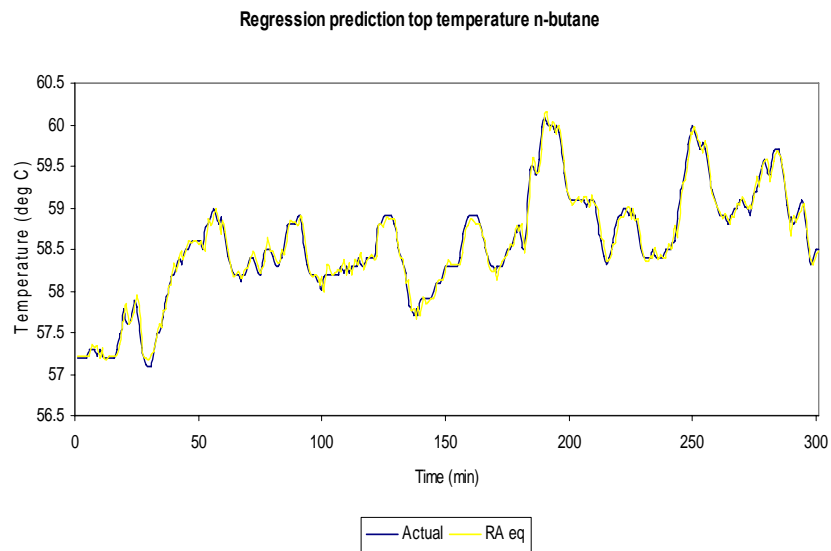


Figure 4.69 Prediction and actual value for top temperature line plot

Figure 4.70 shows the observed versus predicted values of the bottom temperature using regression analysis equation. Figure 4.71, shows the composition line plot of the actual and RA equation n-butane bottom temperature.

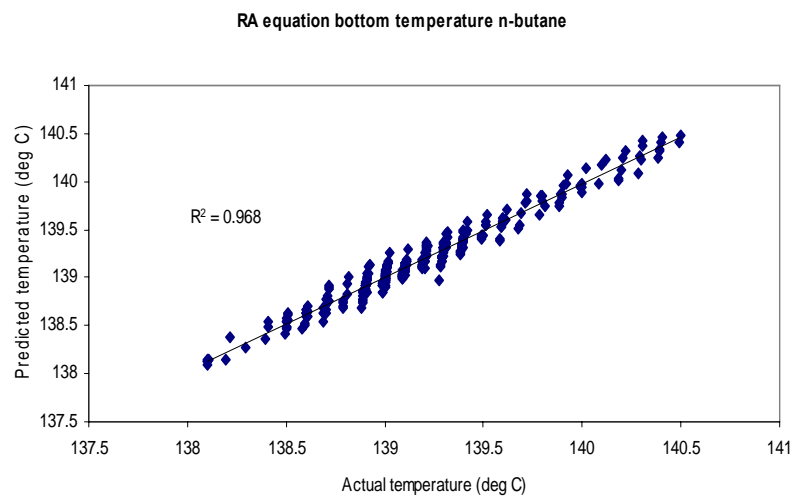


Figure 4.70. Prediction versus actual value RA equation bottom temperature

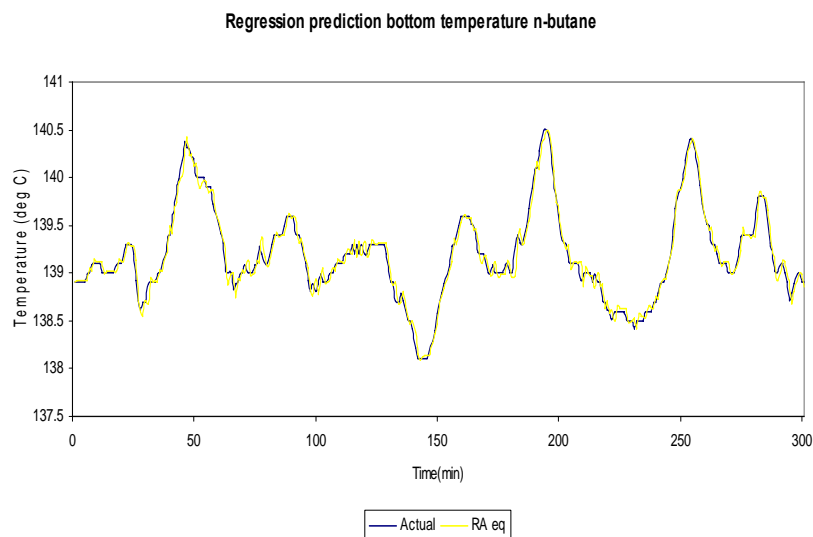


Figure 4.71. Prediction and actual value for bottom temperature line plot

Table 4.15. Statistical analysis of NN equation, PLS equation and RA equation

Parameter	NN eq	PLS eq	RA eq
rmse_bottom	4.74E-07	0.13	0.101
rmse_top	4.28E-08	0.14	0.12
CDC_bottom	79.66	59	59.66
CDC_top	81.66	58.66	56.66
R_bottom	1	0.95	0.97
R_top	1	0.97	0.98
AIC_bottom	63.12	107.09	63.23
AIC_top	293.16	309.72	297.88
BIC_bottom	77.95	121.91	78.063
BIC_top	307.99	324.54	312.71
MAPE_bottom	-3.4E-07	8.65E-06	-4.6E-05
MAPE_top	7.28E-08	-2.8E-06	-0.00763
Cp_bottom	1	0.95	0.97
Cp_top	1	0.97	0.98

4.7.6 Residual analysis

Figure 4.72 and Figure 4.73 shows the residual of the neural network equation, PLS equation and normal regression equation for top and bottom temperature respectively.

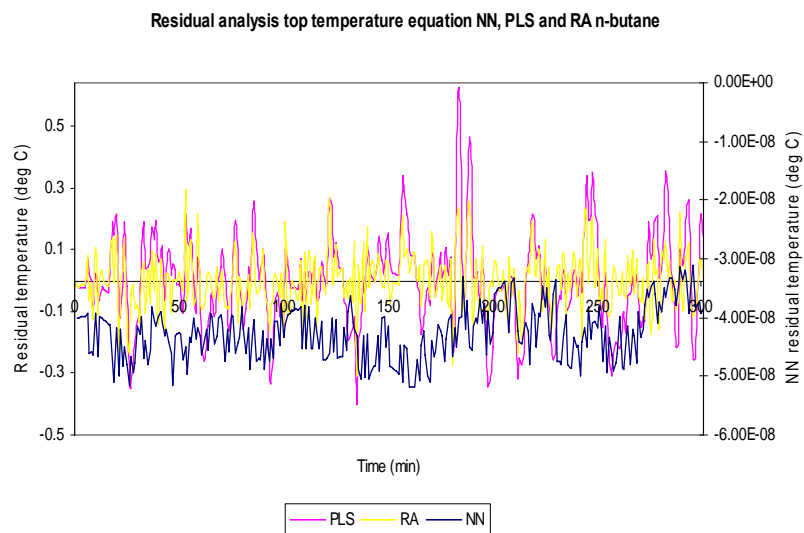


Figure 4.72. Residual analysis for neural network equation, PLS equation and regression analysis equation top temperature

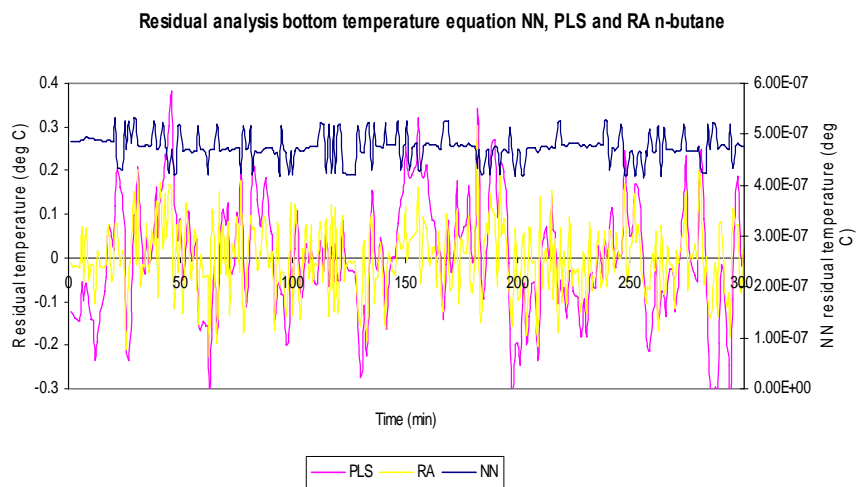


Figure 4.73. Residual analysis for neural network equation, PLS equation and regression analysis equation bottom temperature

The prediction of the composition and temperature at the top and bottom of a debutaniser column using the equation based neural network model which is then compared to other methods such as PLS and regression analysis. All of the results give optimum results in predicting the compositions and temperature but it can be concluded that NN equation gives the best prediction compared to other models based on the RMSE value.

CHAPTER 5: HYBRID NEURAL NETWORK TO ESTIMATE COMPOSITION AND TEMPERATURE FOR THE DEBUTANISER COLUMN

5.1 Introduction

Nonlinear system for process control is a challenging topic at present stage. In the past, neural network and hybrid neural networks were interesting research areas for modeling of nonlinear system. The main contribution of this thesis is in the use of online closed loop and open loop data for training neural network. Hybrid model, the top and bottom composition prediction by first order principle are added together with residual composition predicted using neural network. The second hybrid model also consists of first principle model in terms of energy balance stage by stage for the column. The top and bottom temperature by first order principle are also added together with the residual temperature predicted using neural network. The neural network prediction for residual composition and residual temperature where the inputs were trained, validate and test to obtain the optimum number of neuron in the hidden layer. This research also involves a single dynamic neural network model with lagged inputs to predict the top and bottom composition and temperature simultaneously. Reliable operation and control of such a column normally depends on its ability to measure composition and temperature in an online and accurate fashion. The normal method of utilizing hardware sensors is normally expensive, tedious and non-robust in nature especially for composition measurement which is highly expensive and difficult to handle and operate in an offline manner. This makes it slow in its operation and highly instable when used for online control purposes. A suitable alternative is to utilize soft sensors and one method which is becoming popular is through the use of neural network models. However since these neural network models rely heavily on available data, the use of a combination of first principle model with neural network in a hybrid form is a

more practical approach that is being increasingly applied at the present moment, some of which are given in the next few paragraphs.

The various work presented so far on the use of neural network based hybrid model involves the use of black box model neural network. This is non-versatile and non-robust in nature as well as being difficult to see the correlation between the inputs and outputs to the system. In this work, which has its main novelty and contribution, we have prepared using an equation based neural network model in hybrid with the first principle model for the column. The neural network is MIMO (Multi input and multi output) in nature, where it is used to predict the residual composition and temperature of the top and bottom prediction for the column. The residuals are then added to the first principle model in a hybrid fashion, to predict the actual composition and temperature of the top and bottom for the column. The other contribution of this work is that it utilizes a mixture of online close loop and open loop data and for these data available online and simulation data for those not available online by training the neural network models

5.2 Hybrid model construction

There are 2 types of configuration reported for the hybrid neural network in the literature. There are the series and parallel approaches as seen in Figure 5.1 (Ng & Hussain, 2004). The series approach forces the output from the neural network to be consistent while the parallel approach allows the model to assist the network. The parallel approach is used to estimate the residual of the variable by means of a simplified model, which is the approach we are using in this work.

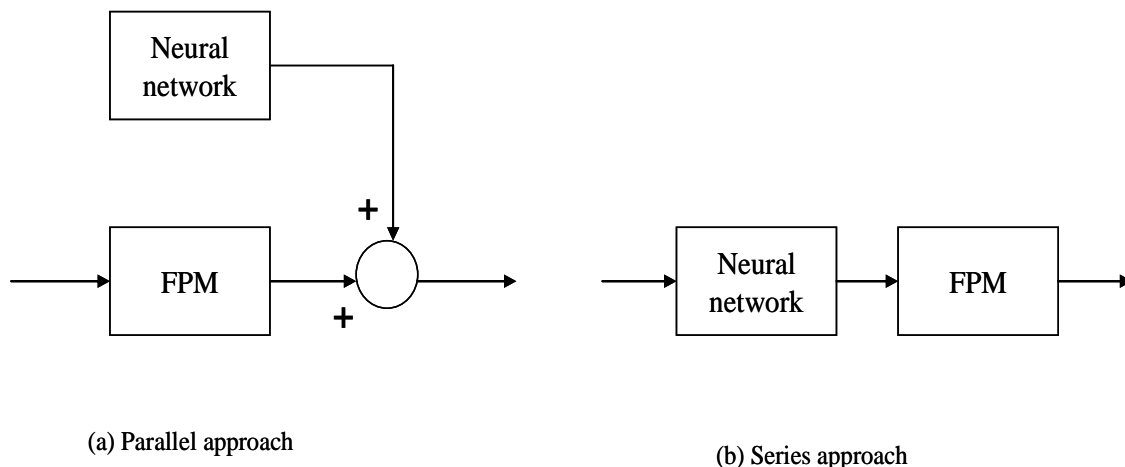


Figure 5.1 Two approaches used in HNN with FPM

5.3 Hybrid simulation of the distillation column

Different combinations could be developed for hybrid models but in order to build them, the detailed knowledge of the process is essential. A conventional method and approach involves applying a first basis, which is established upon the first principles model, while the neural network is used to calculate the unknown parameters (Ng & Hussain, 2004). Our study utilizes the parallel approach, which combines the first principle model with the residual (the difference between model and actual estimation). One of the NN model involves residual composition predictions where the inputs are the manipulated variables that include the reboiler flow rate, reflux flow rate, temperature, as well as the residual top and bottoms composition of n-butane while the outputs are the prediction of the residual top and bottom composition of n-butane while the other NN model is for residual temperature predictions which involve inputs such as the manipulated variables, overhead pressure, reboiler flow rate, reflux flow rate, temperature, residual top and bottoms temperature whereas the outputs are the prediction of the residual top and bottom temperature. The NN model receives these

input variables and predicts the output residual compositions and temperatures accordingly. The outputs results are then combined together with the first principles model to estimate the top and bottoms composition of n-butane as well as the top and bottoms temperature of the column. However in this study, which is one highly novel feature of the work, the neural network predictions utilise an equation based model instead of merely a black box system as in many other applications.

5.4 Mathematical modelling of the distillation column

The dynamic model for the column in terms of mass and energy balances need is first developed. The model is based upon first principles for simulating the column performance.

To simplify the system, the following assumptions were made in this study (Stephanopoulos, 1984):

1. Vapour holdup on each tray was negligible.
2. The molar heat of vaporization of n-butane and i-butane components is equal.
3. The relative volatility was constant throughout the column.
4. The tray efficiency is kept at close to 100%.

The momentum balance for each tray are neglected and it is assumed that the molar flow rate of the liquid leaving each tray is related to the liquid hold up of the tray using the Francis weir formula.

The execution of dynamic simulation was achieved by first simulating the steady state simulation. After that the simulation are turned into the dynamic mode. Then all the controllers are added to the simulation by using dynamic assistant available in HYSYS. The simulations are run from manual mode to automatic mode when the process reaches is set point. The feed composition are measured intermittently by off-line by inputs to

the simulation. To perform the control under dynamic simulation the offline measurement are used

The important step is to develop the dynamic equation of the debutaniser column in terms of the basic mass and energy balance given below:

Mass balance (2 component system i-butane and n-butane)

Feed tray

$$\frac{d(M_{fxf})}{dt} = F_{fc}f + L_{f+1}x_{f+1} + V_{f-1}y_{f-1} - L_{f}x_f - V_{f}y_f \quad (5.1)$$

Top tray

$$\frac{d(M_{nxn})}{dt} = F_{r}x_D + V_{n-1}y_{n-1} - L_{n}x_n - V_{n}y_n \quad (5.2)$$

Bottoms tray

$$\frac{d(M_{1x1})}{dt} = L_{2}x_2 + V_{yb} - L_{1}x_1 - V_{1}y_1 \quad (5.3)$$

i th tray

$$\frac{d(M_{ixi})}{dt} = L_{i+1}x_{i+1} + V_{i-1}y_{i-1} - L_{i}x_i - V_{i}y_i \quad (5.4)$$

Reflux drum

$$\frac{d(M_{RDxD})}{dt} = V_{n}y_n - (F_R + F_D)x_D \quad (5.5)$$

Column base

$$\frac{d(M_{BxB})}{dt} = L_{1}x_1 - V_{yB} - F_{B}X_B \quad (5.6)$$

Antoine equation (Alphaz et al, 2002)

$$y_{n,i} = \frac{p_{n,i}}{p_T} = \frac{x_{n,i}}{p_T} p \quad (5.7)$$

F is the feed molar flow rate (kmol/hr), L is the liquid molar flow rate (kmol/hr) and V is the vapour molar flow rate (kmol/hr). h is the liquid molar enthalpy (kJ/kmol), H is the vapour molar enthalpy (kJ/kmol) and Q is the heat contribution (kJ/hr). All the values in the variables shown in the equations (5.1) to (5.7) are extracted from the process simulator, HYSYS. The specific heat for the energy balance is calculated for every stage. The equation is constructed in a SIMULINK environment in MATLAB. The dynamic mass balance is used to determine the composition of n-butane for every stage in the column. The dynamic energy balance is used to determine the temperature in every stage of the column, which has a total of 35 stages

The vapor pressure, P as a function of temperature;

$$\log_{10} P = A + \frac{B}{T} + C \log_{10} T + DT + ET^2 \quad (5.8)$$

where P = vapor pressure, kPa , A, B, C, D and E = coefficients for chemical compound, T = temperature (K) where P = vapor pressure, kPa , A, B, C, D and E = coefficients for chemical compound n-butane, T = temperature (K). A is 27, B is -1904.9, C is -7.18, D is -6.68×10^{-11} and E is 4.2×10^{-6} . The coefficients for i-butane, A is 31.25, B is -1953, C is -8.8, D is 8.92×10^{-11} and E is 5.75×10^{-6} .

The vapor pressures are used to calculate the top composition n-butane in equation 5.8, where T is the top temperature and the saturated vapor for all the components could be calculated. Equation 5.7 is used to determine the vapor mole fraction of n-butane at the top. The purpose of using a hybrid model for the column is because the first

principles model cannot predict the actual top and bottoms composition and temperature accurately since many of the parameters in this model are empirical in nature and deviate from the actual values, where the neural network is used to estimate this deviation.

V is the vapor molar flow rate, F_R molar reflux flow rate, F_D is the distillate molar flow rate, M_{RD} is the liquid hold up at the reflux drum. L_1 is the liquid flow rate at the column base, V is the vapor molar flow rate, F_B is the bottom product flow rate, M_B is the liquid hold up at the column base. The first principle model is defined as a simple linear model around a certain operating point. Simple linear first principles model to represent the nonlinear dynamics of the distillation column. The FPM model used in the current work is a simplified model that is used in the HYSYS simulation. In other words, the first principle model that has been used is a very crude approximation of the system, and hence, it is not able to predict both the composition and temperature. The results are expected. This is why hybrid prediction is necessary.

The model obtained for the mass balance for the column is obtained by substituting the constants values for vapor molar flow rate, liquid molar flow rate, reflux molar flow rate and distillate molar flow rate as shown below;

The equation n-butane for reflux drum, equation 5.5;

$$M_{RD} \frac{dx_D}{dt} = 1.72y_{35} - 0.71x_D \quad (5.9a)$$

The equation n-butane column base equation 5.6;

$$M_B \frac{dx_B}{dt} = 168x_1 - 81y_B - 82x_B \quad (5.9b)$$

The equation i-butane for reflux drum, equation 5.5;

$$M_{RD} \frac{dx_D}{dt} = 1.68y_{35} - 0.51x_D \quad (5.9c)$$

The equation i-butane column base equation 5.6;

$$M_B \frac{dx_B}{dt} = 160 x_1 - 82 y_B - 75 x_B \quad (5.9d)$$

The model obtained for the mass balance is calculated stage by stage by integration using equations 5.1 to 5.6. By using equations 5.5 and 5.7, top composition could be obtained. Once the mole fraction of n-butane (x_D) is obtained at the distillate, then equation 5.7 is used to determine the mole fraction of vapour (y_D). Equation 5.6 is used to determine the mole fraction of n-butane (x_B) at the bottom. Equations 5.9a and 5.9b are used to solve the dynamic equations of the column. First the calculation starts from the top tray of the column and the calculation is then continued from tray to tray until it reaches the bottom tray by maintaining the feed tray composition. Variable y_{35} is solved using the iteration method. The vapor molar flow rate and the liquid molar flow rate used in Equations 5.9a and 5.9b are obtained from the model created in HYSYS simulation.

The model obtained for the energy balance for the column also by substituting the constants values for vapor molar flow rate, liquid molar flow rate and contribution due to heat are shown below;

Energy balance (Elgue et al., 2004)]

$$\frac{dT}{dt} = \frac{V_{k+1}C_{pk+1}T_{k+1} + L_{k-1}C_{pk-1}T_{k-1} - V_kC_{pk}T_k - L_kC_{pk}T_k + Q_k}{mC_p} \quad (5.9e)$$

where $h=LC_pT$ is the liquid molar enthalpy (kJ/kmol), $H = VC_pT$ is the molar enthalpy of vapour (kJ/kmol) and Q is the contribution due to heat (kJ/hr) for each stage. The

dynamic equation of the debutaniser column in terms of the basic energy balance is shown in equation 5.9e. The specific heat for the energy balance is calculated for every stage. The temperature of each stage is calculated by integration equation 5.9e. Once the composition is calculated by using iteration method stage to stage calculation, the temperature at each stage could also be calculated using iteration method. Once the top temperature could be obtained, then vapour pressure at the top of the column using equation 5.8 could be calculated.

The model obtained for the energy balance for the column is shown below;

$$\frac{dT_{35}}{dt} = 129 T_{34} - 54 T_{35} - 103 \quad (5.9f)$$

$$\frac{dT_1}{dt} = 638 T_1 - 258 \quad (5.9g)$$

The model obtained for the energy balance are calculated stage by stage by integration using equation 5.9e by knowing the enthalpy equation is calculated to be $h = mC_p T$.

5.5 Hybrid neural network (HNN) approach

In this system, the model of the debutaniser column is obtained in section 5.4 is used to produce the given composition of n-butane at the top and bottom of the column. The difference between the actual plant values and the predicted values that is given by the neural network model where the residual model is used as the predicted output for training and validating the neural network model. The training data for the neural network is generated from open loop response functions and the amount of data collected is about 3612 for a sampling time of 541 minutes running time. This modelling is also applied in predicting the top and bottom temperatures. In this scenario, three data sets are prepared which are defined as the training, validation and testing data

sets. These data sets are obtained from combining the simulation and actual open loop data.

The neural network model is used in the hybrid modelling scenario for predicting the residual composition and residual temperature using a forward modelling approach. The residual composition is the difference between the first principle model composition and the actual composition and the residual temperature is the difference between the first principles model temperature and the actual temperature. The outputs from this neural network are added to the mass and energy balance equations which are obtained from the process model to predict the composition and temperature of the column. For the network training it is important to ensure that the prediction of residual match the actual residual compositions.

The residue of real value is obtained from the online data for composition and temperature. The First Principle Model (FPM) is obtained from simulation. The residual is obtained from the deviation between real value and FPM. This also applies for the temperature prediction. The neural network training procedure is very important to determine the accuracy of hybrid modelling in predicting the online composition and temperature accurately and the details of the training approach can be seen in section 5.6.

5.6 Neural network hybrid modeling

The current practice in the industry is to measure the composition at the top and bottom of the column by GC sampling method which is tedious and may delay the determination of results (Fortuna et al., 2005). However neural network model can be used as an alternate because it is able to predict the composition faster and with more accuracy. In addition it can also precisely handle non-linearities in the process variable surrounding the column as proposed in this study. The hybrid model combining neural network with first principles model is a versatile method to execute, which can also be

validated online efficiently. There are two types of hybrid networks developed in this work namely 1) Hybrid model applied for composition prediction and 2) Hybrid model employed for temperature prediction. The input variables to the network include the present composition of n-butane, are lagged values 1 while the output of the network is the future predictions for the composition of n-butane. The purpose for the delayed variable is to develop the dynamic model for the column and to reduce the complexity of the model. This is similar for other networks used to predict the future variation of the top and bottoms temperature respectively. Nonlinear Autoregressive Network with Exogenous inputs (NARX) are employed for training, validation and testing the data set. The training algorithm used is the Levenberg-Marquardt method. Early stopping criteria are implemented to train the network while the performance functions used are outlined in section 4.3.

Tables 4.11 and 4.16 shows the important variables in the neural network for the residual composition n-butane, i-butane and Table 4.38 shows the important variables used in the neural network for residual temperature predictions. The inputs for the neural network residual composition are from $mv2(k)$ to $p_bot(k-1)$ while the outputs from the system are variables $p_top(k+1)$ and $p_bot(k+1)$. The inputs for the neural network residual temperature are from $mv1(k)$ to $T_bot(k-1)$ while the outputs are $T_top(k+1)$ and $T_bot(k+1)$. Figure 4 shows the general procedure in developing the neural network architecture. In the optimum network, the number of layers used is 3 with only 1 hidden layer and the number of hidden nodes is determined using statistical analysis described in section 4.3. The number of inputs to the network is 10 and the outputs are 2 (residual composition of top and bottoms) for composition prediction while the number of inputs to the network is 12 while the outputs are 2 for temperature prediction (residual top and bottom temperature). The transfer function to train the network is purelin (linear) for the entire layer and the networks are trained to

simultaneously predict the top and bottoms residual composition of n-butane and residual top and bottoms temperature of the column.

Prior to implementing the neural network, the data is arranged by combining the open loop response from the simulation and online data. The data set are partitioned according to training which is 65% of the total data, 18% for validation and 17% for testing. The data set is then trained until the network meets its performance criteria. The data set is also validated and tested after the network is trained. After obtaining the neural network structure, and applying the general equation (4.10) for the network, corresponding to the linear activation function, the following equation for the top and bottom residual composition prediction of n-butane is obtained where Δy_1 refers to the top residual composition and Δy_2 refers to the bottom residual composition for a 1 hidden layer network;

$$y = \begin{bmatrix} \Delta y_1 \\ \Delta y_2 \end{bmatrix} = LW^{2,1} \left[IW^{1,1} p + b^1 \right] + b^2 \quad (5.10a)$$

Where;

$IW^{1,1}$ = Input weight at layer 1 (input layer) b^1 = biased value at layer 1

$LW^{2,1}$ = Layer weight at layer 2 (hidden layer) b^2 = biased value at layer 2

The following equation for the top and bottom residual temperature prediction is obtained where Δy_3 refers to the top residual temperature and Δy_4 refers to the bottom residual temperature for a 1 hidden layer network;

$$y = \begin{bmatrix} \Delta y3 \\ \Delta y4 \end{bmatrix} = LW^{2,1} \left[IW^{1,1} p_1 + b^1 \right] + b^2 \quad (5.11b)$$

Where;

$IW^{1,1}$ = Input weight at layer 1 (input layer) b^1 = biased value at layer 1

$LW^{2,1}$ = Layer weight at layer 2 (hidden layer) b^2 = biased value at layer 2

These values can be seen in the Appendix.

n-butane

In this case, p are the inputs to the neural network residual composition given by the vector

$$\left[mv2(k) \ mv2(k-1) \ mv3(k) \ mv3(k-1) \ f(k) \ f(k-1) \ p_{top}(k) \ p_{top}(k-1) \ p_{bot}(k) \ p_{bot}(k-1) \right]^T$$

Where p_1 are the inputs to the neural network residual temperature and for this case study is given by the vector

$$\left[mv1(k) \ mv1(k-1) \ mv2(k) \ mv2(k-1) \ mv3(k) \ mv3(k-1) \ f(k) \ f(k-1) \ T_{top}(k) \ T_{top}(k-1) \ T_{bot}(k) \ T_{bot}(k-1) \right]^T$$

After pruning the neural network structure (simplifying the weights and biases values) the equation above can further be simplified to give the residual composition equation below;

$$\begin{bmatrix} \Delta y1 \\ \Delta y2 \end{bmatrix} = \begin{bmatrix} 1.05 & 0.36 & -0.70 & -0.85 & -0.66 & 1.05 & -0.14 & 1.07 & 1.32 & 0.55 \\ -1.09 & 0.32 & 0.38 & 0.70 & 0.33 & 0.06 & 0.13 & 1.14 & -0.33 & -0.21 \end{bmatrix} p + \begin{bmatrix} -1.35 \\ -0.56 \end{bmatrix} \quad (5.12)$$

The same approach can be applied to the network for predicting the residual temperature as shown below;

$$\begin{bmatrix} \Delta y3 \\ \Delta y4 \end{bmatrix} = \begin{bmatrix} 0.16 & -0.14 & 0.04 & -0.003 & 0.09 & 0.95 & 1.03 & 0.61 & -0.72 & 0.82 & 0.17 & -0.05 \\ 0.42 & 0.07 & 0.05 & 0.21 & -0.30 & 0.19 & 0.12 & 0.28 & 0.36 & -0.29 & -0.48 & 0.17 \end{bmatrix} p1 + \begin{bmatrix} -0.78 \\ -0.004 \end{bmatrix} \quad (5.13)$$

i-butane

In this case, p are the inputs to the neural network residual composition given by the vector

$$[mv2(k) \ mv2(k-1) \ mv3(k) \ mv3(k-1) \ e(k) \ e(k-1) \ o_{top}(k) \ o_{top}(k-1) \ o_{bot}(k) \ o_{bot}(k-1)]^T$$

After pruning the neural network structure (simplifying the weights and biases values) the equation above can further be simplified to give the residual composition equation below;

$$\begin{bmatrix} \Delta y1 \\ \Delta y2 \end{bmatrix} = \begin{bmatrix} -1.52 & -0.2 & -0.16 & 1.32 & -0.88 & 0.47 & 2.00 & 0.16 & -0.04 & 0.038 \\ 0.32 & 0.47 & -0.83 & -0.64 & 0.012 & -1.13 & -0.42 & -0.19 & 0.64 & 0.45 \end{bmatrix} p + \begin{bmatrix} 2.03 \\ -1.38 \end{bmatrix} \quad (5.14)$$

For n-butane, the number of neurons obtained in the hidden layer for the prediction residual composition is 34 while the residual temperature is 12 for n-butane. The number of neuron is determined by evaluating the RMSE values outlined in model adequacy test in section 4.3. The low RMSE values indicate better prediction for the column. The neural network architecture is obtained by running the m-file programming in MATLAB by using the GENSIM(NET) command. This GENSIM command tends to generate the architecture in the SIMULINK environment. From there the hybrid neural network is constructed in SIMULINK environment as shown in Figure 5.2. The neural

network equation for residual composition and residual temperature is developed by extracting the input weights and biases value from the network. Then the equations are constructed in SIMULINK. The hybrid model for composition is obtained by adding the equation 6.1 with the first principle model in terms of the equation used for mass balance of the column to determine the top and bottoms composition. The equations 5.5 and 5.6 respectively are the equations for the mass balance conducted for the top and bottom composition. The hybrid model for the temperature is obtained by adding equation 5.12 with first principles model using an energy balance for the column at the top and bottom temperature. The top and bottoms temperature for the column is by integration equation 5.8 to obtain the top and bottoms temperature.

n-butane

The equation below is the combination of first principle model composition and the residual top and bottom composition

$$\begin{bmatrix} y_1 \\ y_2 \end{bmatrix} = \begin{bmatrix} \int 1.72y_{35} - 0.71x_D \, dt \\ \int 1.68x_1 - 8.1y_B - 8.2x_B \, dt \end{bmatrix} + \begin{bmatrix} 1.05 & 0.36 & -0.70 & -0.85 & -0.66 & 1.05 & -0.14 & 1.07 & 1.32 & 0.55 \\ -1.09 & 0.32 & 0.38 & 0.70 & 0.33 & 0.06 & 0.13 & 1.14 & -0.33 & -0.21 \end{bmatrix} p + \begin{bmatrix} -1.35 \\ -0.56 \end{bmatrix} \quad (5.15)$$

y_1 and y_2 are the outputs for the neural network hybrid prediction model for top and bottom composition. y_{35} is the vapor mole fraction at stage 35, x_D is the liquid mole fraction at distillate, y_B is the vapor mole fraction at the bottoms, x_1 is the liquid mole fraction at stage 1 and x_B is the liquid mole fraction at bottoms. The important equation to generate the equation 5.15 by integrating equation 5.5 and 5.6

The equation below is the combination of first principle model temperature and the residual top and bottom temperature

$$\begin{bmatrix} y3 \\ y4 \end{bmatrix} = \begin{bmatrix} \int 129T_{34} - 54T_{35} - 103dt \\ \int 638T_1 - 258dt \end{bmatrix} + \begin{bmatrix} 0.16 & -0.14 & 0.04 & -0.003 & 0.09 & 0.95 & 1.03 & 0.61 & -0.72 & 0.82 & 0.17 & -0.05 \\ 0.42 & 0.07 & 0.05 & 0.21 & -0.30 & 0.19 & 0.12 & 0.28 & 0.36 & -0.29 & -0.48 & 0.17 \end{bmatrix} p1 + \begin{bmatrix} -0.78 \\ -0.004 \end{bmatrix} \quad (5.16)$$

y3 and y4 are the outputs for the neural network hybrid prediction for top and bottom temperatures. Cp₃₄ and Cp₃₅ are the specific heats of n-butane at stages 34 and stage 35 respectively, while T₃₅, T₃₄ and T₁ are the temperature at stages 35, 34 and 1 respectively.

i-butane

The equation below is the combination of first principle model composition and the residual top and bottom composition

$$\begin{bmatrix} y1 \\ y2 \end{bmatrix} = \begin{bmatrix} \int 1.68y_{35} - 0.5x_D dt \\ \int 160x_1 - 82y_B - 75x_B dt \end{bmatrix} + \begin{bmatrix} -1.52 & -0.2 & -0.16 & 1.32 & -0.88 & 0.47 & 2.00 & 0.16 & -0.04 & 0.038 \\ 0.32 & 0.47 & -0.83 & -0.64 & 0.012 & -1.13 & -0.42 & -0.19 & 0.64 & 0.45 \end{bmatrix} p + \begin{bmatrix} 2.03 \\ -1.38 \end{bmatrix} \quad (5.17)$$

y1 and y2 are the outputs for the neural network hybrid prediction for top and bottoms composition. y₃₅ is the vapor mole fraction at stage 35, x_D is the liquid mole fraction at distillate, y_B is the vapor mole fraction at the bottoms, x₁ is the liquid mole fraction at stage 1 and x_B is the liquid mole fraction at bottoms.

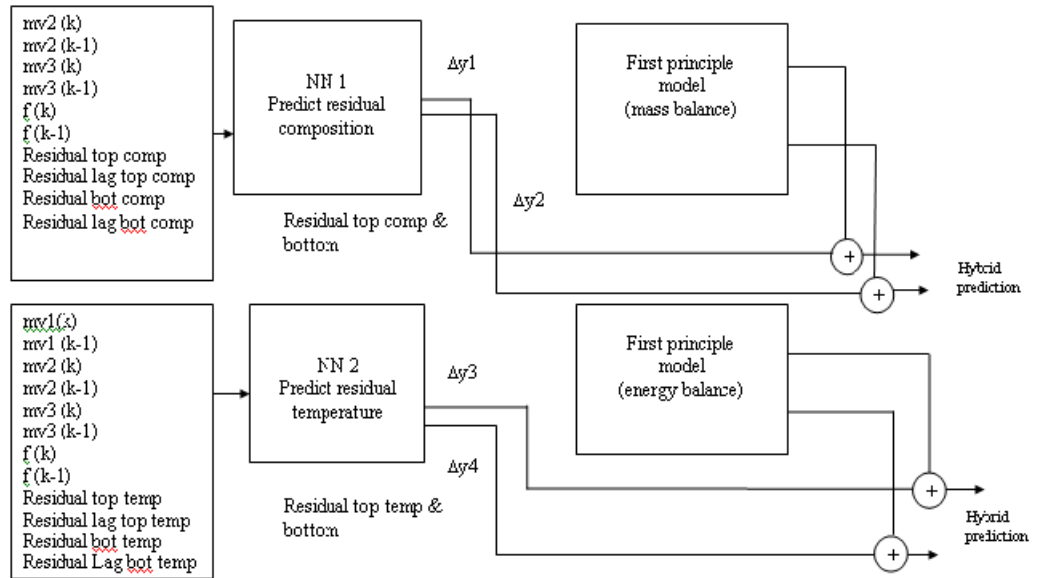


Figure 5.2 Hybrid model for the composition n-butane and temperature

5.7 Residual neural network n-butane

Table 5.1 shows the important variables in the neural network where the data set are combined from the manipulated variable reboiler flow rate and reflux flow rate for n-butane.

Table 5.1 Important variables for neural network prediction

Inputs		
Variable	Symbol	Description
MV2	mv2 (k)	Manipulated reboiler flow rate
	mv2 (k-1)	Lag MV2
MV3	mv3 (k)	Manipulated reflux flow rate
	mv3 (k-1)	Lag MV3
Temp 6	f (k)	Debutaniser feed temp
	f (k-1)	Lag Temp 6
Component 3	p_top (k)	Top residual composition n-butane
	p_top (k-1)	Lag residual composition top
	p_bot (k)	Bottom residual composition n- butane
	p_bot (k-1)	Lag residual composition bottom
Outputs		
	p_top (k+1)	Future predictions n- butane top residual
	p_bot (k+1)	Future predictions n- butane bottom residual

The inputs for the neural network are from mv2 (k) to p_bot (k-1). The outputs are the variable p_top (k+1) and p_bot (k+1).

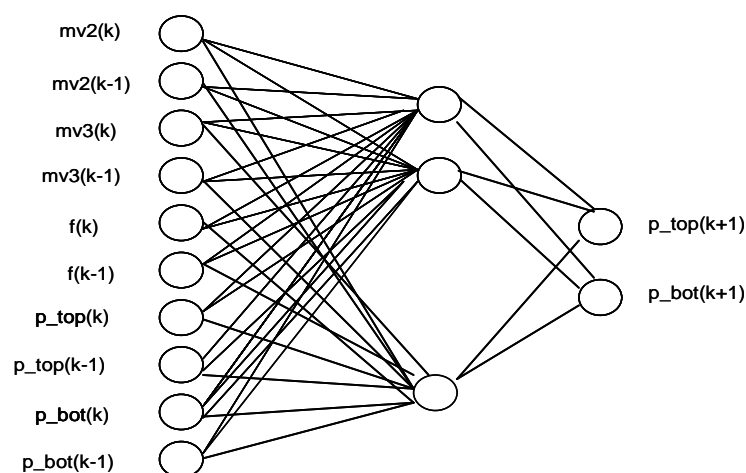


Figure 5.3 Neural network architecture for residual composition prediction of n-butane

Figure 5.3 shows the neural network architecture of the n-butane residual composition prediction

Table 5.2 Neural network architecture

Parameters	Description	
Network	NARX series parallel network (newnarxsp)	
Category	With partitioning divided into 2	with partitioning divided into 3
Training function	TRAINLM	TRAINLM
Adaptation learning function	LEARNGDM	LEARNGDM
Performance function	MSE	MSE
Epochs	1000	1000
Goal	1e-6	1e-6
Number of layers	2	2
Layer 1: Number of Neuron	38	38
Transfer function	PURELIN	PURELIN
Layer 2: Number of Neuron	2	2
Transfer function	PURELIN	PURELIN

5.7.1 With partition into 3

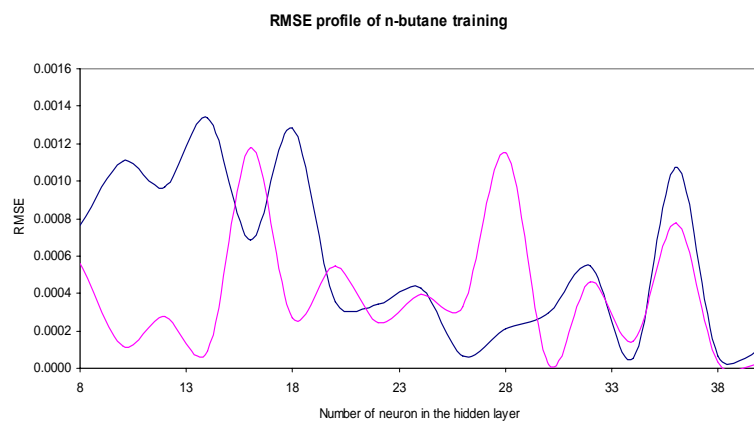


Figure 5.4 Profile of the RMSE of n-butane training

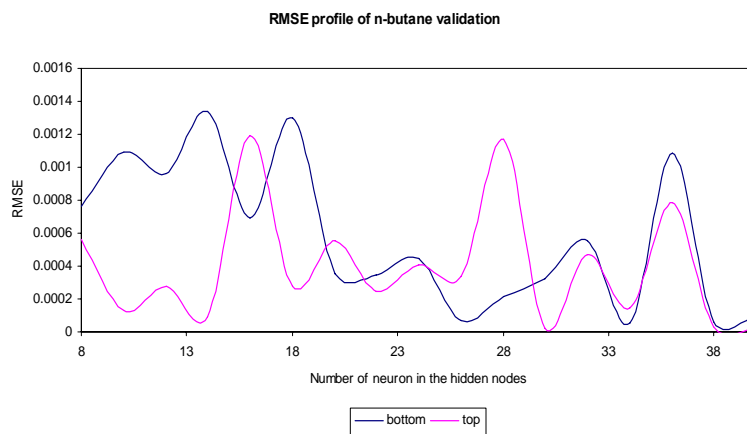


Figure 5.5 Profile of the RMSE of n-butane validation

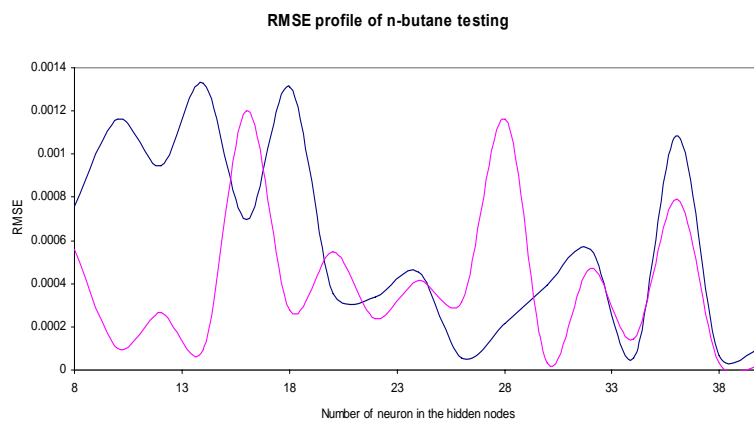


Figure 5.6 Profile of the RMSE of n-butane testing

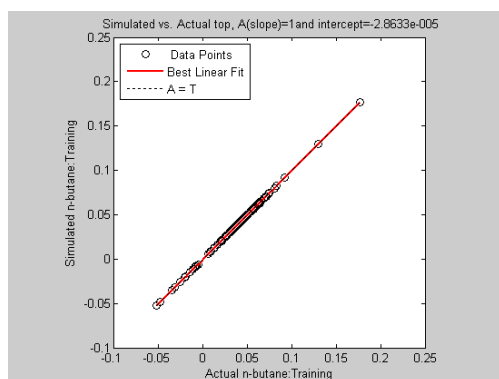


Figure 5.7 Actual and simulated n-butane top residual composition training

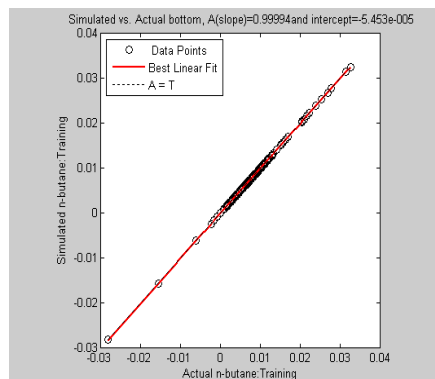


Figure 5.8 Actual and simulated n-butane bottom residual composition training

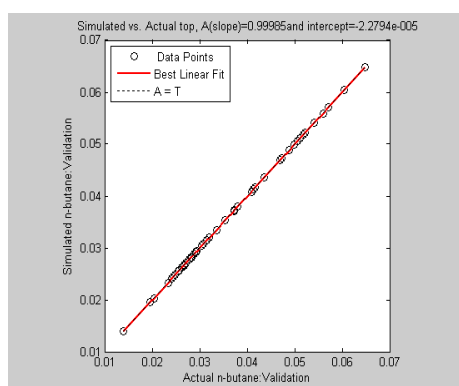


Figure 5.9 Actual and simulated n-butane top residual composition validation

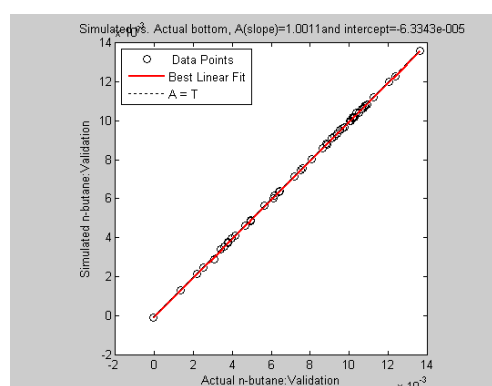


Figure 5.10 Actual and simulated n-butane bottom residual composition validation

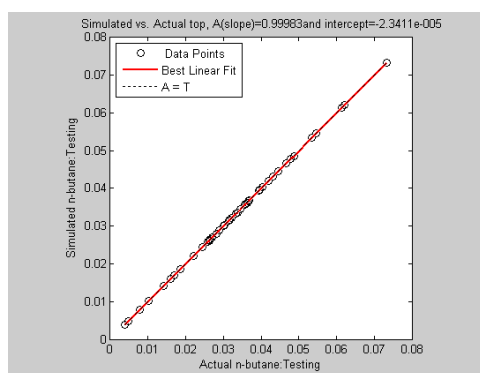


Figure 5.11 Actual and simulated n-butane top residual composition testing

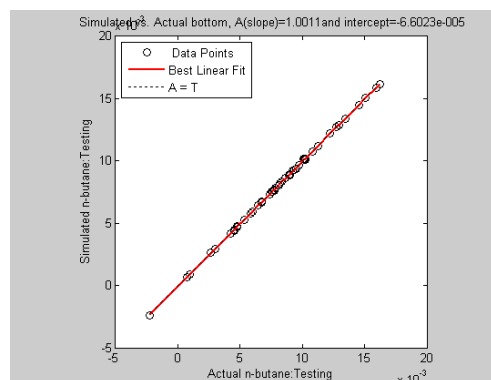


Figure 5.12 Actual and simulated n-butane bottom residual composition testing

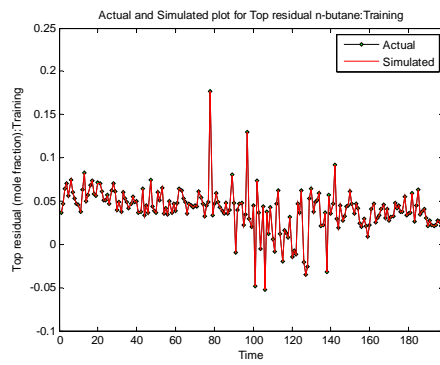


Figure 5.13 Actual and simulated n-butane
top composition line plot training

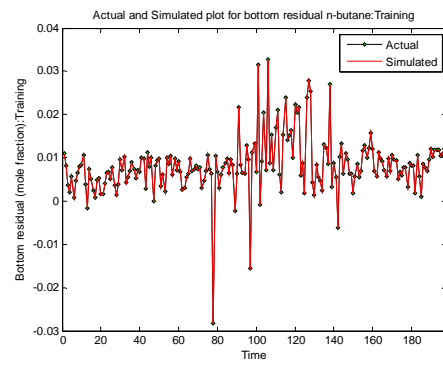


Figure 5.14 Actual and simulated n-butane
bottom composition line plot training

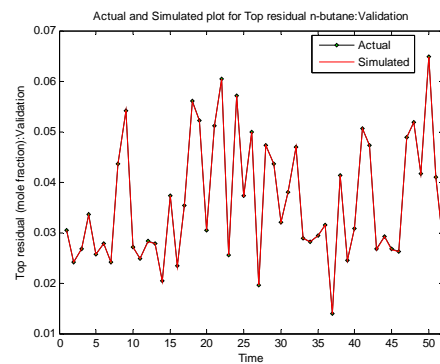


Figure 5.15 Actual and simulated n-butane
top residual composition line plot
validation

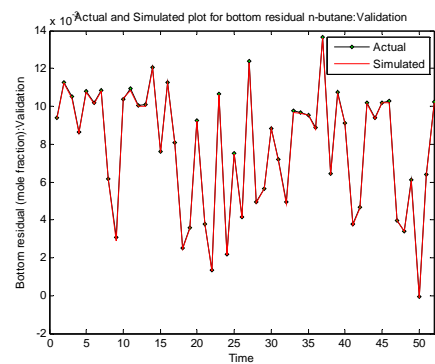


Figure 5.16 Actual and simulated n-butane
bottom residual composition line plot
validation

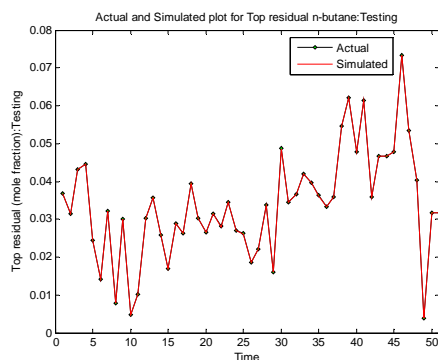


Figure 5.17 Actual and simulated n-butane top residual composition line plot testing

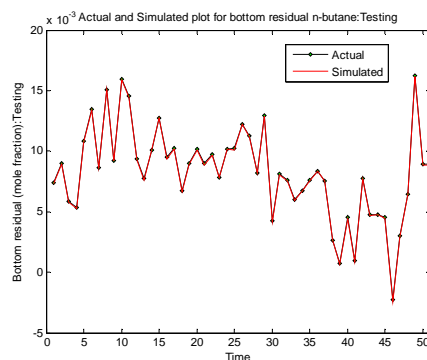


Figure 5.18 Actual and simulated n-butane bottom residual composition line plot testing

Figures 5.4 to 5.6 show the profile with the change in the number of hidden nodes in the hidden layer. Figures 5.7 to 5.18 show the top and bottom residual composition prediction of n-butane for training, validation and testing.

5.8 Residual top and bottom temperature neural network

Table 5.3 shows the important variables in the neural network where the data set are combined from the manipulated variable overhead pressure, reboiler flow rate and reflux flow rate.

Table 5.3 Important variables for neural network prediction

Inputs		
Variable	Symbol	Description
MV1	mv1 (k)	Manipulated overhead pressure
	mv1(k-1)	Lag MV1
MV2	mv2 (k)	Manipulated reboiler flow rate
	mv2 (k-1)	Lag MV2
MV3	mv3 (k)	Manipulated reflux flow rate
	mv3 (k-1)	Lag MV3
Temp 6	f (k)	Debutaniser feed temp
	f (k-1)	Lag Temp 6
Temperature	T_top (k)	Top residual temp
	T_top (k-1)	Lag top residual temperature
	T_bot (k)	Bottom residual temperature
	T_bot (k-1)	Lag bottom residual temperature
Outputs		
	T_top (k+1)	Future predictions top residual temperature
	T_bot (k+1)	Future predictions bottom residual temperature

The inputs for the neural network are from mv1 (k) to T_bot (k-1). The outputs are the variable T_top (k+1) and T_bot (k+1).

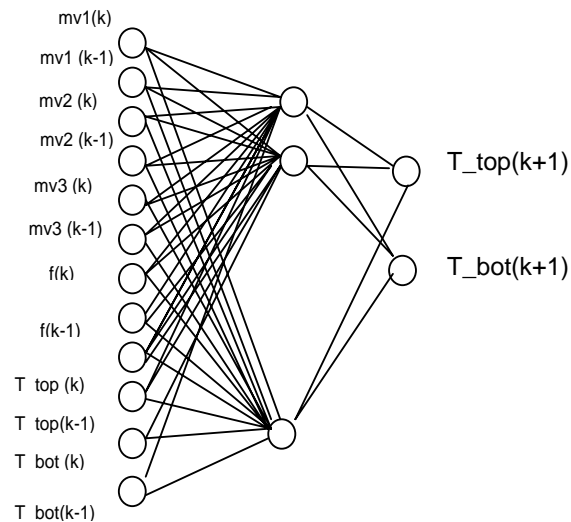


Figure 5.19 Neural network architecture for residual top and bottom temperatures

Table 5.4 Neural network architecture

Parameters	Description	
Network	NARX series parallel network (newnarxsp)	
Category	With partitioning divided into 2	with partitioning divided into 3
Training function	TRAINLM	TRAINLM
Adaptation learning function	LEARNGDM	LEARNGDM
Performance function	MSE	MSE
Epochs	1000	1000
Goal	1e-6	1e-6
Number of layers	3	3
Layer 1: Number of Neuron Transfer function	12	12
	PURELIN	PURELIN
Layer 2: Number of Neuron Transfer function	2	2
	PURELIN	PURELIN

5.8.1 With partition into 3

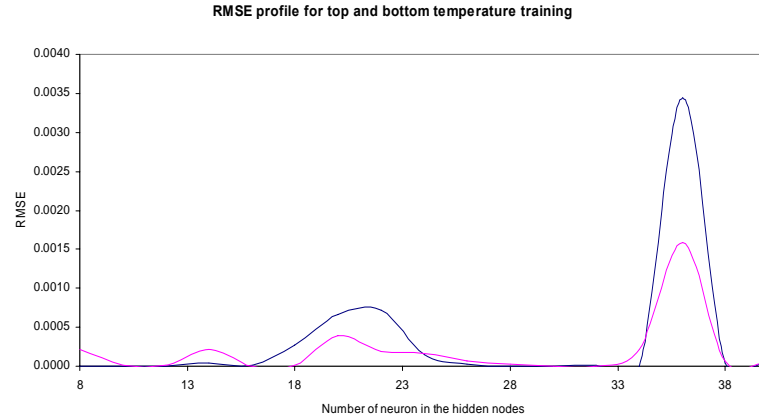


Figure 5.20 Profile of the RMSE training

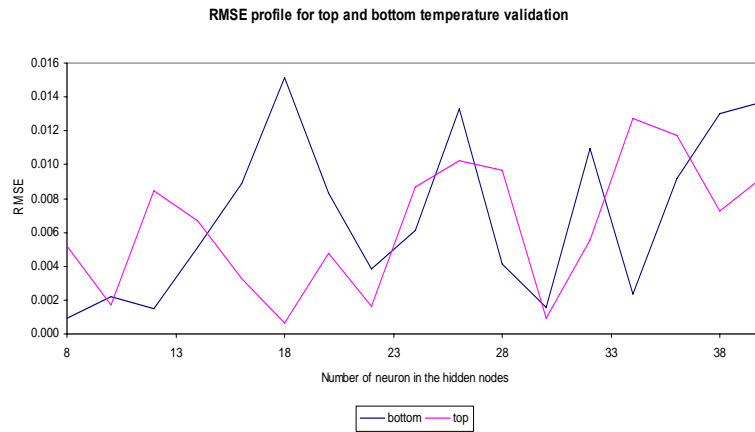


Figure 5.21 Profile of the RMSE validation

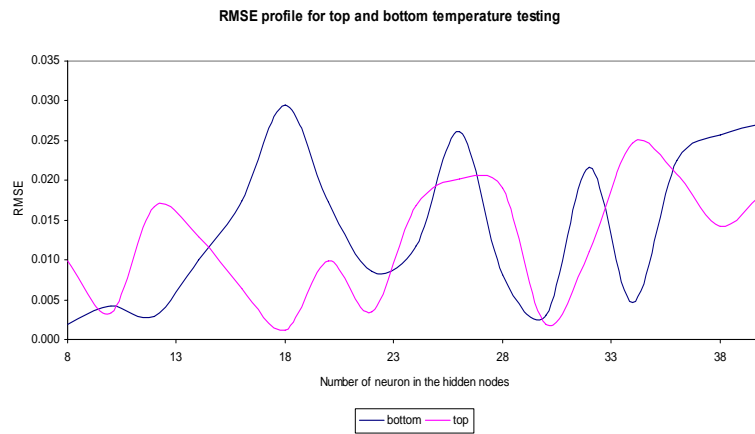


Figure 5.22 Profile of the RMSE testing

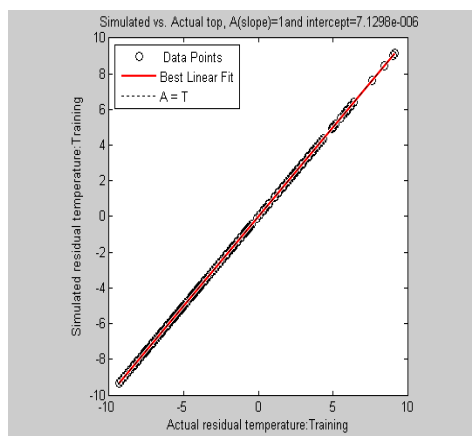


Figure 5.23 Actual and simulated
top residual temperature training

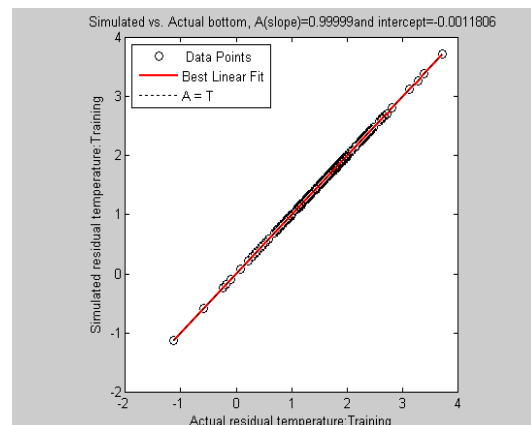


Figure 5.24 Actual and simulated
bottom residual temperature training

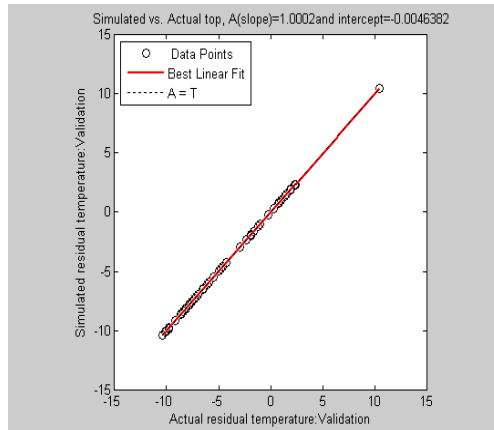


Figure 5.25 Actual and simulated top residual temperature validation

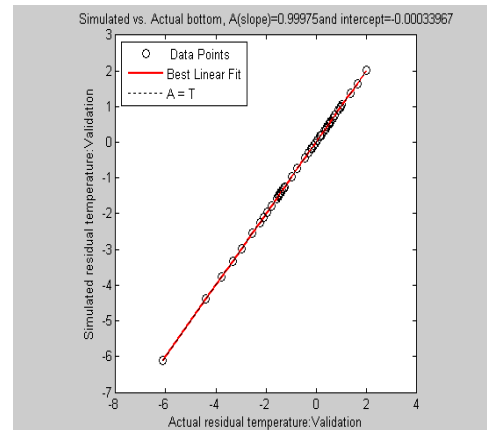


Figure 5.26 Actual and simulated bottom residual temperature validation

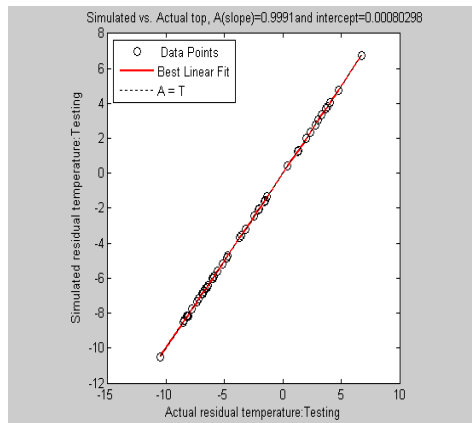


Figure 5.27 Actual and simulated top residual temperature testing

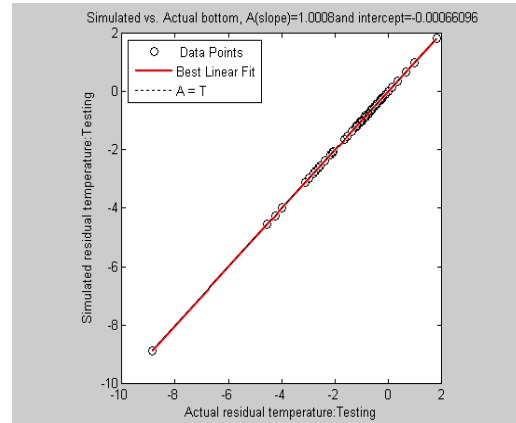


Figure 5.28 Actual and simulated bottom residual temperature testing

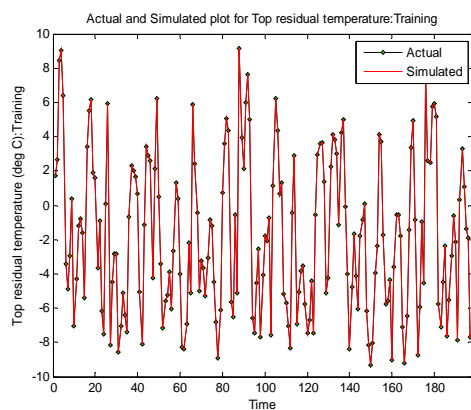


Figure 5.29 Actual and simulated
top residual composition line plot
training

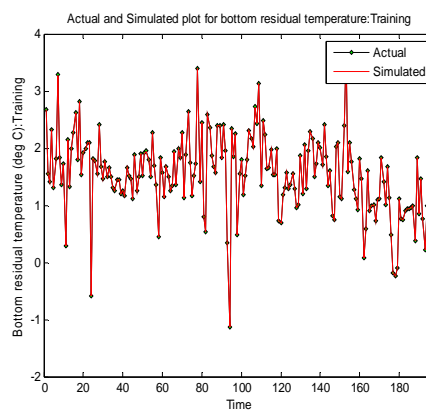


Figure 5.30 Actual and simulated
bottom residual composition line plot
training

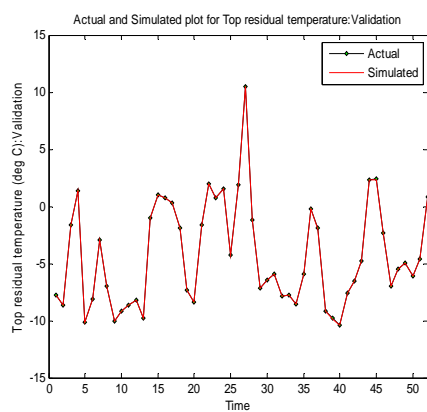


Figure 5.31 Actual and simulated
top residual temperature line plot validation

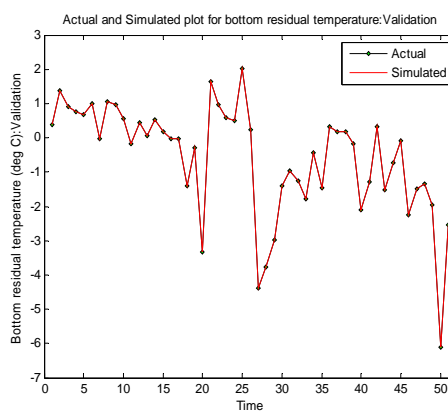


Figure 5.32 Actual and simulated
bottom residual temperature line plot
validation

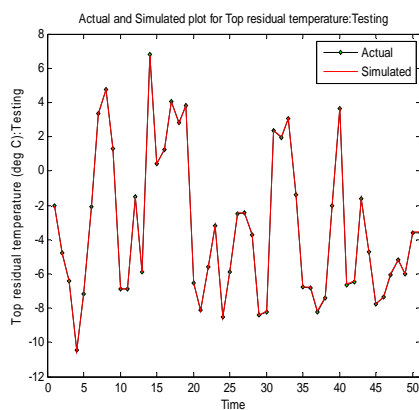


Figure 5.33 Actual and simulated
top residual temperature line plot testing

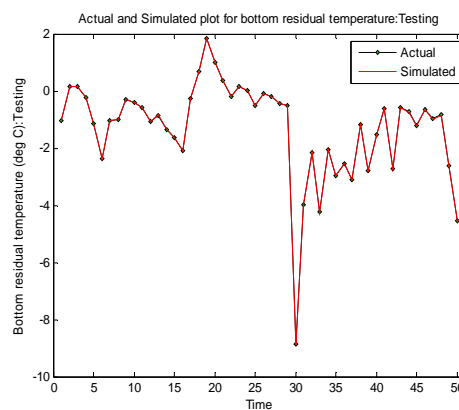


Figure 5.34 Actual and simulated
bottom residual temperature line plot
testing

Figures 5.20-5.22 shows the profile with the change in the number of hidden nodes in the hidden layer. Figures 5.23 to 5.34 show the top and bottom residual temperature prediction of n-butane for training, validation and testing

5.9 Hybrid modeling of n-butane

Figure 5.35-5.36 show the top and bottom composition prediction by first principle model. Figure 5.37-5.38 show the top and bottom temperature prediction by first principle model. From the fluctuations, we could see that the first principle model show large deviation compare to actual online composition.

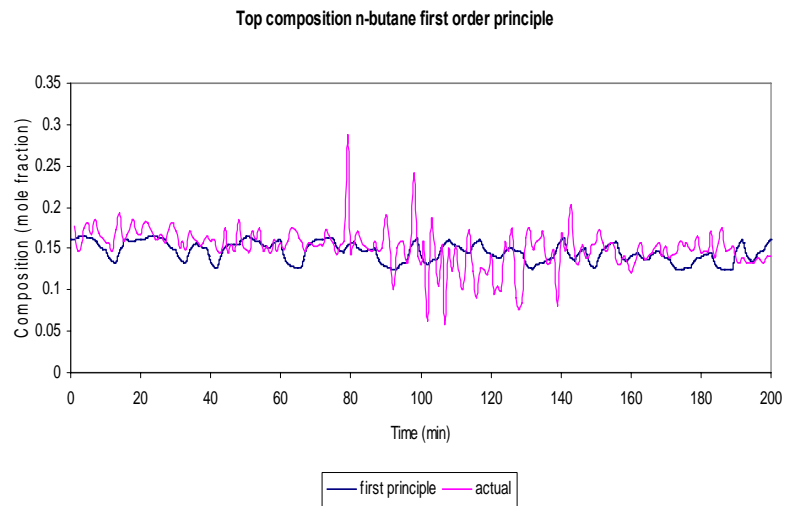


Figure 5.35 Top composition n-butane first principle model

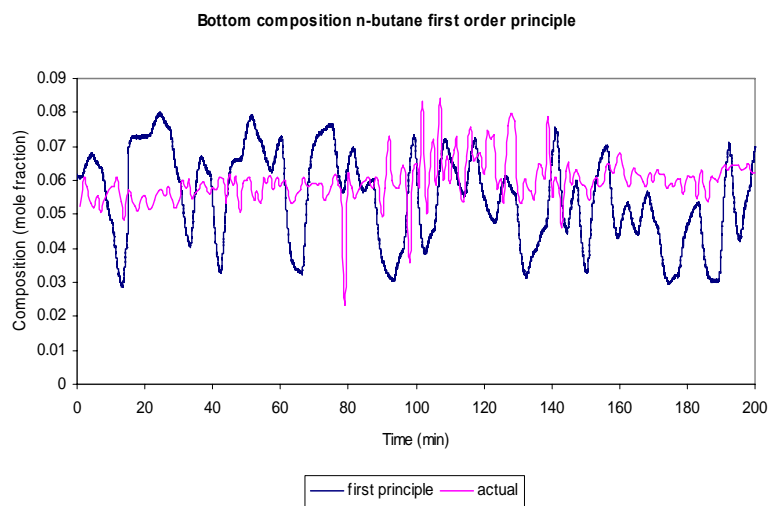


Figure 5.36 Bottom composition n-butane first principle model

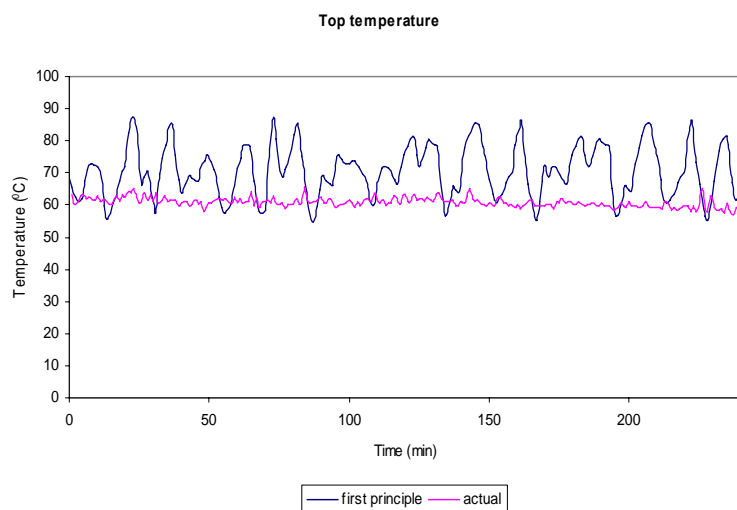


Figure 5.37 Top temperature first principle model

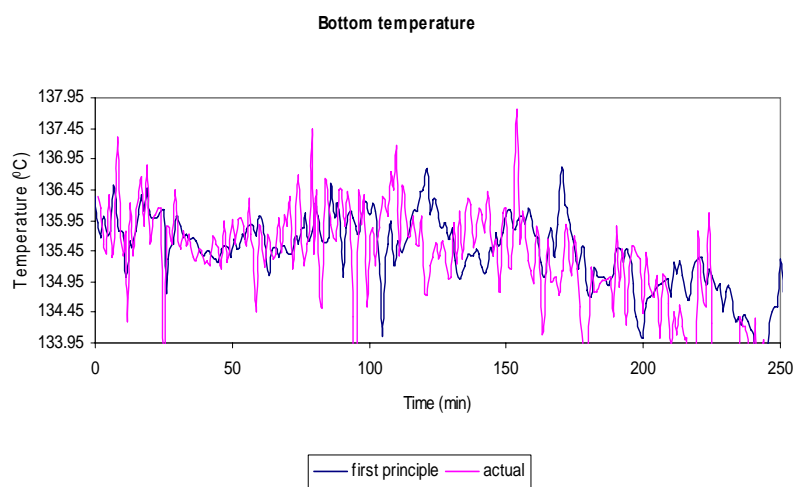


Figure 5.38 Bottom temperature first principle model

Figures 5.39-5.40 show the fluctuation of the actual composition response compared to the hybrid model and neural network. The calculated top and bottoms RMSE for the hybrid equation is 3.65×10^{-9} and 7.24×10^{-9} respectively. The calculated top and bottom RMSE for the neural network is 4.4×10^{-2} and 0.98×10^{-2} . The calculated top and bottom RMSE for hybrid prediction is 3.92×10^{-9} and 7.93×10^{-9} respectively. This indicates that the deviation between actual and predicted top and bottom composition is very small. The prediction results are in good agreement with the actual data as the

regression value of R^2 is close to 1. This confirm that hybrid neural network gives the best for top and bottom composition prediction than the rest.

Hybrid equation gives the best result for top and bottoms composition prediction than the rest. Based on the MAPE values the best prediction is the hybrid equation modeling because the values are close to 0. The MAPE values for top and bottom composition are 1.86×10^{-6} and 6.35×10^{-6} respectively. When having a perfect fit, MAPE is zero. Table 5.1 shows the statistical analysis for composition prediction of n-butane.

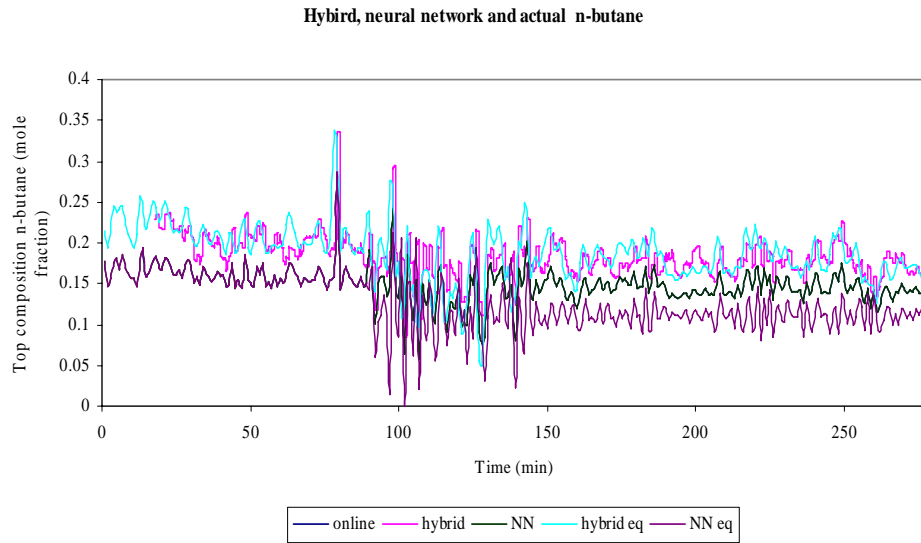


Figure 5.39 Hybrid model, neural network and actual top composition n-butane

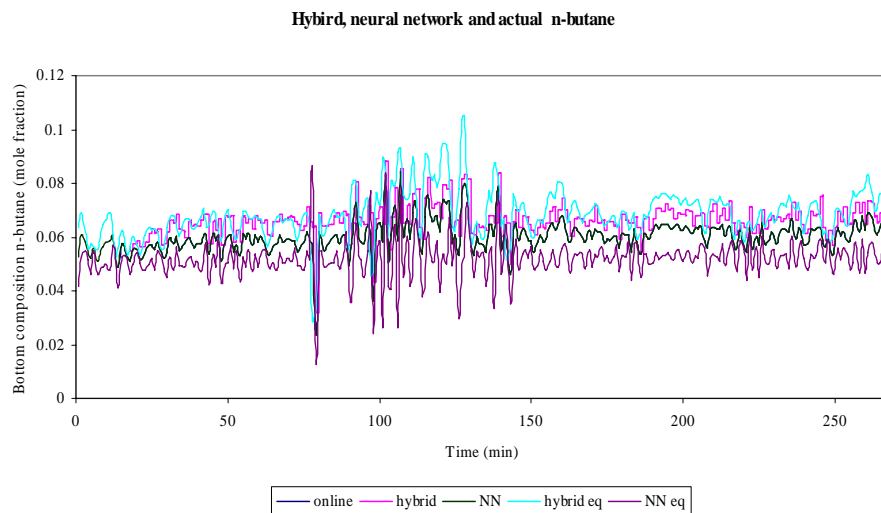


Figure 5.40 Hybrid model, neural network and actual bottom composition n-butane

Table 5.5 Statistical analysis for composition prediction of n-butane.

		Black box model	
		Hybrid eq	NN
rmse_bottom	7.24E-09	7.93E-09	0.0098
rmse_top	3.65E-09	3.92E-09	0.044
R_bottom	1	0.99	0.78
R_top	1	0.99	0.79
MAPE_bottom	6.35E-06	1.49E-05	11.19
MAPE_top	1.86E-06	-3.2E-06	19.05

Figures 5.41 and 5.42 show the fluctuation of the actual temperature response compared to hybrid model and neural network. The calculated top and bottoms RMSE for the hybrid equation is 2.86×10^{-3} and 5.25×10^{-5} respectively. The calculated top and bottom RMSE for neural network is 4.4×10^{-2} and 0.98×10^{-2} . The calculated top and bottom RMSE for the hybrid prediction is 1.32×10^{-2} and 5.2×10^{-4} respectively. The prediction results are in good agreement with the actual data as the regression value of R is close to 1. Hybrid equation gives the best result for top and bottom temperature prediction than the rest is because the R value is 1. Hybrid equation gives the best for top and bottom composition prediction than the rest. Based on the MAPE values the best prediction is the hybrid equation because the values are close to 0. The MAPE values for top and bottom temperature are -4.17×10^{-4} and 3.07×10^{-5} respectively. When having a perfect fit, MAPE is zero. This shows that the hybrid network perform well than the rest of the predictions for composition and temperature prediction. Table 5.2 shows the statistical analysis for temperature prediction. This shows that hybrid neural network is the optimum composition and temperature prediction with high accuracy and small error compared to the rest of the prediction.

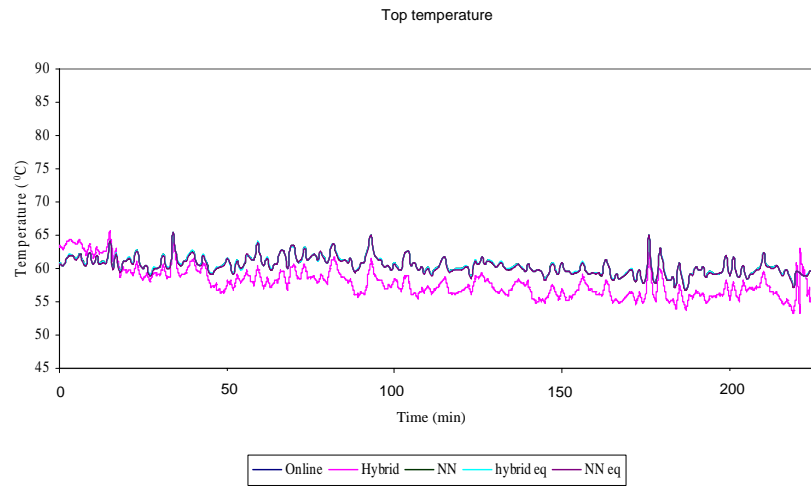


Figure 5.41 Hybrid model, neural network and actual top temperature

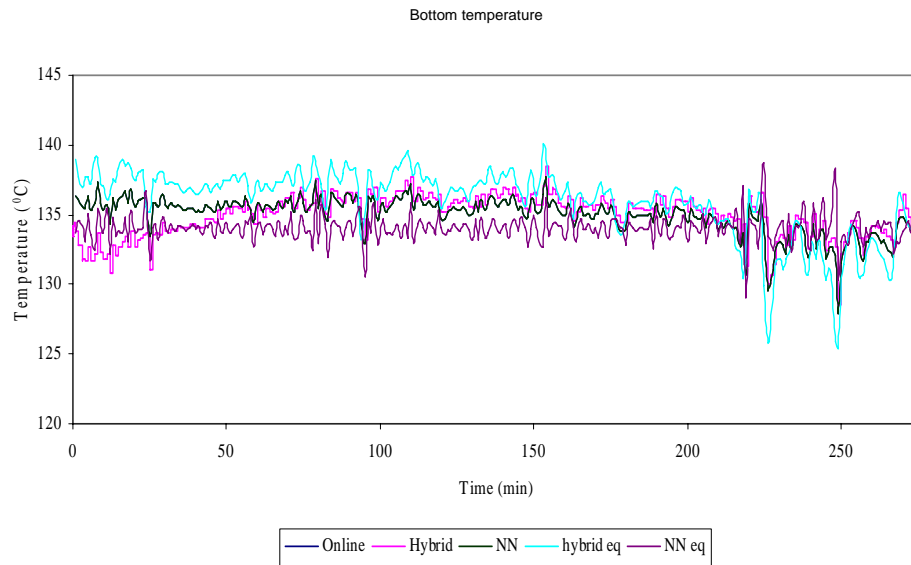


Figure 5.42 Hybrid model, neural network and actual bottom temperature

Table 5.6 Statistical analysis for temperature prediction.

	Hybrid eq	Black box model	
		Hybrid	NN
rmse_bottom	5.25E-05	5.20E-04	1.782703
rmse_top	2.86E-03	1.32E-02	0.044306
R_bottom	0.99	0.99	0.33
R_top	0.99	0.99	0.99
MAPE_bottom	3.07E-05	1.01E-04	-0.51
MAPE_top	-4.17E-04	-1.37E-03	-0.063

From the results it may be concluded that the prediction by NN using the neural network conventional approach is based on black box model would not be able to predict the composition and temperature compared to the hybrid equation. The prediction using residual composition and the residual temperature equation is robust in nature by pruning the input weights and biases in order to obtain a relationship between the inputs of the network by relating them to the outputs prediction. The hybrid model is used to minimize the deviation between the first principles model and the actual composition. By training the residual composition, the hybrid model is able to predict the actual composition accurately and gives decent prediction with comparison to the other counterparts. The hybrid equation is robust in nature compared to the rest of the prediction because we determine the equation required which consists of first principles model and residual composition and temperature.

In order to determine the robustness, process parameter need to be evaluated. One of the methods that could be used is to introduce the measurement error as one of the inputs to the neural network and maintain the other variables. Then hybrid model for the composition and temperature are simulated again in order to see its performance. The measurement error is introduced to a variable while the other variables are maintained. The variable that is tested for robustness analysis is the variable Temp 6 by introducing some 5% measurement error and observes the performance of the hybrid prediction. Table 5.4 shows the statistical analysis for robustness analysis for Temp 6.

Then variable $\Delta p_{top}(k)$ and $\Delta p_{top}(k-1)$ are introduced with some 5% measurement error and to observe the performance of the hybrid prediction. The process parameter could also be change by adjusting the feed composition in the first principle model and perform the hybrid simulation. From the analysis above, the hybrid prediction show similar fluctuation although there are some process parameter where evaluated. So therefore the hybrid prediction is robust in nature.

Table 5.7 Statistical analysis for robustness analysis variable Temp 6

Parameter	Composition	Temperature
rmse_bottom	118E-10	2E-05
rmse_top	6.4E-10	4.6E-04
R_bottom	1	1
R_top	1	1
MAPE_bottom	1.3E-07	5.3E-06
MAPE_top	2.1E-07	6.5E-05

The hybrid neural network equation performs better in comparison to the rest of the neural network prediction methodologies as evidenced by the error values which are smaller with respect to the other prediction procedures. This work could be developed for online prediction, monitoring and control of composition and temperature of the column. Based on the hybrid model, the effect of key operation conditions is analyzed and some useful guiding rules are obtained. Because the predicting performance of the hybrid equation neural network depends on the quality and range of the sample data, the performance of the hybrid model also depends on the quality and range of the sample data. The other advantage of the hybrid equation is that we could determine the relationship between the inputs and outputs for these predictions and could be easily applied for model based control strategies in the future.

CHAPTER 6: ADVANCED PROCESS CONTROL

6.1 Introduction

Controlling two compositions requires more complex instrumentation. The top and bottom composition loops interact and dynamic stability problems can arise. Holding heat input or reflux constant simplifies the control system and avoid interaction problem. Composition control of the column requires an on-line measurement performance variable directly related to composition. The common measurement is temperature. However, temperature-composition relationship is influenced by column pressure control (Alpbaz et al., 2002). If temperature is used as a control variable, the sensing element is usually not placed directly in the product stream. Often, product streams are relatively pure so that boiling point is relatively insensitive to small changes in concentration. The steady state column temperature profile should be investigated instead the sensing element should be located several trays away from the end, at a point where the gradient is larger (L Smith, 1979). At this point, a fixed change in product composition causes a larger temperature change. Controlling the temperature gives tight control on product composition despite wide variations in other factors such as internal reflux ratio (L Smith, 1979). The variables that need to be controlled are the top and bottom temperatures and the variables that need to be estimated is top and bottom compositions. Application of composition control to both ends of a debutaniser column has been considered with generally little success. The difficulty results because two individual control loops interact. The top loop controls the heavy key in the overhead stream and the bottom loop controls the light key in the bottom stream. Some disturbances cause the light key concentration in the bottom stream to increase. The lower loop acts to reduce the concentration by adding heat. This action lowers the light key concentration sends more heavy key up the column. If both loops are tuned tightly,

the column becomes unstable, and the system can be stable by detuning one loop. Processes with only one output being controlled by a single manipulated variable are classified as single input single output (SISO) system. Many processes do not conform to such a simple control configuration. In the process industries, any unit operation cannot do so with only a single loop. In fact each unit operation requires control over at least two variables, product rate and product quality. Systems with more than one control loop are known as multi input multi output (MIMO) or multivariable control system. There will therefore be a composition control loop and temperature control loop. Minimization of energy usage is possible if the compositions of both the top and bottom product streams are controlled to their design values, dual composition control. A common scheme is to use reflux flow to control top product composition while the heat input is used to control bottoms product composition. Loop interaction may also arise as a consequence of process design, typically the use of recycle streams for heat recovery purposes. Changes in the feed temperature will in turn influence bottom product composition. It is clear that interaction exists between the composition and pre heat control loops. The simple approach in dealing with loop interactions is by the design of multivariable control strategies. This is to eliminate interactions between control loops. The research that has been done on advanced process control from previous researchers is outlined in the previous chapter under literature review. The outline in the thesis for this chapter is the multivariable controller used consists of neural network equation based for the forward model and inverse model. The multivariable control system is to control the top and bottom temperature and estimating the top and bottom composition. The use of the neural network based controller compared to conventional PID controllers is because all the process variables surrounding the debutaniser column are non-linear in nature and PID could not handle non-linearities. As shown in Figure 3.2, the column configuration exist interaction loops

to maintain the top and bottom compositions and to control the top and bottom temperatures.

6.2 Neural network based control strategies

There are 2 types of control strategies for neural networks to be implemented for the inverse model based control schemes. The two different ways are the Direct Inverse Control (DIC) and the Internal Model Control (IMC) methods. These methods are described briefly as shown in Figure 6.1 and Figure 6.2.

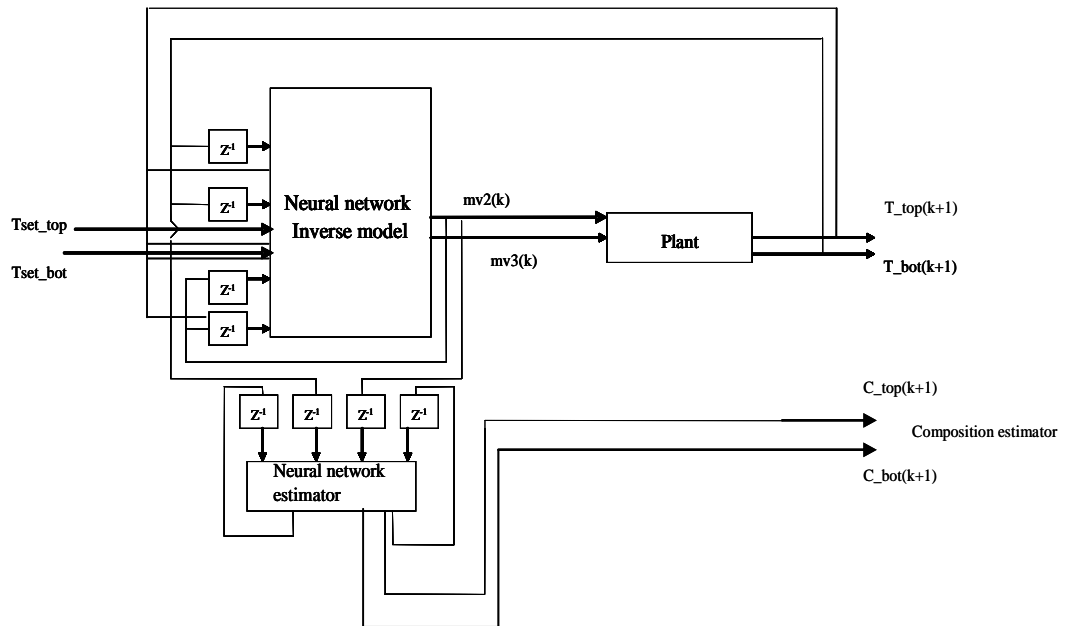


Figure 6.1 Control loop of neural network based Direct Inverse Model Control (DIC)

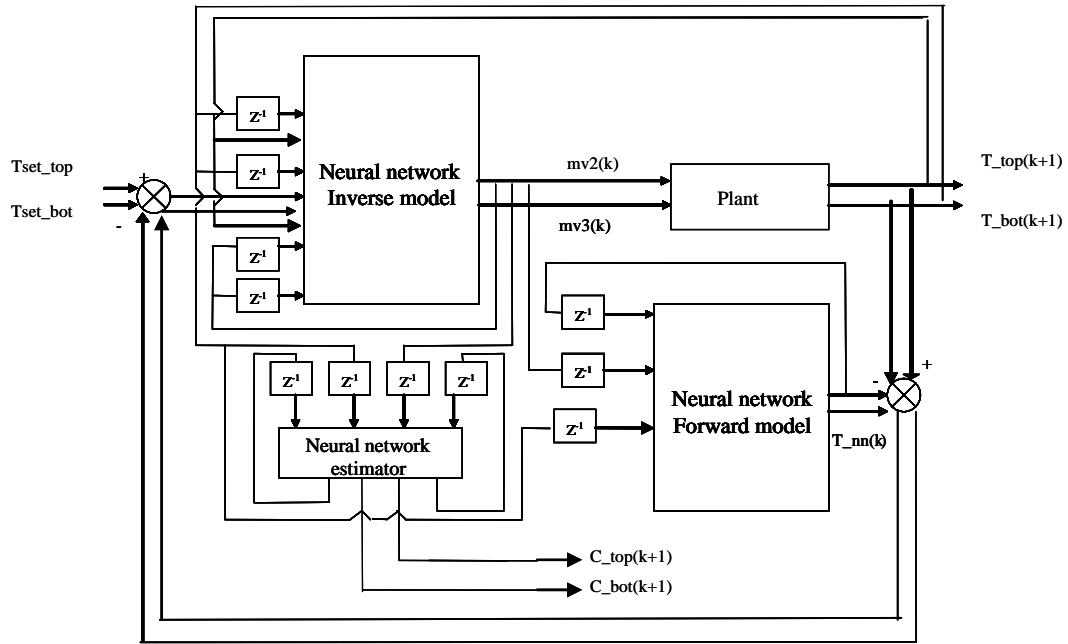


Figure 6.2 Control loop of neural network based Internal Model Controller (IMC)

6.2.1. Direct Inverse Control (DIC) method

This strategy consists of the process control which is placed in series with neural network inverse models that act as the controllers. In this scheme, the outputs predict the desired current system input, while the desired set-point acts as the desired output which is fed to the network together with the past plant inputs. In this case, the appropriate control parameter for the desired target will be predicted based on its input. Neural networks acting as the controller has to learn to supply at its input. As shown in Figure 6.1, the inverse model is then utilized in the control strategy by cascading it with the controlled system or plant. This method depends on the accuracy of the inverse model. The controlled variables are the top and bottom temperature and the manipulated variables are the reflux and reboiler flow rate for the DIC method.

6.2.2. Internal Model Control (IMC) method

Neural network based IMC method incorporate both inverse and forward model in the control scheme. The dynamic of the process is the forward model which it represents is placed in parallel with the system. This is to cater for plant or mismatches of the model during implementation (Mujtaba et al., 2006). On the other hand, the inverse model will act as a controller. In this scheme, the error between the neural network forward model and plant output is then subtracted from the set- point before being fed into the inverse model, as seen in Figure 6.2. With the mismatch detection feature, the internal model based controller can be used to drive the controlled parameter to the desired set-point even when noise and disturbances are present in the system. The optimum performance for controller performance is the IMC method. The error produced by the process model could be minimized and compensated by the error produced by the neural network forward process model (Mujtaba et al., 2006). The controlled and manipulated variables used in the IMC method are similar to the DIC method.

6.2.3. Neural networks models

Before applying the inverse model neural network control strategies for the debutaniser column, it is crucial to discuss the development and configuration of the forward and inverse models. Using neural network architecture and equation based neural network are important fundamentals to these model based control strategies as necessary.

6.2.3.1. Forward models

The procedure of training a neural network in which to represent the forward dynamics of a column is by predicting the outputs using the required inputs. This is

called forward modeling and the model obtained from this method is referred to as the forward models. The most straightforward and popular approach is to augment the network inputs data signals in real number forms, from the model or system being identified (Ng & Hussain,2004). Other fundamental state variables can also be fed into the network and considered as part of the inputs. In this method, the network is fed with the present input, past inputs as well as the past outputs to predict the necessary output. The neural network is placed in parallel with the model or system. The error between the network output and system output which are the prediction error is used as the training signal for the neural network. The forward models that have been mentioned previously are used to determine the inverse model. The forward model which is inversed to get the inverse model is then changed to the equation based. The equation based method has been used to replace the black box model neural network for IMC and DIC method. The inverse models as controllers are used in the IMC and DIC methods. The composition forward models are used as a neural network estimator to predict the top and bottom compositions.

The forward model for temperature is as follows;

In this case, p are the inputs to the neural network temperature given by the vector

$$\begin{bmatrix} mv1(k) & mv1(k-1) & mv2(k) & mv2(k-1) & mv3(k) & mv3(k-1) & f(k) & f(k-1) & T_{top}(k) & T_{top}(k-1) & T_{bot}(k) & T_{bot}(k-1) \end{bmatrix}^T$$

After pruning the neural network structure (simplifying the weights and biases values)

the equation above can be further simplified to give the equation below;

$$y = \begin{bmatrix} T_1 \\ T_2 \end{bmatrix} = \begin{bmatrix} -0.16 & -0.14 & 0.04 & -0.002 & -0.094 & -0.951 & 0.03 & -0.61 & -0.71 & 0.81 & 0.16 & -0.049 \\ 0.42 & 0.07 & 0.04 & 0.20 & -0.30 & -0.19 & 0.12 & -0.28 & 0.35 & -0.29 & -0.48 & 0.168 \end{bmatrix} p + \begin{bmatrix} -0.28 \\ -0.22 \end{bmatrix} \quad (6.1)$$

T_1 and T_2 is the output neural network top and bottom temperature prediction.

6.2.3.2. Neural network estimator

The forward model for neural network for composition is similar as the neural network estimator composition n-butane used for control system IMC method extracted from chapter 4 are as follows;

In this case, p are the inputs to the neural network composition given by the vector

$$\begin{bmatrix} mv2(k) & mv2(k-1) & mv3(k) & mv3(k-1) & f(k) & f(k-1) & p_{top}(k) & p_{top}(k-1) & p_{bot}(k) & p_{bot}(k-1) \end{bmatrix}^T$$

After pruning the neural network structure (simplifying the weights and biases values) the equation above can further be simplified to give the composition equation below;

$$\begin{bmatrix} y1 \\ y2 \end{bmatrix} = \begin{bmatrix} -0.26 & 0.15 & 0.37 & 0.23 & 0.38 & 0.40 & -0.50 & 0.97 & 0.12 & -0.31 \\ -0.09 & 0.006 & 0.31 & -0.10 & 0.02 & 0.02 & -0.42 & -0.12 & 0.36 & -0.085 \end{bmatrix} p + \begin{bmatrix} -0.28 \\ -0.21 \end{bmatrix} \quad (6.2)$$

The forward model for composition i-butane is as follows;

In this case, p are the inputs to the neural network composition given by the vector

$$\begin{bmatrix} mv2(k) & mv2(k-1) & mv3(k) & mv3(k-1) & e(k) & e(k-1) & o_{top}(k) & o_{top}(k-1) & o_{bot}(k) & o_{bot}(k-1) \end{bmatrix}^T$$

After pruning the neural network structure (simplifying the weights and biases values) the equation above can further be simplified to give the composition equation below;

$$\begin{bmatrix} y1 \\ y2 \end{bmatrix} = \begin{bmatrix} 0.36 & 0.23 & 0.42 & -0.28 & 0.78 & 0.004 & -0.48 & 0.70 & 0.18 & -0.76 \\ -0.41 & -0.24 & -0.30 & 0.35 & -0.21 & -0.11 & 0.06 & -0.19 & -0.105 & 0.45 \end{bmatrix} p + \begin{bmatrix} 1.24 \\ 0.69 \end{bmatrix} \quad (6.3)$$

$y1$ and $y2$ is the output neural network top and bottom composition predictions.

6.2.3.3. Inverse models

Inverse models are basically the neural net structure representing the inverse of the system dynamics at the completion of training. The methods for inverse models are achieved by switching the inputs with the required outputs. The important manipulated variable that is used for switching the inputs of the neural net is the manipulated variable reboiler and reflux. The outputs predicted which are the future predictions of top and bottom temperatures are switched with the manipulated variables. The sequence of the inputs of the network needs to be maintained. The training procedure in this case is called inversed modeling and $y(k+1)$ corresponds to the required reference signal or set-point. The final network representation of the inverse is given below;

$$u(k) = f^{-1}[y_p(k+1), y_p(k), y_p(k-1), u(k), u(k-1)] \quad (6.4)$$

where, f^{-1} represents the inverse map of the forward model

In this case for the inverse model is to predict the reboiler and reflux flow rate. The prediction of the control output, $mv2(k)$ and $mv3(k)$ is performed for a one-step ahead prediction, inconformity with that of the forward model and the application of a one-step ahead control action in the control strategies involving the neural network based strategies.

The training and validation data set generated for the networks are similar to that used for forward modeling but with different input and output configuration.

The inverse model for temperature is as follows;

In this case, p are the inputs to the neural network inverse temperature given by the vector

$$\begin{bmatrix} mv1(k) & mv1(k-1) & mv2(k-1) & mv3(k-1) & f(k) & f(k-1) & T_{top}(k+1) & T_{top}(k) & T_{top}(k-1) & T_{bot}(k+1) & T_{bot}(k) & T_{bot}(k-1) \end{bmatrix}^T$$

After pruning the neural network structure (simplifying the weights and biases values) the equation above can further be simplified to give the inverse temperature equation below

$$\begin{bmatrix} mv2(k) \\ mv3(k) \end{bmatrix} = \begin{bmatrix} -0.16 & 0.14 & 0.039 & -0.004 & -0.09 & -0.95 & 1.03 & -0.61 & -0.72 & 0.81 & 0.17 & -0.05 \\ 0.42 & 0.077 & 0.039 & 0.20 & -0.30 & -0.19 & 0.13 & -0.27 & 0.34 & -0.28 & -0.47 & 0.16 \end{bmatrix}^p + \begin{bmatrix} -0.79 \\ -0.008 \end{bmatrix} \quad (6.5)$$

$mv2(k)$ and $mv3(k)$ is the manipulated variable reflux and reboiler flow rate respectively. The equation is implemented in SIMULINK in MATLAB by having the system with more than one control loop which are multi-input and multi-output (MIMO) or multivariable control. Figure 6.2a shows the forward and inverse model to control temperature.

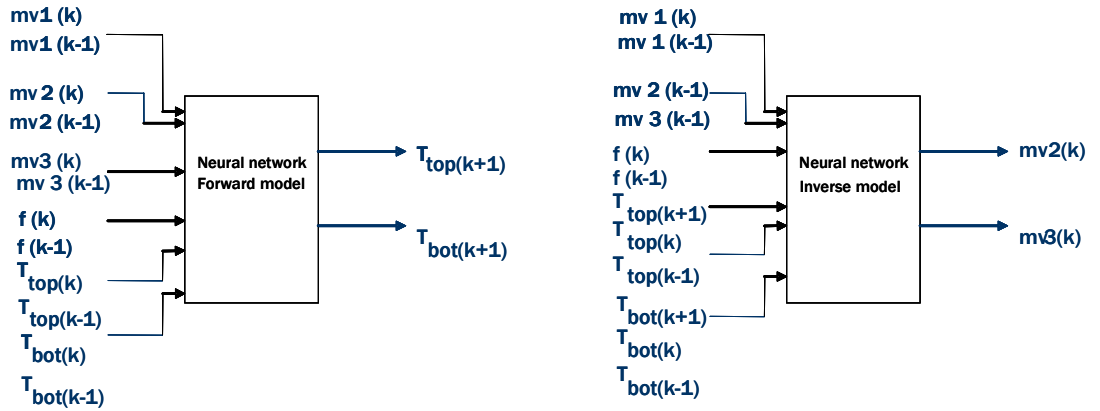


Figure 6.2a Forward and inverse models to control temperature

6.3 Neural network development

The control strategies used in this work are DIC and IMC method. In order to develop and analyze the controller performance for the debutaniser column, there are two criteria for advanced process control which are the set point changes and disturbances changes applied to the column. The set point changes is the step increases for the temperature and the disturbances changes is by introducing a disturbance of the column feed temperature. To perform the control performance for the compositions using a neural network estimator.

6.3.1 Set point changes

First the top temperature is increased from 30 to 58°C. The bottom temperature is increased from 60 to 137°C. The starting point for the top temperature is 30 °C and for bottom temperature is 60°C. This is because the starting point temperature mentioned here is based on the experience of the engineers to maintain and control that particular temperature. There are 3 types of control strategies implemented for the control strategies which are the IMC, DIC and PID controller. It can be seen that IMC and DIC show similar trends with small error, no overshoot, and fast settling time and straight goes to the set point. The settling time for top and bottom temperatures fluctuation is at 200 minutes. The IMC and DIC method gives the least fluctuations for step up tracking of the set point. The fluctuations during step up for the conventional PID controller give unacceptable results because it exhibits very large overshoot and small decay ratio. The settling time for PID also is larger compared to the IMC and DIC methods. The PID controller also produces offset when set point changes have been made. This applies to the top and bottom temperatures respectively. Table 6.1 shows the performance of the controller to control the top and bottom temperature. The results indicate that IMC

equation gives the optimum performance as the IAE, ISE values and ITAE values is the smallest compared to the result of the controller. Figures 6.5 and 6.6 show the fluctuation of the manipulated variables to control temperature. The neural network would be able to predict the manipulated variable for reboiler and reflux accurately compared to PID controller. Therefore the performance of neural network is better. The fluctuations of the manipulated variable for the reboiler and reflux are very important to see how the controller calculates the error for a control system. The fluctuations for reboiler and reflux flow rate for temperature based on PID show similar trends as time progresses. The units for the calculated IA, ISE and ITAE are dimensionless.

Table 6.1 PID tuning

Parameter	K_c	T_i	T_d
Top temperature	0.71	1.41	20
Bottom temperature	1.76	3.25	15
Top composition	137.32	3.26	10
Bottom composition	87.36	3.26	5

Table 6.2 Controller performance during set point changes

	IMC eq	DIC eq	PID
IAE top	830.76	912.78	1219.70
IAE bottom	3809	4289	4666

	IMC eq	DIC eq	PID
ISE top	2.10E+04	2.23E+04	2.69E+04
ISE bottom	1.21E+05	2.67E+05	3.06E+05

	IMC eq	DIC eq	PID
ITAE top	4.25E+04	4.48E+04	1.44E+05
ITAE bottom	1.92E+05	2.16E+05	4.45E+05

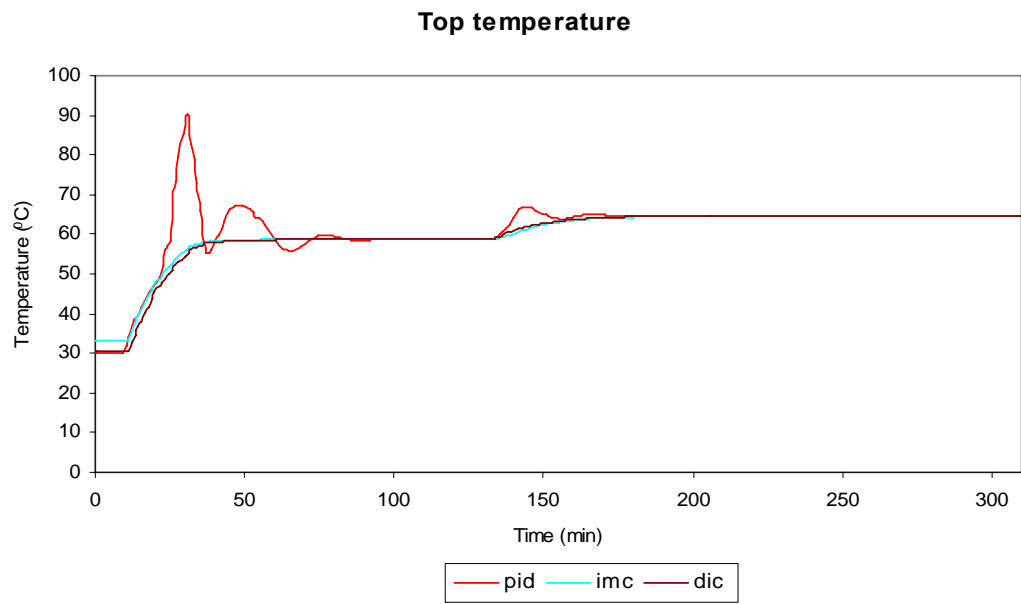


Figure 6.3 Set point top temperature

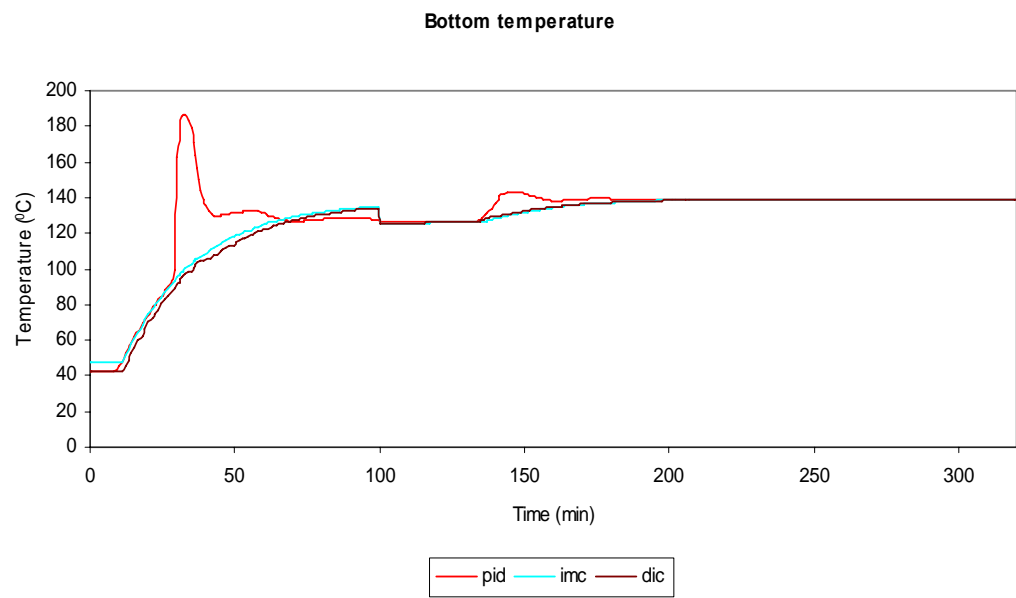


Figure 6.4 Set point bottom temperature

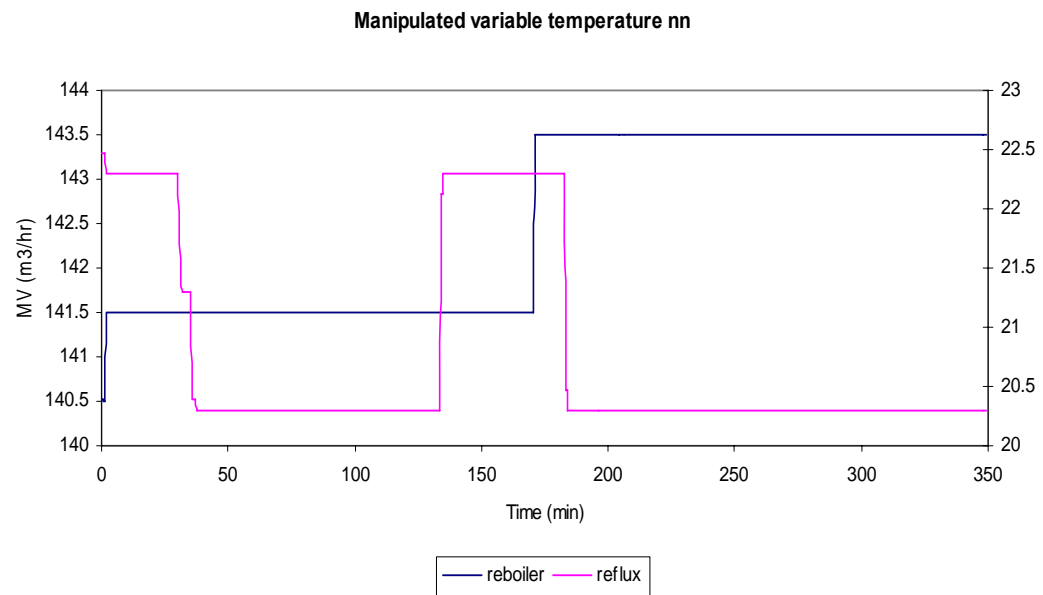


Figure 6.5 Manipulated variable temperature neural network

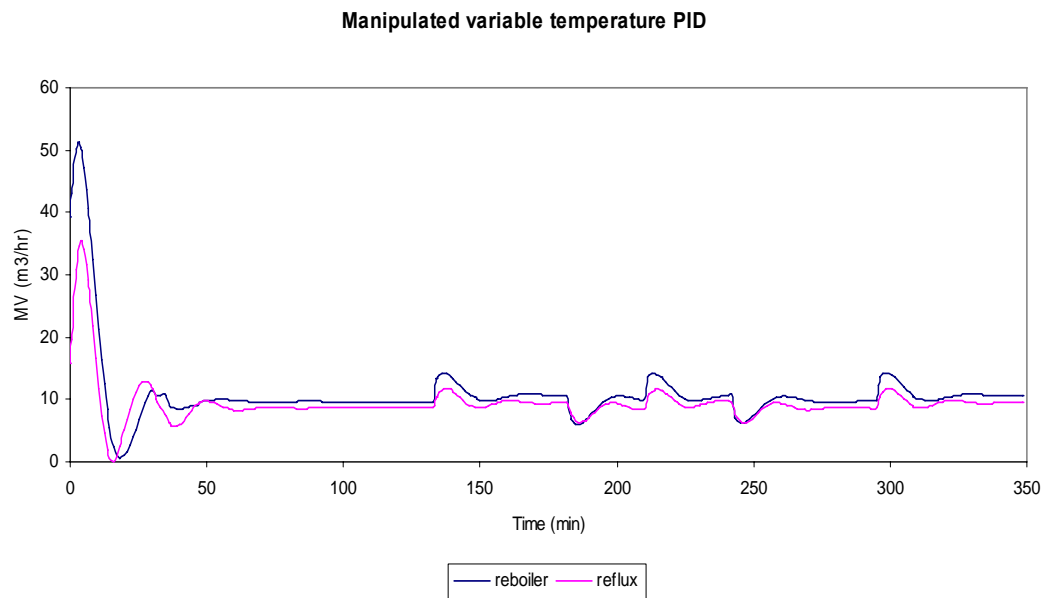


Figure 6.6 Manipulated variable temperature PID

6.3.2 Disturbances test

Figures 6.7 and 6.8 show the fluctuations for the top and bottom temperatures due to disturbances. The disturbances introduced to the debutaniser column are the feed temperature. Similar trends are observed for DIC and IMC methods for the top and bottom temperatures because of disturbances. The neural network control performs well compared to PID controller because there is no overshoot, fast settling time and small error. The PID controller gives unacceptable results as they perform with high overshoot, some offset and large error. This also applies to the top and bottom temperatures. Table 6.2 shows the performance of the controller to control the top and bottom temperatures. Results indicate that IMC equation gives the optimum performance as the values of IAE, ISE and ITAE are the smallest compared to other controller. Figures 6.9 and 6.10 show the fluctuation of the manipulated variable to control temperature. The neural network would be able to predict the manipulated variable for reboiler and reflux accurately compared to PID controller. Therefore the performance of neural network is better. The fluctuation of the manipulated variable for the reboiler and reflux flow rate is very important in order to see how the controller calculates the error for a given control system. The fluctuations for reboiler and reflux flow rate for temperature based on PID shows similar trends as time progresses.

Table 6.3 Controller performance during disturbance changes

	IMC eq	DIC eq	PID
IAE top	817.21	836.95	1736.30
IAE bottom	2811.80	2876.00	7891.20

	IMC eq	DIC eq	PID
ISE top	6.02E+03	6.63E+03	3.37E+04
ISE bottom	1.14E+05	1.23E+05	1.75E+06

	IMC eq	DIC eq	PID
ITAE top	7.78E+04	7.90E+04	1.78E+05
ITAE bottom	1.28E+05	1.30E+05	4.64E+05

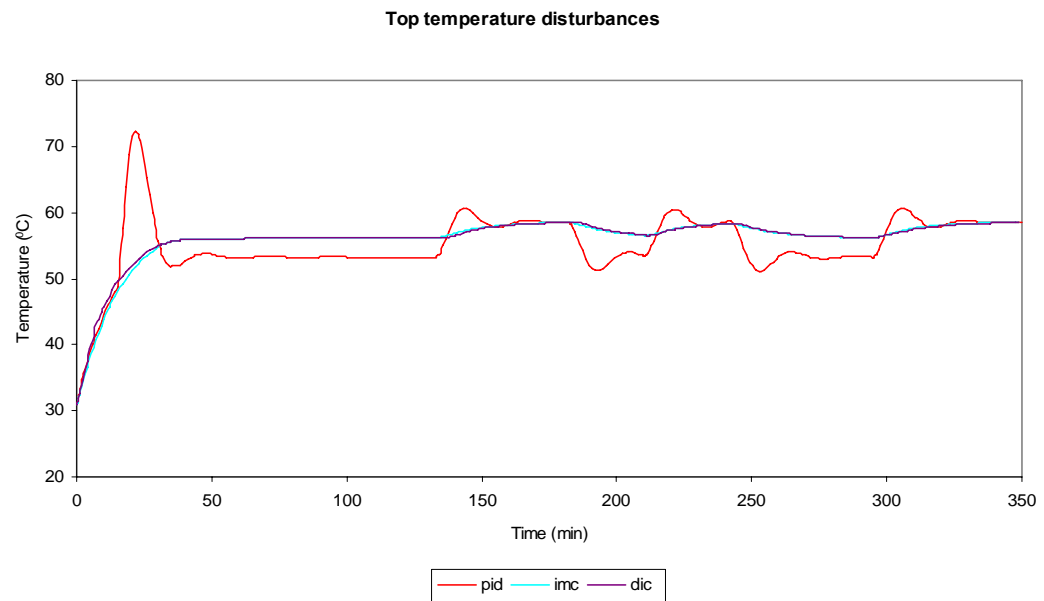


Figure 6.7 Disturbances top temperature

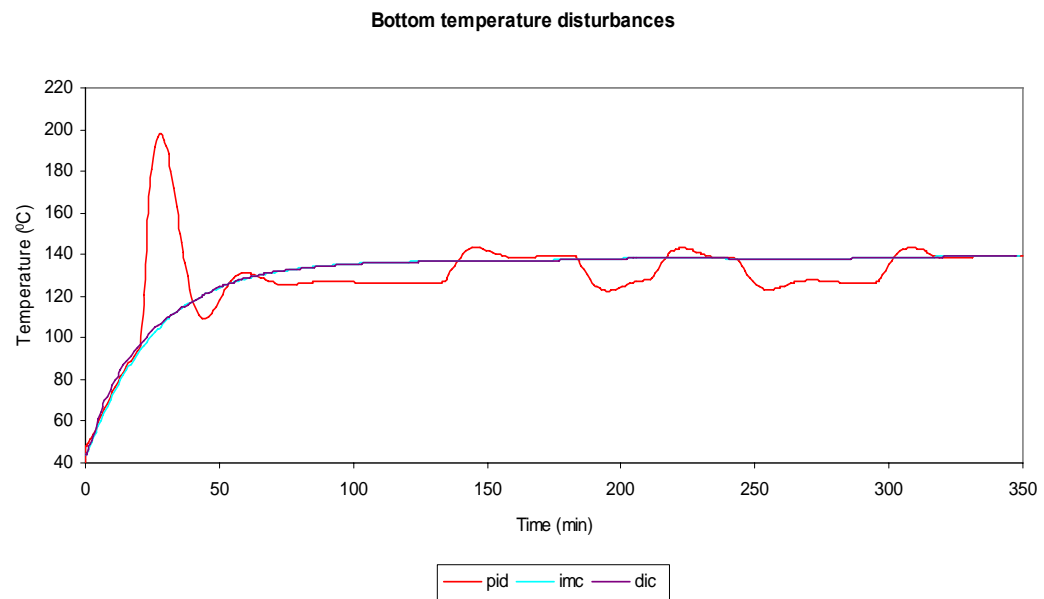


Figure 6.8 Disturbances bottom temperature

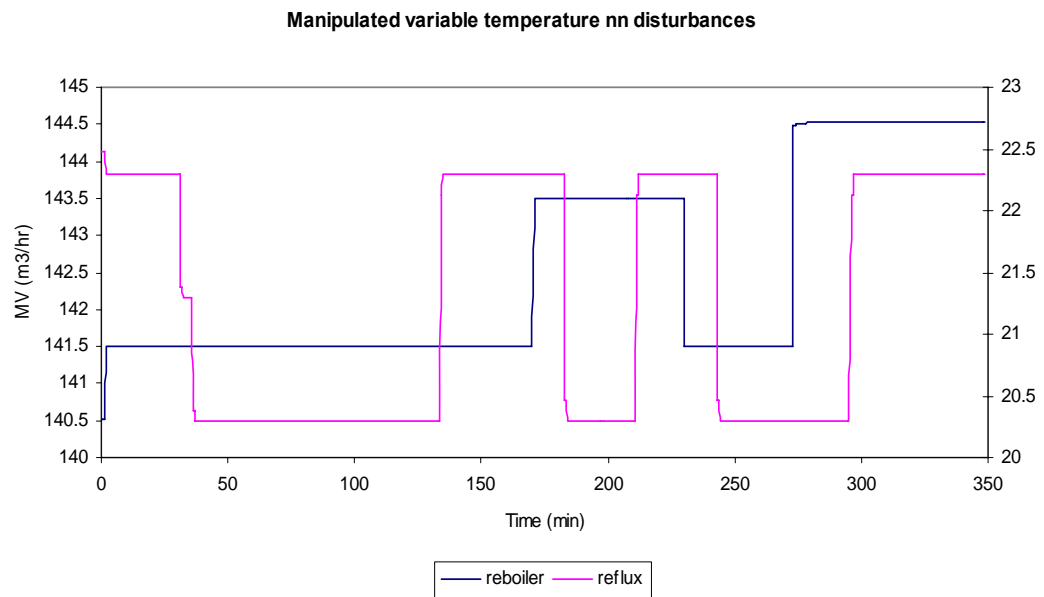


Figure 6.9 Manipulated variable temperature neural network disturbances

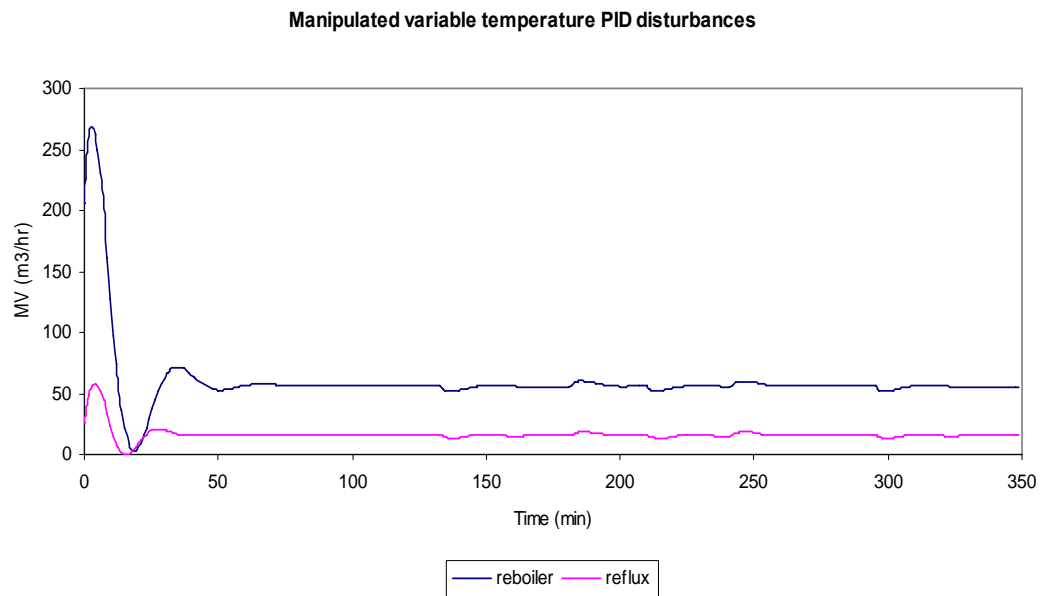


Figure 6.10 Manipulated variable temperature PID disturbances

n-butane

6.3.3 Neural network estimator

The neural network estimator used in the IMC and DIC method is to monitor and estimate the top and bottom composition. Figures 6.11 and 6.12 show the fluctuations for the top and bottom compositions which are due to set point changes. For the top composition for neural network controller for IMC and DIC methods, it could be concluded that the IMC trend shows optimum result compared to DIC. This is because the settling time to settle to the required set point for the composition is faster. Both IMC and DIC method are superior comparison to the conventional PID controller. This is because the error is small with no overshoot. The results for PID controller are unacceptable because of large overshoot, large error and longer settling time. For the bottom composition fluctuations, the IMC and DIC methods show similar trends. Both methods show better fluctuations compared to PID controller. Figure 6.13 shows the fluctuation of the manipulated variable for composition.

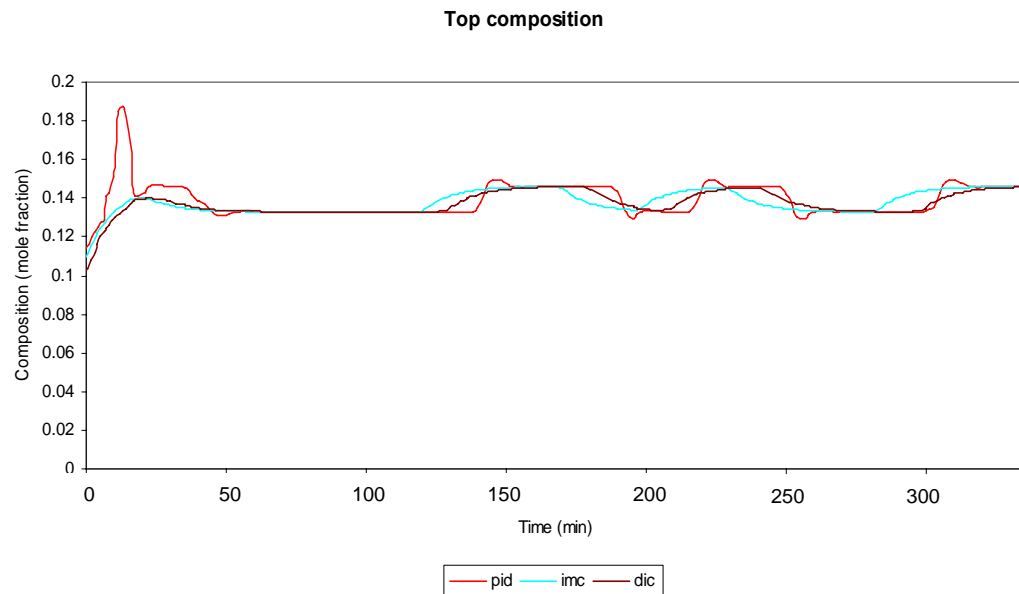


Figure 6.11 Neural network estimator for the top composition

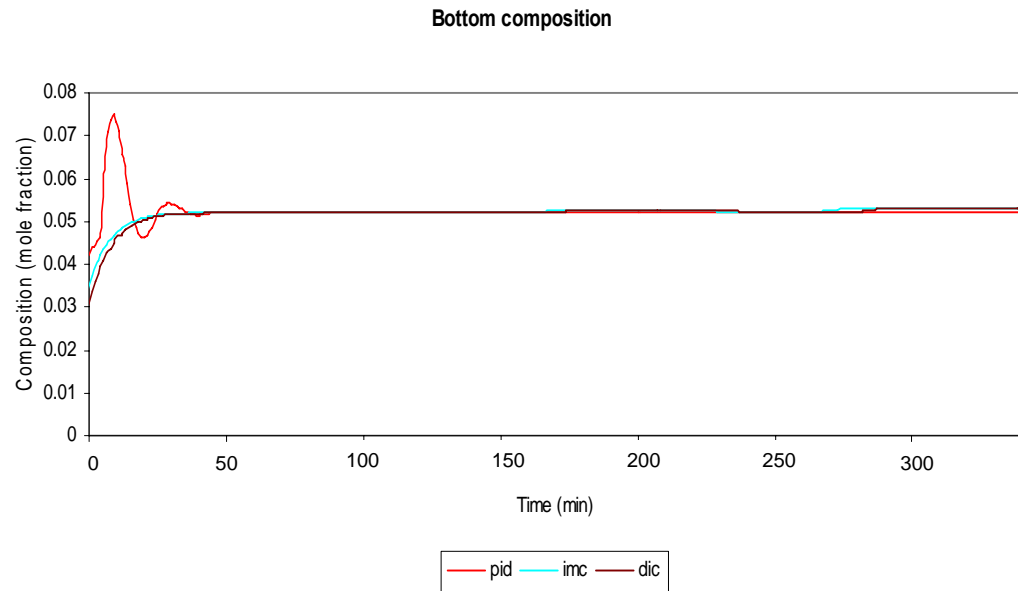


Figure 6.12 Neural network estimator for the bottom composition

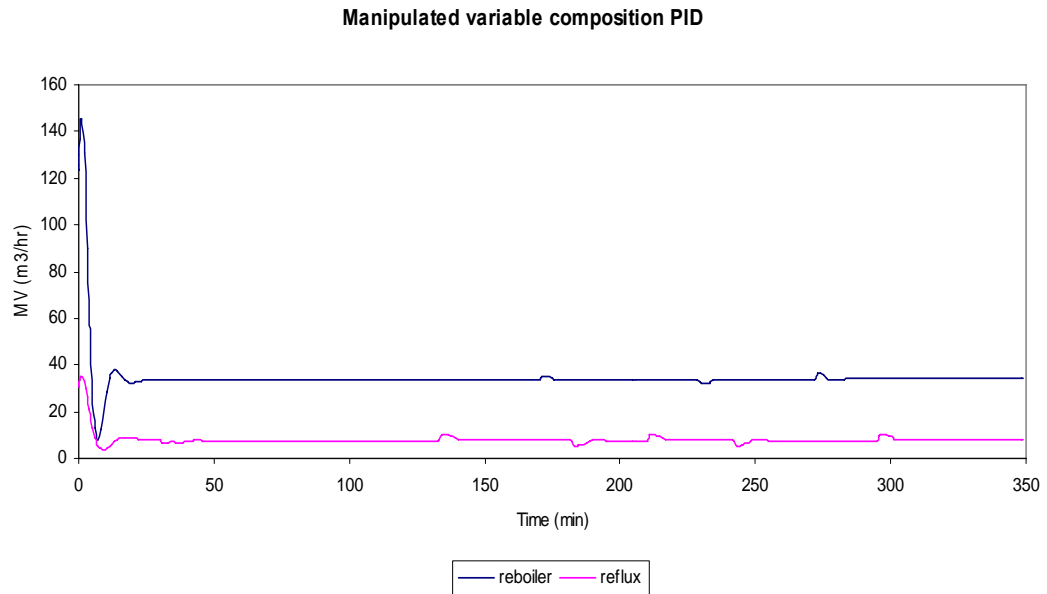


Figure 6.13 Manipulated variable compositions for PID

Figures 6.14 and 6.15 show the fluctuations for the top and bottom compositions due to disturbances. For the top composition for neural network controller for IMC and DIC methods, it could be concluded that the IMC trend shows similar results to the DIC method. The settling time for the required set point for the composition is similar. Both IMC and DIC methods are superior in comparison to the conventional PID controller.

This is because the error is small with no overshoot. The results for PID controller are unacceptable that are due to large overshoot, large error and longer time to settle. For the bottom composition fluctuations, the IMC and DIC methods show similar trends. Both methods shows better fluctuations compared to PID controller. Figure 6.16 shows the fluctuation of the manipulated variable for composition PID which is due to disturbances.

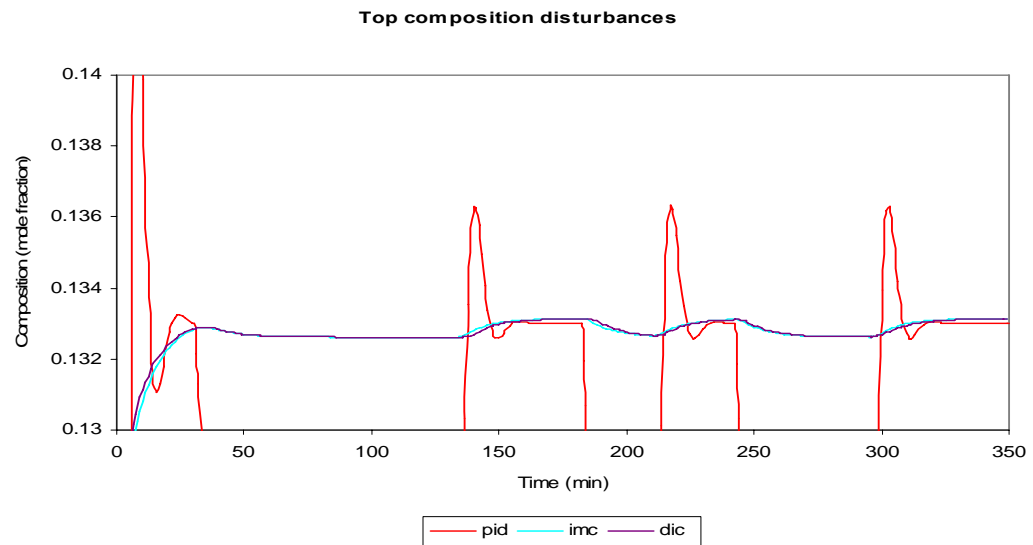


Figure 6.14 Top composition disturbances

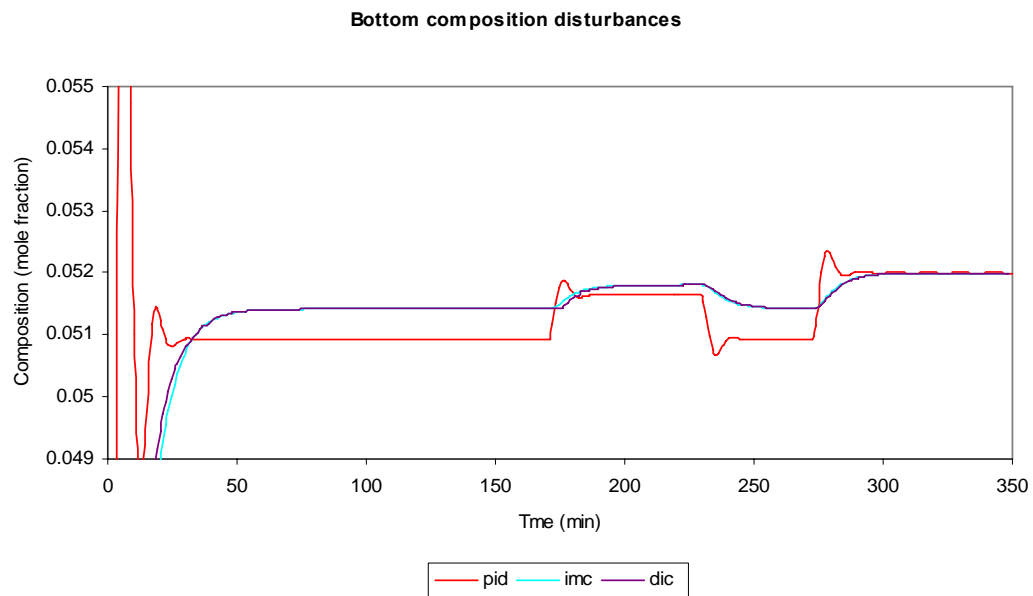


Figure 6.15 Bottom composition disturbances

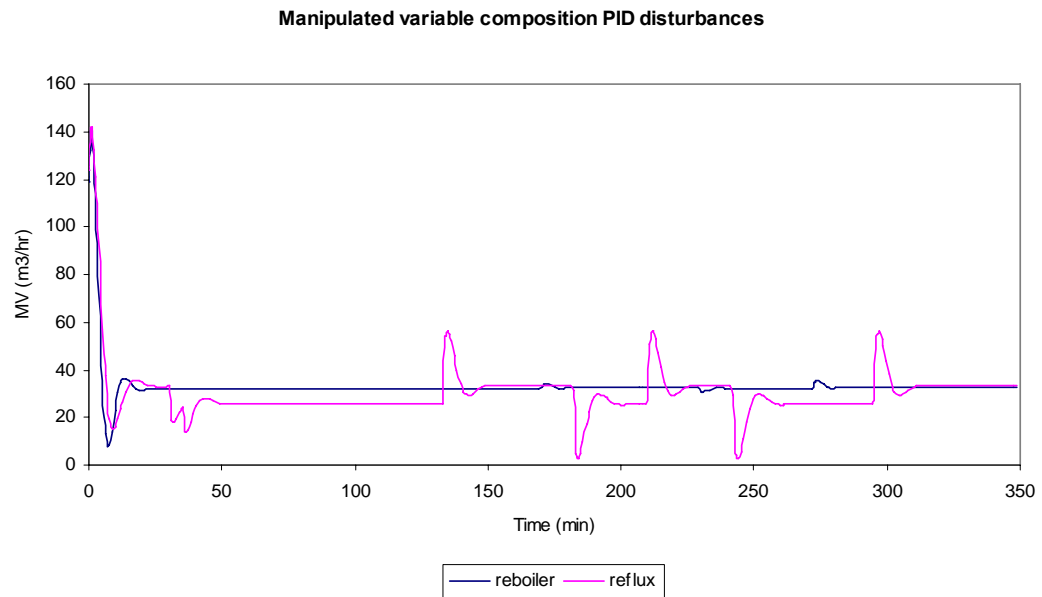


Figure 6.16 Manipulated variable compositions PID due to disturbances

6.3.4 Neural network steady state error

Figures 6.17 and 6.18 show the fluctuations of the steady state error for the neural network for the column. It could be observed that the steady state error is small compared to the PID controller and less fluctuations.

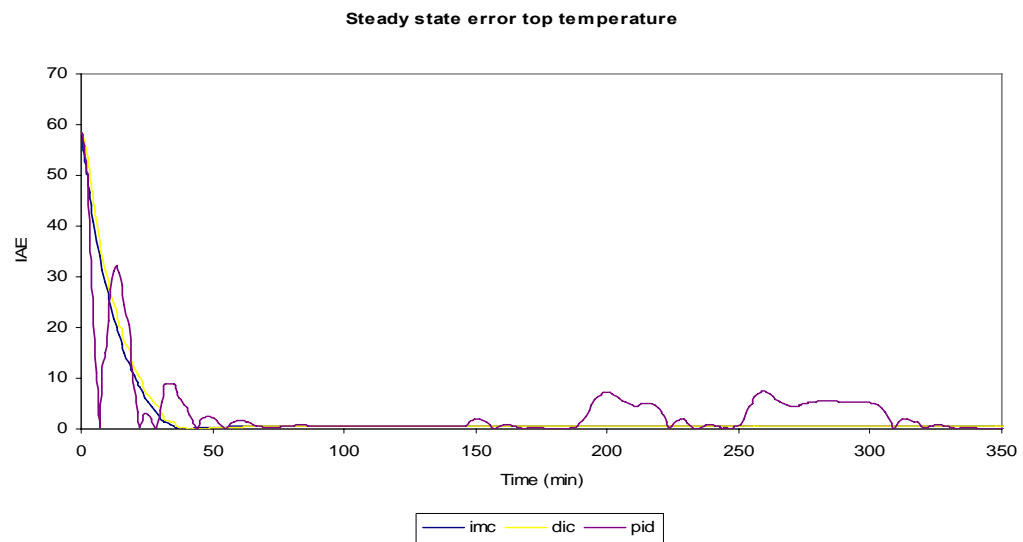


Figure 6.17 Steady state error top temperature

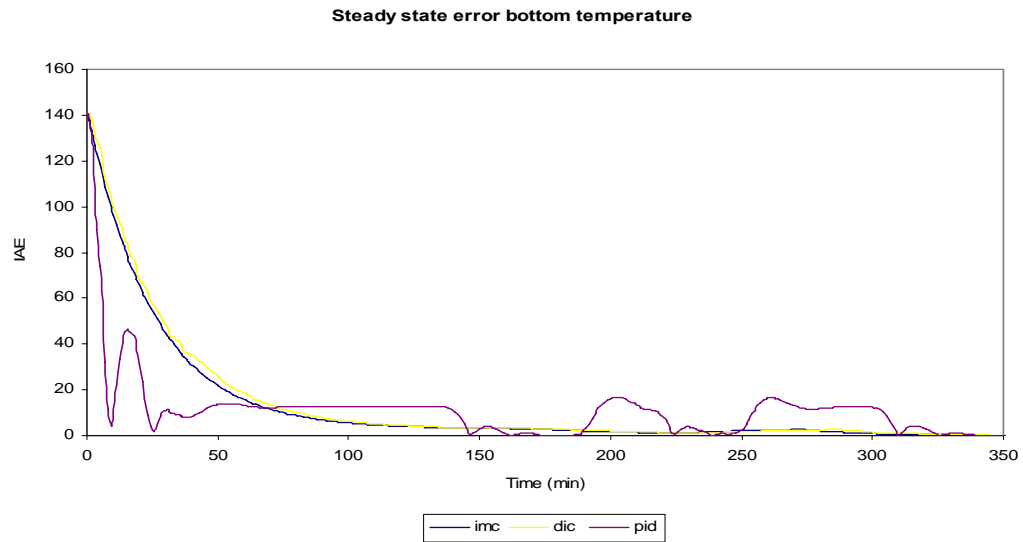


Figure 6.17 Steady state error bottom temperature

Established control system design techniques rely on the availability of non-linear system models. This is to ensure that the resulting control scheme is closely matched to the dynamics of the process. The multivariable system must therefore first be modeled using set of differential equations to describe their behavior to an assumed structure of the process, black box modeling. However, for the control system design purposes, the input output model obtained using equation based method approach is often robust, adequate and can be used for control of multivariable processes such as the debutaniser column system.

The difference in computing time using these different approaches are shown in Table 6.4 where the NN model takes less than 5 seconds to compute which more faster than the PLS (45 seconds) and RA method (1 minute). Hence it is suitable for online measurement since the industrial method takes more than 1 day to analyse and compute.

Table 6.4. Computing time

	NN eq	PLS eq	RA eq
Computing time	5 second	45 second	1 minute

CHAPTER 7: SUMMARY AND MAJOR CONTRIBUTION

7.1 Introduction

This chapter presents the summary and conclusion of the research work carried out in this thesis. The contribution of this work is also presented to highlight the findings and results from this study. Finally, recommendations for possible future work extension are suggested for further improvement in designing debutaniser column and extended to other types of advanced non-linear control methods.

7.2 Summary of work

1. A neural network model is able to model the top and bottom composition as well as temperature prediction of a debutaniser column. The model makes use of online closed loop data, open loop data and simulation data making it robust and highly suitable for online application. PCA and PLS analyses have also been found to facilitate the correct and right inputs of the variables for the column since a large number of industrial data are available. The neural network prediction of n-butane and i-butane gives high accuracy and small error between the prediction and actual composition and actual temperature. This ensures that neural network could also be used as an inferential estimator for composition estimation online. From the statistical analysis for the top and bottom composition of n-butane and i-butane it indicates that RMSE is smaller for the extract from the closed loop compared to the open loop response. Therefore the extract from the closed loop tends to perform better than the open loop response.
2. An equation based neural network model can be used to estimate and predict the top and bottom compositions of n-butane and i-butane of a debutaniser column

satisfactorily. The collected data is then compared to other methods such as PLS and regression analysis. All of the results are able to give optimum results in predicting the compositions and temperature. However based on the RMSE values, it could be concluded that NN equation seems to give the best prediction compared to other models. This is especially true for nonlinear system, where linear controllers are not able to perform satisfactorily.

3. A satisfactory hybrid prediction model of a debutaniser column using equation-based model has been developed. The results are compared to the hybrid neural network black box model and conventional neural network black box models. The hybrid neural network equation seems to perform better in comparison to the rest of the neural network prediction methodologies. This is based on the estimated error values which are smaller with respect to the other prediction procedures. This work could be developed for online prediction, monitoring and control of composition and temperature of the column. Based on the hybrid model, the effect of key operation conditions is analyzed and some useful guiding rules are established. The performance prediction of the hybrid equation neural network is a function of the quality and range of the sample data. Thus performance of the hybrid model will also depend on the quality and range of the sample data. The other advantage of the hybrid equation is it allows the user to determine the relationship between the inputs and outputs for these predictions and could be easily applied for model based control strategies in the future.
4. A new model has successfully been developed and used to simulate the dynamic responses of compositions and temperature when the controllers were applied into the system. The control strategies namely, internal model controller (IMC) and

Direct Inverse Control (DIC) are implemented in simulation within the control system. The forward model and inverse model are used to develop the control strategies for temperature fluctuations. Neural network estimator is used to predict the composition fluctuations. The entire models developed for the controller are used based on equation based method. The controllers were on the ability to track set-point changes and disturbances test changes in the system. Based on the result, IMC equation was found to perform better than the conventional controllers

7.3 Major contribution of this work

In general, this work has contributed in various aspects to the implementation of neural network based process controllers in debutaniser column control. Among the significant contributions that can be outlined for this work include the following:-

1. Online and simulation data are used for modeling the debutanizer column. Data generation is an important step to identify the responses of all the variables surrounding the column to obtain the neural network model. A mixture of online close loop and open loop data for those data available online and simulation data for those not available online, for training the neural network models.
2. In many practical control problems, typically a number of variables are controlled and are manipulated. Therefore the neural network model that is developed in this work is based on Multi input and multi output (MIMO) process. The MIMO process is more complex than the Single input single output (SISO) because process interaction occurs between controlled and manipulated variables.

3. The prediction of the composition and temperature at the top and bottom of a debutaniser column are achieved using the equation based neural network model. This proposed equation based NN model is useful for online composition and temperature prediction since it is robust and versatile and can be easily applied as a soft sensor for the distillation column.
4. The hybrid model which includes neural network prediction where the model is presented using equation based method. The neural network is used to predict the residual composition and temperature of the top and bottom prediction for the column simultaneously. The residual is the difference between the actual and simulated values. The residuals are then added to the first principle model in a hybrid fashion, to predict the actual composition and temperature of the top and bottom for the column.
5. The development of inverse and forward model based neural network control strategies to control top and bottom temperature. The compositions are estimated using forward model neural network estimator. The control strategies that are used in simulation for the neural network model are based on equation based model.

CHAPTER 8: CONCLUSIONS AND RECOMMENDATION

8.1 Conclusions

1. PCA is multivariate projection method designed to extract and display systematic variation in data. Prior to PCA, data are pretreated in order to transform the data into analysis. PLS is regression extension of PCA which is used to relate the input and output variables. PLS provides model parameter which are useful for the regression model. The SIMCA-P environment is powerful tool to address PCA and PLS for the debutaniser column.
2. The proposed equation based NN model is useful for online composition prediction since it is robust and versatile and can be easily applied as a soft sensor for the distillation column. It could also easily be further applied as an inverse controller in the equation form especially for nonlinear system, where linear controllers are not able to perform successfully. This proposed model based NN method is also easier to visualize and apply for various applications as compared to the black box neural network structure which is cumbersome and non-portable in nature.
3. By extracting the matrix input weight and biases is another way to represent the neural network black box model. All NN models, used by other researchers are black box models. Putting the weights and biases in the equation based could be easily utilized because we could determine the relationship between the input and output predictions. Extracting the weights and biases from the neural network are just another way to represent NN equation based model.

3. The proposed hybrid equation model is also useful for online composition and temperature prediction since it is versatile with fast computing time and easily be applied as a soft sensor for the debutaniser column. It could predict both the top and bottom compositions as well as temperatures through the use of a single vector equation.
4. The resulting control strategy performance depends on the accuracy of the model. In the process industries, where there is a high degree of uncertainty about process behavior, the black box modeling approach is often employed. However, for the control system design purposes, the input output model obtained using equation based method approach..

8.2 Recommendations and future work

Possible proposed future work is as follows:-

1. Other advanced control strategies such as fuzzy logic, sliding mode control, self tuning PID and auto tuning PID can be implemented to control different various processes. Further research should also focus on the study of different schemes of advanced control strategies which are available.
2. System identification using neural network control strategies can be further developed by using graphical user interface. This method would enhance the communication with online processes through available communication. User will be able to select the inputs and outputs to the process controller directly. The GUI will carry out the modelling for the inverse and forward model incorporated in the control strategies. It will assign the optimum neural network structure to be used for the models and come out with a process controller. The product will be

integrated with online data acquisition and data processing where it can be able to analyze and plot the results.

3. The forward model that are used for hybrid prediction for the debutaniser column to predict composition and temperature could be used as an inverse model so that it could then be implemented as a controller in the IMC and DIC control strategies.
4. Optimization of the debutaniser column is important. Modification in process design and operating procedure could be implemented to reduce costs and meet constraints with an emphasis on improving efficiency and profitability. Optimization of the column using mathematical programming could be carried out. The process model of the column comprises the equality constraints. Emphasis on how to formulate optimization appropriately helps engineers and scientists understand the difficult phase of the process.

REFERENCES

- Alpaz M., Karacan S, Cabbar Y., Hapoglu H. (2002). Application of model predictive control and dynamic analysis to a pilot distillation column and experimental verification. *Chemical Engineering Journal* 88: 63-174
- Balchen J G., Sandrib B., (1995). Elementary nonlinear decoupling control of composition in binary distillation columns. *Journal of Process Control*.5, No. 4: 241-247,
- Baratti R., Corti S., (1997). A feedforward control strategy for distillation column. *Artificial Intelligence in Engineering* 11: 40-412
- Bertsekas, D.P., Tsitsiklis, J.N. (1996). Neuro-dynamic programming. *Athena Scientific*
- Bettoni A., Bravi M., Chianese A., (2000). Inferential control of a sidestream distillation column. *Computers and Chemical Engineering* 23: 1737–1744
- Biswas P. P., Ray S., Samanta A N., (2007). Multi-objective constraint optimizing IOL control of distillation column with nonlinear observer. *Journal of Process Control* 17: 73–81
- Biswas P. P., Ray S, Samanta A., N., (2009). Nonlinear control of high purity distillation column under input saturation and parametric uncertainty. *Journal of Process Control* 19: 75–84
- Bollas G M., Papadokonstadakis S., Michalopoulos J., Aramatzis G., Lappas A.A., Vasalos I A., Lygeros A., (2003). Using hybrid neural networks in scaling up an FCC model from a pilot plant to industrial unit. *Chemical Engineering and Processing*, 42: 697-713
- Chang J S., Lu S., Chiu Y., (2007). Dynamic modeling of batch polymerization reactors via hybrid neural network rate function approach. *Chemical Engineering Journal*, 130: 19-28.
- Chawankul N., Budman H., Douglas P., (2005) The integration of design and control: IMC control and robustness. *Computers and Chemical Engineering* 29: 261–271
- Chen G, McAvoy Thomas J., Piovoso Michael J, (1998). A multivariate statistical controller for online quality improvement. *Journal of Process Control* 8: 139-149

- Cubillos F A, Alvarez P I, Pinto J C, Lima E L., (1996).Hybrid neural modeling for particulates solid drying processes. *Powder Technology* 87: 153-160
- Demuth H., Beale M and Hagan M., (2007). Neural network Toolbox User Guide Version 5, *Mathworks*
- Deng Hua, Xu Zhen & Li Han-Xiong., (2009). A novel neural internal model control for multi-input and multi-output nonlinear discrete time processes. *Journal of process control*, 19: 1392-1400
- Dutta P., Rhinehart R. R., (1999).Application of neural network control to distillation and an experimental comparison with other advanced controllers. *ISA Transactions* 38: 251-278
- Dwyer Aidan O., (2003).Handbook PI and PID Controller Tuning Rules. *World Scientific*
- Elgue S., Prat L., Cabassud M., Le Lann J M., Cezerac J. (2004).Dynamic models for start up operations of batch distillation columns with experimental validation. *Computers and Chemical Engineering* 28: 2735-2747
- Enagandula S., Riggs James B., (2006).Distillation control configuration selection based on product variability prediction. *Control Engineering Practice* 14: 743–755
- Eriksson L., Johansson E., Kettaneh-Wold N., Trygg J., Wilstrom C., Wold S., (January 2006). Multi and Megavariate Data Analysis Part I Basic Principles and Applications. *Umetrics Academy* 2nd edition,
- Fernandez de Canete J, Gonzalez S, del Saz-Orozco P & Garcia I., (2010).A harmonic balance approach to robust neural control of MIMO nonlinear processes applied to a distillation column. *Journal process control*, 20: 1270-1277
- Fernandez de Canete J, del Saz-Orozco P, Gonzalez S, & Garcia-Moral I., (2012)..Dual composition control and soft estimation for a pilot distillation column using a neurogenetic design. *Computers and Chemical Engineering*, 40: 157-170
- Fortuna L., Graziana S., Xibilia M.G. (2005). Soft sensors for product quality monitoring debutanizer distillation columns. *Control Engineering Practice* 13: 499-508

- Gonzalez-Trejo J., Ramirez J. A., Fernandez G., (1999). Robust control with uncertainty estimation for feedback linearizable systems: application to control of distillation columns. *Journal of Process Control* 9: 221-231
- Guo B, Shen Y, Li D, Zhao F., (1997). Modeling coal gasification with a hybrid neural network. *Fuel* 76, 12: 1159-1164
- Gupta, S., Ray, S., Samanta, A. N. (2009). Nonlinear control of debutanizer column using profile position observer. *Computers & Chemical Engineering*, 33(6): 1202-1211
- Hagglblom K E., (1996). Combined internal model and inferential control of a distillation column via closed-loop identification. *Journal of Process Control*. 6, 4: 223-232,
- Hori E. S., Skogestad S., (2007). Selection of control structure and temperature location for two product distillation columns. *Chemical Engineering Research and Design*, Trans IChemE Part : 121-134
- Horn J., (2001). Trajectory tracking of batch polymerization reactor based on input-output linearization of a neural process model. *Computers and Chemical Engineering* 25: 1561-1567
- Hu Bin, Zhao Zhao & Liang Jun., (2012). Multi-loop nonlinear model controller design under nonlinear dynamic PLS framework using ARX-neural network model. *Journal of process control*, 22: 207-217
- Huang K., Wang S. J., Iwakabe K., Shan L., Zhu Q., (2007). Temperature control of an ideal heat-integrated distillation column (HIDiC). *Chemical Engineering Science* 62: 6486 – 6491
- Iruthayarajan M.W., Baskar S., (2009). Evolutionary algorithms based design of multivariable PID controller. *Expert Systems with Applications* doi:10.1016/j.eswa.2008.12.033
- Jan A. K., Samanta A. N., Ganguly S., (2009). Nonlinear state estimation and control of a refinery debutanizer column. *Computers and Chemical Engineering*, 33: 1484–1490
- Jana A. K., (2010). Analysis and control of a partially heat integrated refinery debutanizer. *Computers and Chemical Engineering*. 34: 1296–1305

- Jana A K., Samanta A. N., Ganguly S., (2005). Nonlinear model-based control algorithm for a distillation column using software sensor. *ISA Transactions* 44: 259–271
- Kahrs O., Marquardt W., (2008). Incremental identification of hybrid process models. *Computers and Chemical Engineering* 32: 694–705
- Kano M., Miyazaki K., Hasebi S., Hashimoto I. (2000). Inferential control system of distillation compositions using dynamic partial least squares regression. *Journal of Process Control* 10: 157–166
- Karacan S., (2003). Application of a non-linear long range predictive control to a packed distillation column. *Chemical Engineering and Processing* 42: 943–953
- Karacan S., Hapoglu H., Albaz M., (2007). Multivariable system identification and generic model control of a laboratory scale packed distillation column. *Applied Thermal Engineering* 27, 1017–1028
- Khaisongkram W., Banjerdpongchai D., (2006). Linear controller design and performance limits of binary distillation column subject to disturbances with bounds on magnitudes and rates of change. *Journal of Process Control* 16: 845–854
- L Smith Cecil, (1979). Industrial process control. *Proceedings of the workshop American Institute of Chemical Engineers Continuing Education Department*, 70–75
- Lim J S, Hussain M A & Aroua M K., (2010). Control of a hydrolyzer in an oleochemical plant using neural network based controllers. *Neurocomputing*, 73: 3242–3255
- Linhart A., Skogestad S., (2009). Computational performance of aggregated distillation models. *Computers and Chemical Engineering* 33: 296–308
- Liu X., Kruger U., Littler T., Xie L., Wang S., (2009). Moving window kernel PCA for adaptive monitoring of nonlinear processes. *Chemometrics and Intelligent Laboratory Systems* 96: 132–143
- M Ramli Nasser., Hussain M A., (1–2 December 2009). Dynamic modeling and control of a debutanizer column. *16th ASEAN Regional Symposium on Chemical Engineering* (RSCE 2009) Manila, Philippines.

- M Ramli N., Hussain M A., Mohamed Jan B., (2011).Principal component analysis of a debutanizer column. *International conference of Chemical Engineering and Industrial Biotechnology with 25th Symposium of Malaysian Chemical Engineers*, 28 November – 1 December 2011, Kuantan, Pahang, Malaysia
- Madar J, Abonyi J., Szeifert F., (2005).Feedback linerizing control using hybrid neural networks identified by sensitivity approach. *Engineering Applications of Artificial Intelligence* 18: 343-351
- Maiti S. N., Saraf N., (1995).Adaptive dynamic matrix control of a distillation column with closed-loop online identification. *Journal of Process Control* 5: 315-327
- Mohamed Ramli N., Hussain M A., Mohamed Jan B., (2012). Hybrid neural network to estimate composition and temperature of a debutanizer column. *4th International conference on Chemical and Bioprocess Engineering with 26th Symposium of Malaysian Chemical Engineers* 21 – 23 November 2012, Kota Kinabalu, Sabah.
- Mohamed Ramli N., Hussain M A., Mohamed Jan B., (2014). Composition prediction of a debutanizer column using equation based artificial neural network model. *Neurocomputing* 131: 59-76
- Mohd Ramli N., Hussain M A., Mohamed Jan B., (2010). Neural network model for composition prediction in debutanizer column. *conference proceeding 17th Regional Symposium on chemical engineering* 22-23 November 2010, Bangkok, Thailand
- Molga E., Cherbanski R., (1999).Hybrid first principle neural network approach to modelling of the liquid liquid reacting system. *Chemical Engineering Science*, 54: 2467-2473
- Monedero I., Biscarri F., León C., Guerrero J I., González R., Pérez-Lombard L., (2012). Decision system based on neural networks to optimize the energy efficiency of a petrochemical plant. *Expert Systems with Applications* 39: 9860–9867
- Mujtaba I M, Aziz N & Hussain M A., (2006).Neural network based modeling and control in batch reactor. *Chemical Engineering Research and Design*, 84: 635-644
- Murlidhar G. M., Jana A. K., (2007).Nonlinear adaptive control algorithm for a multicomponent batch distillation column. *Chemical Engineering Science* 62: 1111 – 1124

- Ng C W & Hussain M A., (2004).Hybrid neural network prior knowledge model in temperature control of a semi batch polymerization process. *Chemical Engineering and Processing* 43 :559-570
- Nooraii A., Figueroa J., Romagnoli J A., (1997). Robustness analysis and control of a pilot-scale distillation column. *Computers and Chemical Engineering* 21 : 703-717,
- Oliverira R., (2004) Combining first principle modeling and artificial neural networks: a general framework. *Computers and Chemical Engineering*, 28 : 755-766
- Peng B., Li Xi., Sheng M., Song S., Zhao G., Li Xi, (2007). Study of dual temperature control method on cyclic total reflux batch distillation. *Chemical Engineering and Processing*, 46: 769–772
- Prasad V., Wayne Bequette B., (2003).Nonlinear system identification and model reduction using artificial neural networks. *Computer and Chemical Engineering* 27: 1741-1754
- Qi, H., Zhou X., Liu L.,Yuan W.K., (1999).A hybrid neural network first priciple model for fixed bed reactor *Chemical Engineering Science*, 54: 2521-2526
- Ramchandran S., Rhinehart RR., (1995). A very simple structure for neural network control of distillation. *Journal of process control*. 5 : 115-128
- Ramli S. A., (2008). Study of Neural Network for Heat exchanger with development of graphical user interface *Thesis, Universiti Teknologi PETRONAS*
- Seader, J D., Header E. J. (2006) Separation process principle *John Wiley and Sons 2nd edition*
- Seborg Dale E., Edgar Thomas F., Mellichamp Duncan A., (2003). Process Dynamic and Control. *John Wiley and Sons 2nd edition*
- Sen D, Roy A, Bhattacharya, Banerjee D., Bhattacharjee C., (2011). Development of a knowledge based neural network for studying the effect of diafiltration of whey. *Desalination* 273 :168-178
- Shamsuzzoha M., Lee M., (2008).Analytical design of enhanced PID filter controller for integrating and first order unstable processes with time delay. *Chemical Engineering Science* 63: 2717 – 2731

- Sharma R., Singh K., Singhal D., and Ghosh R., (2004). Neural network applications for detecting process faults in packed towers. *Chemical Engineering and Processing* 43: 841–847.
- Shin J., Seo H., Han M., Park S., (2000). A nonlinear profile observer using tray temperatures for high-purity binary distillation column control. *Chemical Engineering Science* 55: 807-816
- Singh V., Gupta I., Gupta H.O., (2005). ANN based estimator for distillation—inferential control. *Chemical Engineering and Processing* 44: 785–795
- Singh V., Gupta I., and Gupta H.O., (2007). ANN-based estimator for distillation using Levenberg–Marquardt Approach. *Engineering Applications of Artificial Intelligence* 20: 249–259
- Srinivas G R., Arkun Y., Chien I L., Ogunnaike B A., (1995). Nonlinear identification and control of a high-purity distillation column: a case study. *Journal of Process Control*.5: 149 162
- Stephanopoulos, George (1984). Chemical Process Control: An Introduction to Theory and Practice. *Prentice Hall*
- Stevanovic J S., (1996). Neural Net controller by inverse modeling for a distillation plant. *Computers and Chemical Engineering* 20: 925-930
- Trotta A., Barolo M., (1995). Nonlinear model based control of a binary distillation column. *Computer and Chemical Engineering* 19: 519-524
- Wan J., Huang M., Ma Y., Guo W., Wang Y., Zhang H., Li W., Sun X., (2011). Prediction of effluent quality of a paper mill wastewater treatment using an adaptive network-based fuzzy inference system, *Applied Soft Computing* 11: 3238–3246.
- Warner R M. (2008). Applied Statistics *Sage Publication*.
- Wilson J A., Zorzetto L F M., (1997). A generalised approach to process state estimation using hybrid artificial neural network/mechanistics models. *Computers Chemical Engineering* 21, 9 :951-963

- Xuefeng Y., (2010).Hybrid artificial neural network based on BP-PLSR and its application in development of soft sensors. *Chemometrics and Intelligent Laboratory Systems 103*: 152-159
- Yaws, Carl L (1999). Chemical properties handbook for organic and inorganic chemicals. *McGraw Hill*, 2nd edition
- Zahedi, G., Elkamel A., Lohi A., Jahanmiri A., Rahimpour M.R., (2005). Hybrid artificial neural network-first principle model formulation for the unsteady state simulation and analysis of a packed bed reactor for CO₂ hydrogenation to methanol. *Chemical Engineering Journal, 115* :113-120
- Zamprogna E., Barolo M., Seborg D E., (2004).Estimating product composition profile in batch distillation via partial least square. *Chemical Engineering Practice 12*: 917-929
- Zamprogna E., Barolo M., Seborg Dale E., (2005).Optimal selection of soft sensor inputs for batch distillation columns using principal component analysis. *Journal of Process Control 15*: 39-52
- Zilochian A., Bawazir K., (2001).Chapter 7: Application of Neural Network in Oil Refineries. *CRC Press*, 2nd edition

LIST OF PUBLICATIONS AND PAPERS PRESENTED

- M Ramli N., Hussain M A., Mohamed Jan B., (2011) Principal component analysis of a debutanizer column. *International conference of Chemical Engineering and Industrial Biotechnology with 25th Symposium of Malaysian Chemical Engineers* 2011, 28 November – 1 December 2011, Kuantan, Pahang, Malaysia
- M Ramli Nasser., Hussain M A., (2009) Dynamic modeling and control of a debutanizer column. *16th ASEAN Regional Symposium on Chemical Engineering (RSC E 2009)* 1 -2 December 2009 Manila, Philippines.
- Mohd Ramli N., Hussain M A., Mohamed Jan B., (2010). Neural network model for composition prediction in debutanizer column. *conference proceeding 17th Regional Symposium on chemical engineering (RSCE 2010)* 22-23 November 2010, Bangkok, Thailand
- Mohamed Ramli N., Hussain M A., Mohamed Jan B. (2014), Composition prediction of a debutanizer column using equation based artificial neural network model. *Neurocomputing 131*: 59-76
- Mohamed Ramli N., Hussain M A., Mohamed Jan B., (2012). Hybrid neural network to estimate composition and temperature of a debutanizer column. *4th International conference on Chemical and Bioprocess Engineering with 26th Symposium of Malaysian Chemical Engineers* 21 – 23 November 2012, Kota Kinabalu, Sabah.